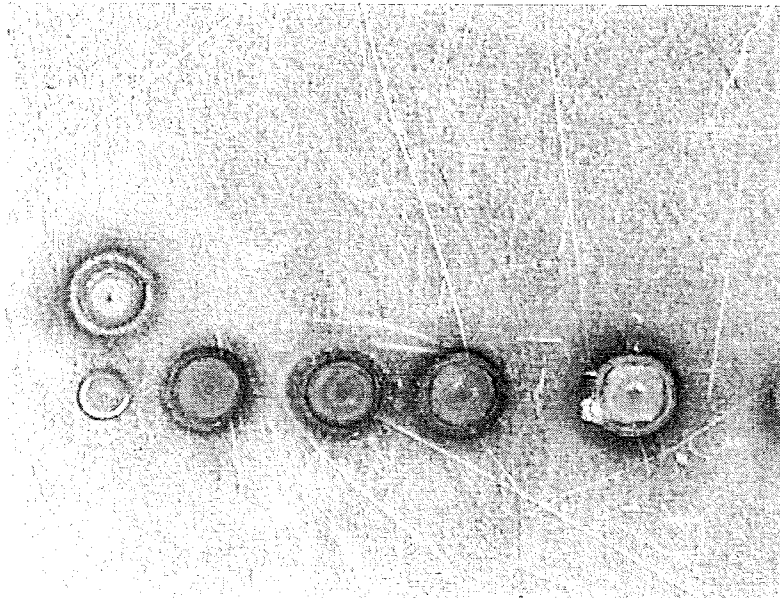


# Laser Assisted Micro Arc Welding

a feasibility study

Z.Z. Moeniralam



Master thesis

Delft University of Technology  
Faculty of Chemical Technology and Materials Science  
Section Welding Technology and Non-Destructive Testing

June 1997

Supervisors: Prof. Dr. G. den Ouden (TU Delft)  
J.J.C. Buelens (Philips-CFT)  
Ir. E.C.M. Verhoeven (Philips-CFT)  
Dr. W. Hoving (Philips-CFT)



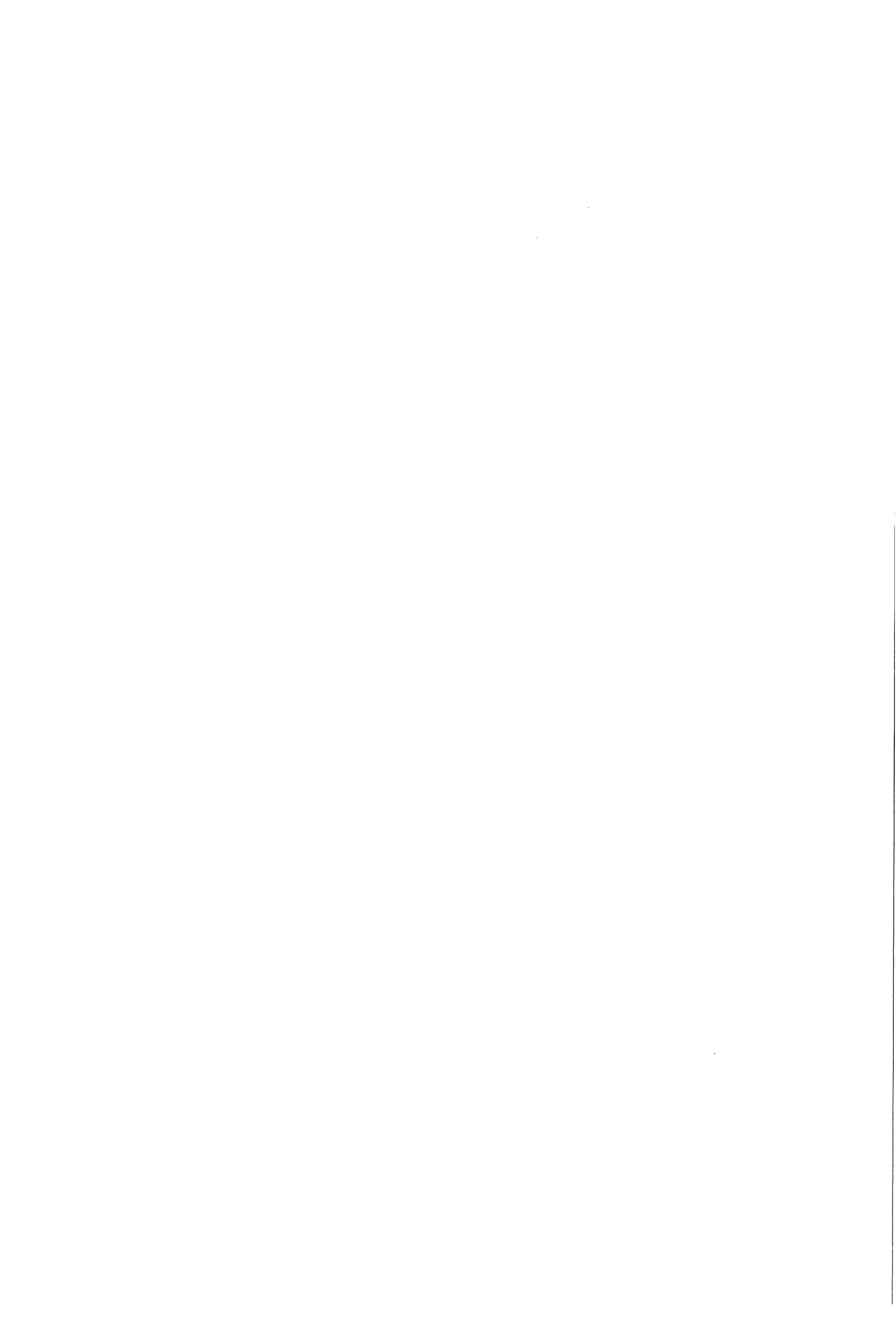
## SAMENVATTING

Micro-booglassen wordt wereldwijd op grote schaal toegepast. Een belangrijke parameter bij dit proces is de manipuleerbaarheid van de boog. Het doel van het onderzoek dat in dit verslag wordt gepresenteerd is systematisch na te gaan wat de mogelijkheden zijn de manipuleerbaarheid van de boog te vergroten met behulp van een laser. Dit is in principe mogelijk doordat de laser een pluim genereert bestaande uit neutrale en geladen deeltjes, die beter geleidend is dan het proefstuk en zo de boog aantrekt en geleidt naar de gewenste positie van de laserspot op het proefstuk (antenne functie).

Er is gekeken naar de grootst mogelijke (horizontale) afstand waarover de boog nog aangehouden wordt door de laserpluim en welke parameters hierop van invloed zijn. Dit is onderzocht voor het gepulst TIG-lassen gecombineerd met een gepulste Nd:YAG-laser, waarbij het testmateriaal uit Cr/Ni-stalen (N 286) plaatjes bestaat. Er zijn echter ook testen uitgevoerd op fosforbrons (R 1178/1179).

De van invloed zijnde parameters blijken te zijn: de boogstroom, de lengte (tijdsduur) van de boogpuls, de lengte van de laserpuls, het tijdsverschil tussen de triggering van de laserpuls en de boogpuls, de geometrie van het werkstuk, het type proefstukmateriaal, de intensiteit van de laser en de lasatmosfeer.

Op basis van de experimentele resultaten is een model opgesteld, waarmee de boog-laser interactie kan worden voorspeld.



## SUMMARY

Arc welding is a widely used welding process. One of the most important parameters during micro arc welding is the manipulability of the arc.

The objective of the study presented in this report is to systematically examine the possibilities of increasing the manipulability of the arc by means of a laser. Principally, this is possible because the laser generates a plume, consisting of neutral and charged particles, by which the plume becomes better conductive than the workpiece and thus guides the arc to the desired laser spot position on the workpiece surface (antenna function).

Tests are conducted to determine the largest distance over which the arc is still attracted to the laser plume/spot and to determine which parameters influence this distance. The arc welding process used during these tests is pulsed TIG welding. The laser is a pulsed Nd:YAG laser. The testing material is mostly Cr/Ni-steel (N 286, small plates). However, tests have also been conducted on phosphor bronze (R 1178/1179, small plates and pins).

The influencing parameters proved to be: the arc current, the pulse duration of the arc, the pulse duration of the laser, the delay time between the triggering of the laser pulse and the arc pulse, the geometry of the workpiece, the intensity of the laser, the type of material of the workpiece and the welding atmosphere.

Based on the experimental results a model is proposed, with which the arc-laser interaction can be predicted.



<b>CONTENTS</b>	
<b>Samenvatting</b>	i
<b>Summary</b>	ii
<b>Contents</b>	iii
<b>List of symbols</b>	iv
<b>1. Introduction</b>	1
<b>2. Theoretical background</b>	2
2.1 Arc welding	2
2.2 The anode fall region	2
2.3 The cathode fall region	3
2.4 The arc column	4
2.5 Physical properties of the plasma	4
2.5.1 Ionisation and dissociation	4
2.5.2 Thermal conductivity	5
2.5.3 Electrical conductivity	6
2.6 Ignition of the arc	7
2.7 Arc welding process	7
<b>3. Laser welding</b>	9
3.1 The laser	9
3.2 Laser welding	10
3.3 Laser spot welding phenomena	11
<b>4. Experimental procedure</b>	14
4.1 Experimental set-up	14
4.2 Materials	14
4.3 Experimental procedure	15
4.3.1 Initial tests	15
4.3.2 Standard	16
4.3.3 Variations	16
<b>5. Results &amp; Discussion</b>	18
5.1 Influencing parameters on the attraction of the arc for plates	18
5.1.1 Standard	18
5.1.2 Influence of arc length	18
5.1.3 Influence of polarity	19
5.1.4 Influence of arc current	19
5.1.5 Influence of the pulse duration of the TIG pulse	19
5.1.6 Influence of laser power and laser intensity	20
5.1.7 Influence of laser pulse duration	21
5.1.8 Influence of delay time	22
5.1.9 Influence of shielding gas	23
5.1.10 Influence of workpiece material	25
5.2 Results of experiments on phosphor bronze pins	25
5.3 High speed video camera	26
5.4 Model	27
<b>6. Conclusions &amp; Recommendations</b>	31
<b>References</b>	33
<b>Appendix A</b>	



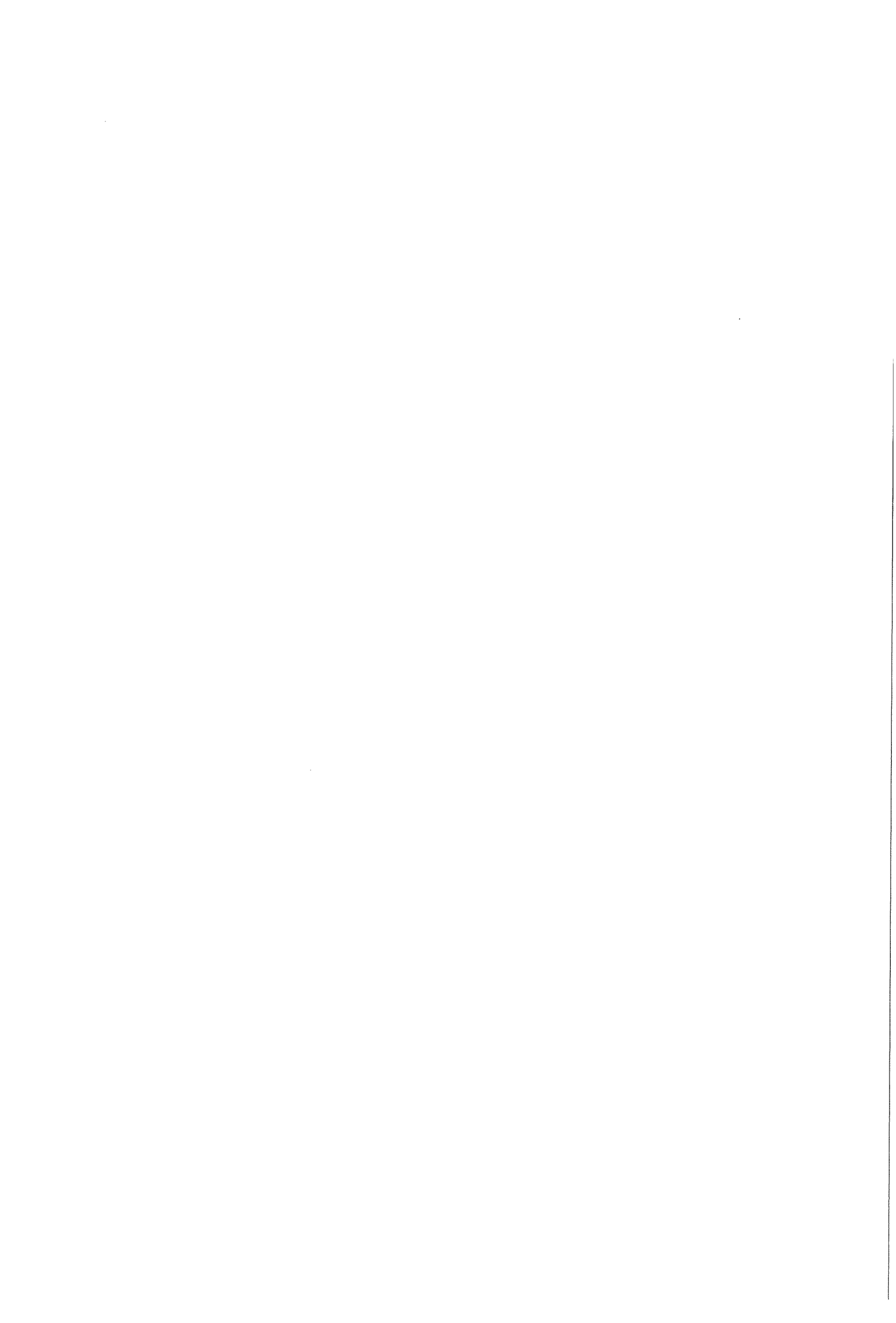
**LIST OF SYMBOLS**

## Theoretical background

- $e$  : electron charge (eV)  
 $E$  : electric field strength (V/m<sup>2</sup>)  
 $E_d$  : dissociation energy (eV)  
 $E_i$  : ionisation energy (eV)  
 $j$  : current density (A/m<sup>2</sup>)  
 $j_e$  : electron current density ()  
 $j_i$  : ion current density ()  
 $k$  : Boltzmann constant ( $1.3807 \times 10^{-23}$  J/K)  
 $l_e$  : electron mean free path (m)  
 $m_e$  : electron mass (kg)  
 $m_i$  : ion mass (kg)  
 $n_e$  : electron density (particles/m<sup>2</sup>)  
 $p$  : gas pressure (N/mm<sup>2</sup>)  
 $\Delta Q$  : thermal conductivity (W/m<sup>2</sup>)  
 $T$  : absolute temperature (K)  
 $x$  : distance used in determining temperature gradient (m)  
 $\alpha_d$  : degree of dissociation  
 $\alpha_i$  : degree of ionisation  
 $\eta_p$  : process efficiency  
 $\kappa$  : thermal conductivity coefficient (W/m.K)  
 $\sigma$  : electrical conductivity (1/ $\Omega$ .m)  
 $\Phi$  : work function (eV)

## Laser welding

- $C_p$  : specific heat at constant pressure (J/kg.K)  
 $c\rho$  : volume specific heat (J/kg.K)  
 $d_s$  : diameter of laser spot (m)  
 $E_p$  : energy of pulse of length  $t_p$  (J)  
 $\Delta H_m$  : enthalpy of fusion (J)  
 $k$  :  $K/c\rho$  = thermal diffusivity (kg.K/m.s)  
 $k_e$  : extinction coefficient  
 $K$  : thermal conductivity (W/m<sup>2</sup>)  
 $n$  : refractive index  
 $P_p$  :  $E_p/t_p$  = pulse power (W)  
 $q$  :  $P_p/\pi r_s^2$  = power density delivered to the hot spot of radius  $r_s$  (W/m<sup>2</sup>)  
 $Q$  : heat given by heat source (J)  
 $r^2$  :  $x^2 + y^2$  (square distance from heat source to a point (x,y)) (m<sup>2</sup>)  
 $r_s$  : radius of laser beam (m)  
 $R$  : reflection coefficient  
 $S_m$  : entropy of fusion (J/K)  
 $t$  : time (s)  
 $t_p$  : pulse duration (s)  
 $T$  : absolute temperature (K)  
 $T_b$  : boiling temperature (K)  
 $T_m$  : melting temperature (K)



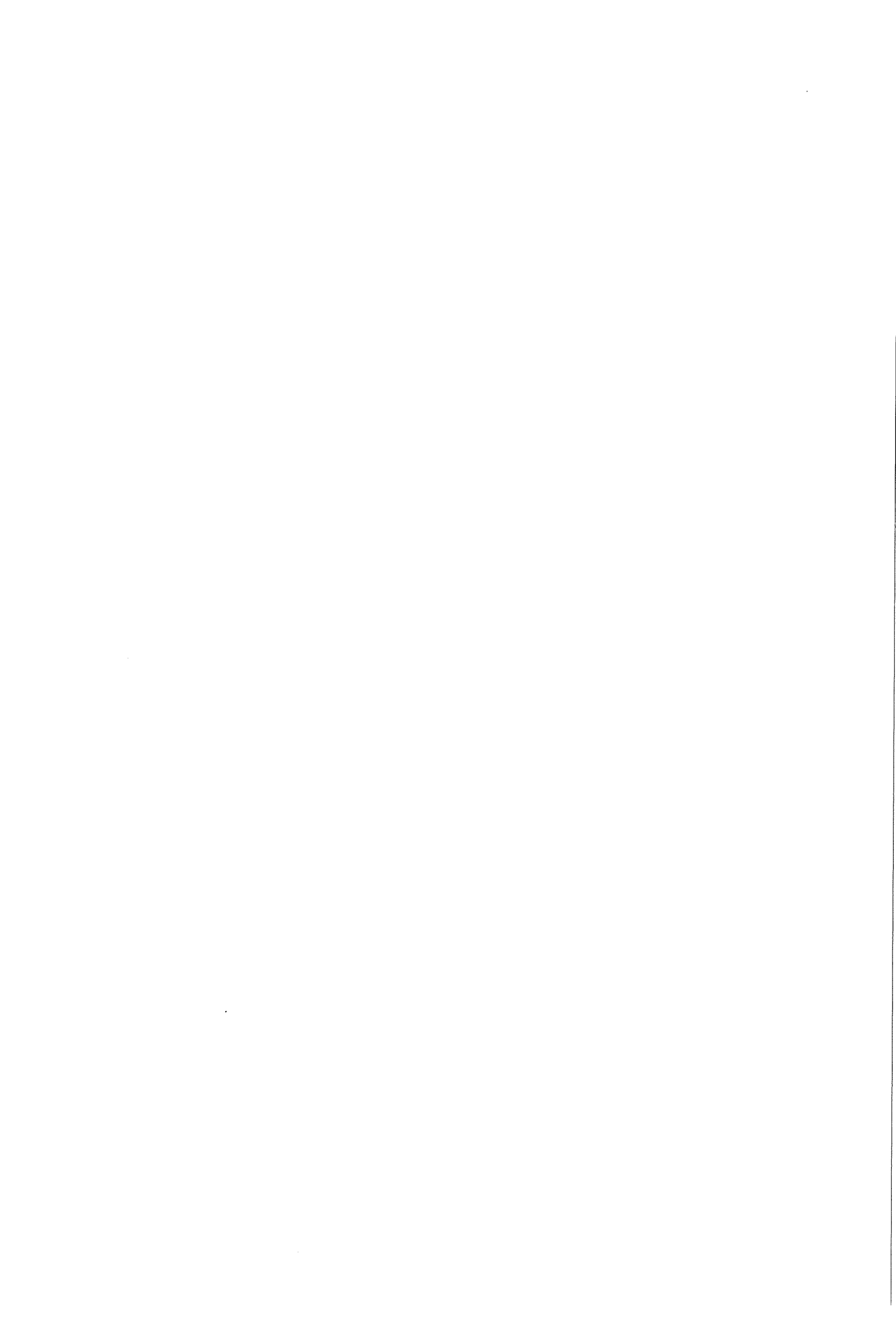
- $\alpha$  : heat transfer coefficient ( $\text{W}/\text{m}^2\cdot\text{K}$ )  
 $\alpha'$  :  $2\alpha/c\rho\delta$  = factor accounting for the surface heat transfer to the environment ( $\text{kg}/\text{m}\cdot\text{s}$ )  
 $\delta$  : thickness of plate (m)

#### Experimental procedure

- $l_c$  : critical distance (m)  
 $l_a$  : arc length (m)  
 $I$  : arc current (A)  
 $P$  : laser power (W)

#### Results & Discussion

- $d$  : diameter spot (m)  
 $f$  : focal length (m)  
 $h$  : visible area ( $\text{m}^2$ )  
 $I_a$  : arc current (A)  
 $I_L$  : laser intensity (expressed by spot diameter) (m)  
 $l_a$  : arc length (m)  
 $l_c$  : critical distance (m)  
 $P$  : laser power (W)  
 $t_a$  : TIG pulse duration (s)  
 $t_l$  : laser pulse duration (s)  
 $\Delta t$  : delay time (s)



## 1. INTRODUCTION

Tungsten Inert Gas welding is a widely used process. In industry it is often used in micro welding applications. Although most applications are rather successful, there still is need for a way to control the position of the arc spot. For instance, the position of the weld spots will not be the same during a series of spot welds with a fixed position between the electrode and the workpiece. Under these conditions often a cluster of spots is formed.

The goal of this feasibility study is to examine the possibilities of positioning and/or controlling the arc (and its spot position) by means of a laser during pulsed micro welding techniques.

On the basis of a literature search [1] it can be shown that the arc can be assisted by a laser in order to control its position. In the tests which are described in this study, continuous arc welding (with relatively high arc currents) and laser welding techniques were used. Several improvements of the arc welding process were obtained by adding a laser to the arc: the travel speed, penetration depth and the efficiency all increase. Also the stability and ignition of the arc and the quality of the welds are improved. Furthermore, the ignition can take place at higher arc lengths. The most important result in relation to the goal of the work presented in this report is the fact that the arc is attracted to the laser spot position and follows the laser exactly when it is moved.

First of all, the physical properties of the arc welding and laser welding processes will be discussed (chapter 2 and 3) in order to have an understanding of what takes place during these processes. In the combination the laser will only have a guiding function. In order for this combination to be able to compete with the relatively "cheap" TIG welding process, the laser power needs to be as low as possible. The higher the laser power, the more expensive the combined process becomes. Thus, it was tried to keep the laser power as low as possible and even avoid actual laser welding. However, even for the low laser power the laser/material interaction will, in principle, be the same as during laser welding. Therefore, it is necessary to briefly discuss what takes place during laser welding. This will help explaining the attraction of the arc.

In chapter 4 the set-up of the experiments is discussed. The influencing parameters and how they will be investigated are mentioned.

In chapter 5 the results of these experiments are presented, as well as the discussion of the obtained results. At the end of chapter 5 the model with which it is tried to explain the attraction behaviour of the arc by the laser is presented and discussed.

Finally, chapter 6 deals with the conclusions and recommendations.

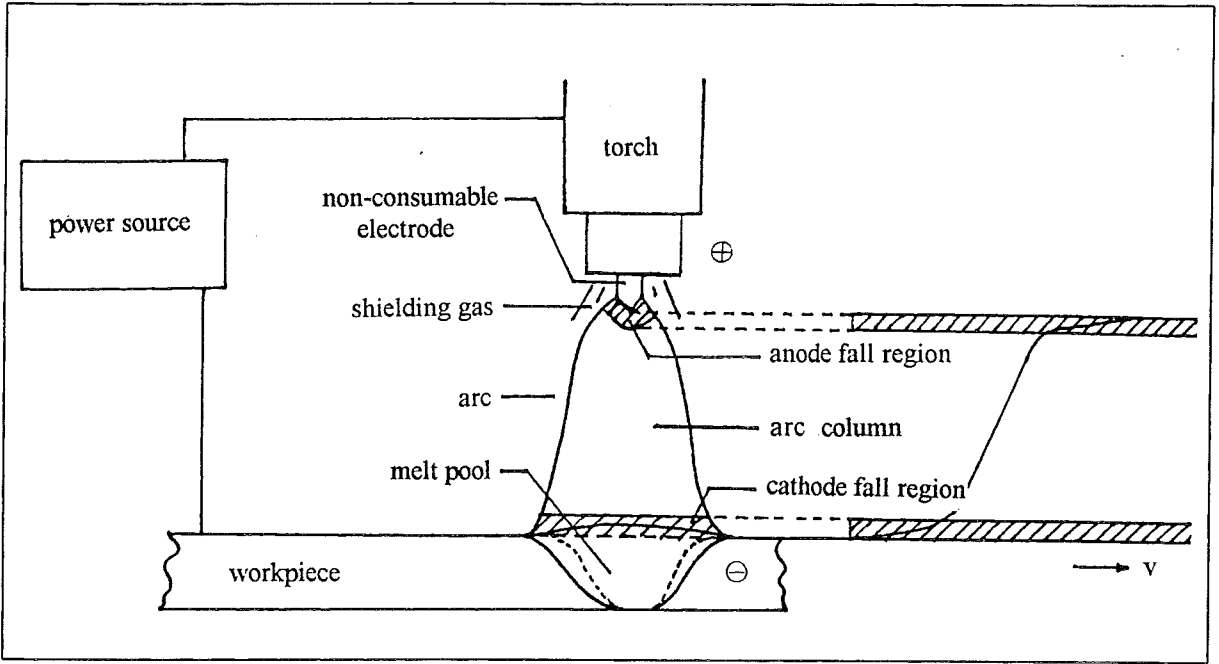


Figure 1: Schematic view of arc welding [2].

## 2. THEORETICAL BACKGROUND

In order to obtain more insight in what occurs during the combined laser/arc welding process, it is necessary to have a closer look at the physical aspects of the arc welding process as well as the laser welding process. These processes will be discussed in this and the next chapter (chapter 3). The emphasis will not be on the welding processes itself, but on the arc and on the laser plume.

### 2.1. Arc welding

The electric arc is an electric discharge in a partially ionised gas (plasma). Electric arcs can be distinguished from other types of gas discharges by their relatively high current (10 to 1000 A) and relatively low voltage (10 to 40 V). In arc welding the arc burns between a cylindrical (consumable or non-consumable) electrode and the workpiece to be welded. In figure 1 the general arc welding process is presented schematically. Due to the heat produced by the arc a weld pool is formed in the workpiece, which after solidification turns into the required weld. A shielding gas is used to protect the liquid metal and the electrode against oxidation, which is caused by the surrounding atmosphere. In most cases this will be helium or argon or a mixture of both gases.

The behaviour of the arc at the sides of the electrode and the workpiece differs from the part in-between. Therefore the arc can be divided in three parts, which are [2-8]:

- the anode fall region;
- the arc column (or plasma column);
- the cathode fall region.

These three regions are also shown in figure 1. In this figure it can be seen that a small but constant voltage gradient is typical for the arc column, while the cathode and anode fall regions are characterised by a voltage drop.

In the following sections the three regions and some physical aspects of the plasma will be briefly discussed [2-8].

### 2.2. The anode fall region

The anode fall region is the boundary region between the anode and the arc column. It is an extremely thin layer ( $10^{-7}$  m). The voltage drop lies between 1 to 10 V.

Contraction of the arc occurs near the anode at relatively low arc currents ( $\leq 40$  A). The formed anode spot is rapidly leaping from point to point which contributes to the unstable behaviour of the arc.

The anode only receives electrons. Besides their kinetic energy, they also transfer the energy corresponding with the work function.

The anode fall region forms in fact the transition between the pure electron current right in front of the anode and the positive ion current which is part of the total current in the arc column. The ionisation which takes place in this region provides the positive ions, which travel towards the arc column and electrons which travel towards the anode. The anode itself can not produce ions.

Table 1: Work function of some metals [2].

metal	work function (eV)
Al	4.0
Cu	4.3
Fe	4.4
Ni	5.0
W	4.6

### 2.3. The cathode fall region

The cathode fall region is the boundary region between the cathode and arc column. This layer is also extremely thin ( $10^{-8}$  m) and is also characterised by a voltage drop ( $\pm 10$ -20 V), which results in a high field strength in the order of  $10^9$  V/m.

The most important role of the cathode is emission of electrons. These electrons will be transported towards the anode under influence of the field strength. Emission of electrons from the cathode can occur in the presence of a high electric field (field emission), or as a result of high temperature (thermal emission). Thermal emission is the most common mechanism in the case of refractory metals, as used in TIG cathodes. The electron current density  $j_e$  is related to the temperature by the Richardson's equation [2,3,5]:

$$j_e = AT^2 \exp\left(-\frac{\phi}{kT}\right) \quad (1)$$

in which:  $j_e$  = electron current density

A = constant depending on the cathode material. The value of A is typical  $6 \cdot 10^5$  A/m<sup>2</sup>K<sup>2</sup> for most metals.

T = absolute temperature

$\phi$  = work function of the cathode

k = Boltzmann constant

In table 1 the work energy of several metals is given. From the table one can see that the work function of tungsten is relatively high. Oxides have lower ( $\pm 2$  eV) work functions and therefore they are often added to the metals to facilitate electron emission.

Field emission only takes place when the electric field strength is high enough. When field emission occurs, the current density is extremely high ( $\sim 10^{11}$  A/m<sup>2</sup>).

The physical processes occurring in the cathode fall region may be described as follows [5]. Electrons are emitted due to the high temperature and the high electric field strength at the cathode surface. This results in electron evaporation cooling, because in evaporating an electron, an energy equal to the work function of the cathode material is dissipated. After travelling a distance equal to the electron free path, electrons collide with heavy particles and thermal ionisation takes place. In this collision zone, electrons leave in the direction of the anode, whereas the less mobile ions travel slowly to the cathode. Because of the limited mobility of the ions, a positive space charge is formed, producing the cathode voltage drop. The ions travelling to the cathode transfer part of their kinetic energy to the cathode. During contact with the cathode the ions are neutralised, releasing their ionisation energy. This increases the cathode temperature, favouring thermal emission of electrons.

The part of the total arc energy that is transferred to the workpiece is given by the process efficiency  $\eta_p$ . This can be expressed for a non-consumable electrode (direct current, electrode negative) by [2]:

$$\eta_p = \frac{Q_a}{VI} \times 100\% \quad (2)$$

in which:  $Q_a$  = energy available for heating the anode



VI= total arc energy

For TIG welding with electrode negative  $\eta_p$  lies between 50-80 %.

## 2.4. The arc column

The largest part of the arc is formed by the arc column. The arc column consists of neutral particles (like atoms and molecules) and particles which are electrically loaded (electrons and ions). Due to the field strength present, the electrons travel in the direction of the anode and the positive ions travel in the direction of the cathode. Under normal conditions the field strength is in the order of  $10^3$  V/cm. The arc column is electrically neutral i.e. one unit of volume consists of an equal amount of positive and negative loaded particles. This is called a plasma. As a consequence of the electrical neutrality, the field strength in the arc column is constant. Well established plasma physics theories can be applied in this region.

The plasma in the arc column is considered to be in Local Thermodynamic Equilibrium (LTE), i.e. the energetic coupling between electrons and heavy particles is relatively strong and electrons and heavy particles are in mutual equilibrium ( i.e. have the same temperature). Total equilibrium does not exist, since the electrons and heavy particles are not in equilibrium with the photons, which can escape from the plasma. The temperature in the arc column varies between 5000-25000 K.

## 2.5. Physical properties of the plasma

The characteristics of the plasma in the welding arc are determined by various parameters like temperature distribution, thermal and electrical conductivity etc. The following sections discuss the major parameters: the ionisation and dissociation within the plasma, and its thermal and electrical conductivity.

### 2.5.1. Ionisation and dissociation

Welding usually takes place at atmospheric or higher pressure, when the electron temperature is virtually equal to the gas temperature in the plasma arc column. This means that the plasma is in thermal equilibrium. As a result of the relatively high temperature part of the atoms and molecules will be ionised according to [2]:



The ionisation takes place according to the Eggert-Saha equation and can be expressed as [2,3]:

$$\frac{\alpha_i^2}{1 - \alpha_i^2} = C_1 \frac{T^{5/2}}{p} \exp\left(\frac{-E_i}{kT}\right) \quad (4)$$

in which:  $\alpha_i$  = degree of ionisation

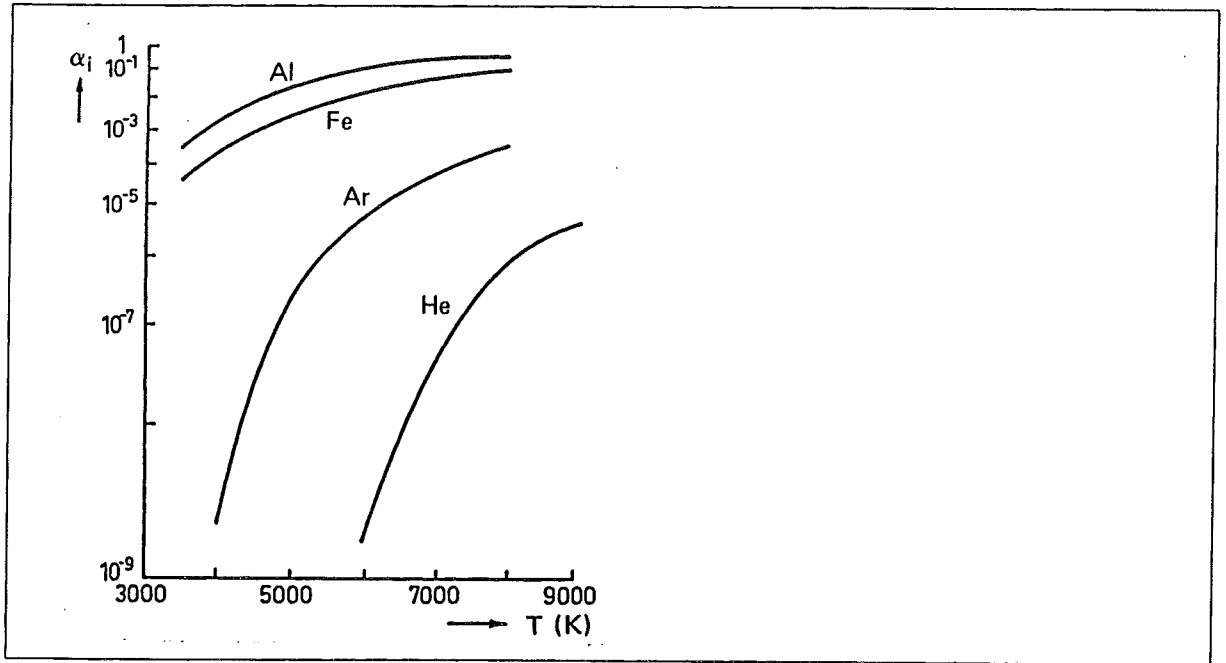


Figure 2: Degree of ionisation as function of the temperature [2].

Table 2: Ionisation energy of some atoms and molecules [2].

element	E(eV)
H <sub>2</sub>	15.6
Ar	15.8
Al	6.0
Cu	7.7
Fe	7.9
W	7.9
Sn	7.3

Table 3: Dissociation energy for hydrogen/nitrogen/oxygen and carbon dioxide [2].

gas	H <sub>2</sub>	N <sub>2</sub>	O <sub>2</sub>	CO <sub>2</sub>
E <sub>d</sub> (eV)	4.48	9.76	5.08	4.3

- $C_1$  = constant  
 $T$  = absolute temperature  
 $p$  = pressure  
 $E_i$  = ionisation energy  
 $k$  = Boltzmann constant

From equation (4) it can be seen that the ionisation strongly depends on the temperature. Figure 2 shows the degree of ionisation as function of the temperature for some metal vapours and gases. In addition to the temperature, the ionisation energy of the plasma gas is also an important parameter. In table 2 the values of the ionisation energies for a number of atoms and molecules are presented.

From figure 2 and table 2 one can see that generally the ionisation energy of metal vapours is lower in comparison to that of gases. As a consequence metallic elements, which vaporise from the weld pool and enter the arc during welding, will play a dominant part in the electrical conductivity of the plasma.

When molecular gases are present in the shielding gas, a part of these molecules will be dissociated due to the high temperature, according to [2]:



The degree of dissociation can be expressed by [2,3]:

$$\frac{4\alpha_d^2}{1-\alpha_d^2} = C_2 \frac{T^{5/2}}{p} \exp\left(-\frac{E_d}{kT}\right) \quad (6)$$

- in which:  $\alpha_d$  = degree of dissociation  
 $C_2$  = constant  
 $T$  = absolute temperature  
 $p$  = pressure  
 $E_d$  = dissociation energy  
 $k$  = Boltzmann constant

From equation (6) it can be seen that the degree of dissociation is strongly dependent on the temperature. Values of the dissociation energy are listed in table 3 for hydrogen, nitrogen, oxygen and carbon dioxide. At the high temperatures in the core of the arc when welding ( $\geq 6000$  K) an important part of these gases will be dissociated, which implies that the dissociation energy is an important parameter.

### 2.5.2. Thermal conductivity

During welding an important part of the energy is transferred by means of thermal conduction. The energy loss also depends on the thermal conductivity. The thermal conductivity determines the temperature gradient in the arc.

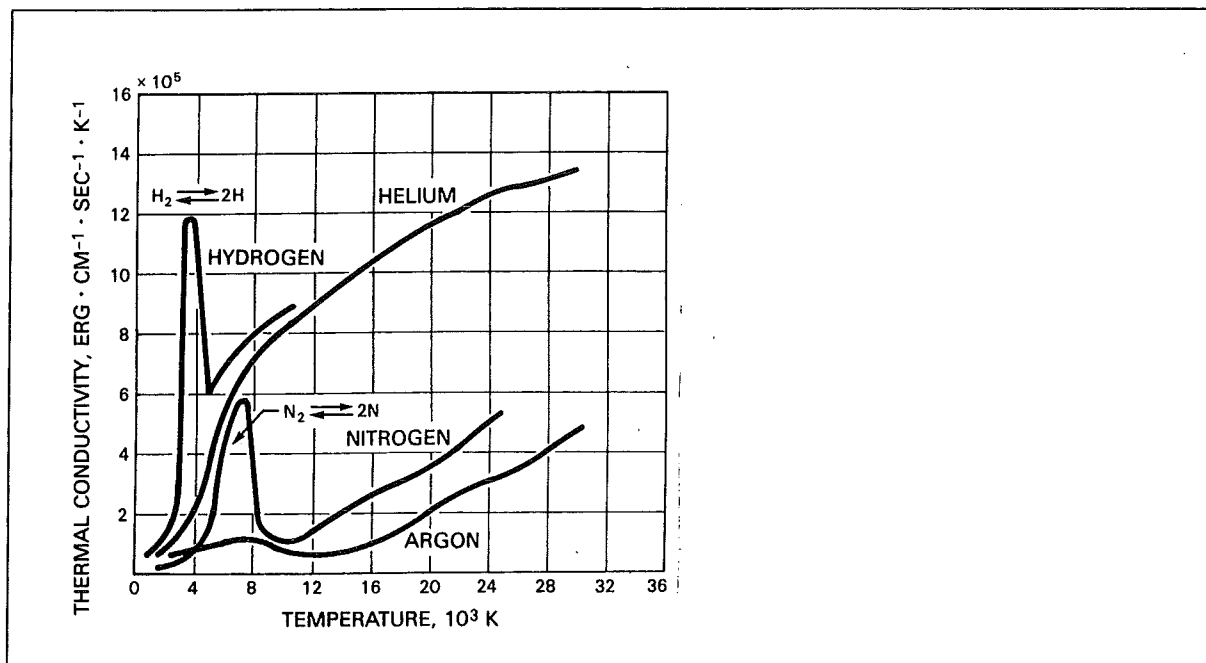


Figure 3: Thermal conductivity of some gases as a function of temperature [4].

This means that the arc diameter is strongly dependent on the thermal conductivity of the plasma. The thermal conductivity is defined as [2]:

$$\Delta Q = \kappa \frac{dT}{dx} \quad (7)$$

in which:  $\Delta Q$  = heat flow through unit surface area per unit time  
 $\kappa$  = thermal conductivity coefficient  
 $dT/dx$  = temperature gradient in direction x

The total thermal conductivity is determined by several mechanisms which gives [2]:

$$\kappa = \kappa_g + \kappa_e + \kappa_f + \kappa_d \quad (8)$$

in which:  $\kappa$  = total thermal conductivity coefficient  
 $\kappa_g$  = thermal conductivity coefficient due to the collisions of heavy particles  
 $\kappa_e$  = thermal conductivity coefficient due to the collisions between electrons and heavy particles  
 $\kappa_f$  = thermal conductivity coefficient due to the diffusion of ionised pairs (electrons and positive ions)  
 $\kappa_d$  = thermal conductivity coefficient due to the diffusion of dissociated molecules

Figure 3 shows the thermal conductivity of several important gases as a function of temperature. The peaks in the hydrogen and nitrogen lines are due to the effect of thermal dissociation and association.

### 2.5.3. Electrical conductivity

An important arc parameter is the electrical conductivity  $\sigma$ . This parameter determines the current density and plays a decisive role in the heat balance of the arc. The electrical conductivity can be expressed as [2,3]:

$$\sigma = \frac{j}{E} = \frac{e^2 n_e l_e}{\sqrt{8m_e kT} / \pi} \quad (9)$$

in which:  $\sigma$  = electrical conductivity  
 $j$  = current density  
 $E$  = electrical field strength  
 $e$  = electron charge  
 $n_e$  = electron density  
 $l_e$  = electron mean free path  
 $m_e$  = electron mass  
 $k$  = Boltzmann constant  
 $T$  = absolute temperature

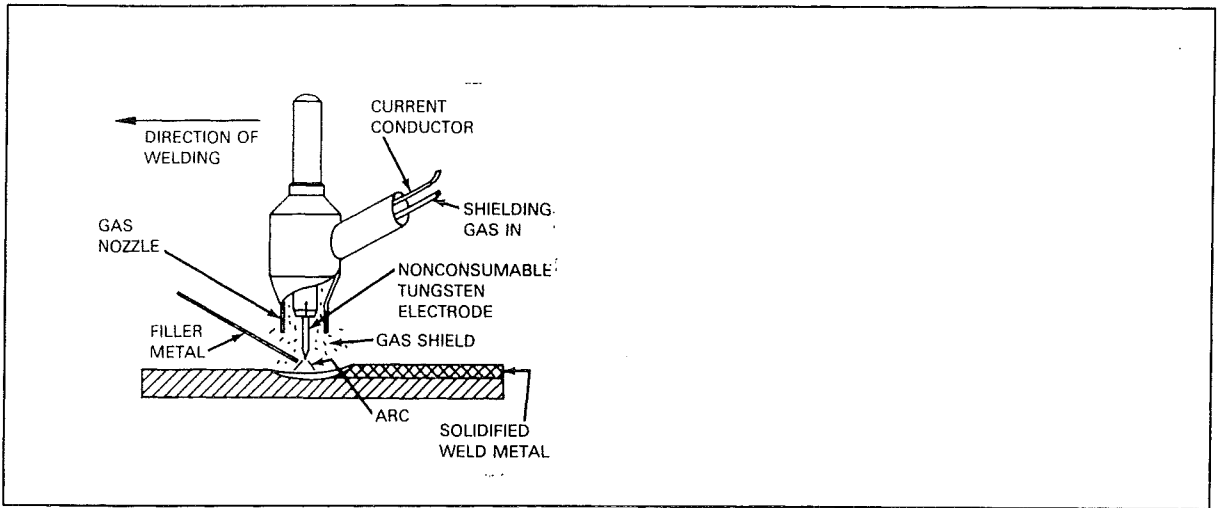


Figure 4: Schematic view of TIG welding process [4].

The electron density and the mean free path of the electron are only dependent on temperature. This means that also the electrical conductivity is only a function of the temperature. In addition to electrons, ions also contribute to the charge transport in the arc. However, as the mass of electrons is much smaller than that of ions, the charge transport is realised primarily by electrons. A good estimate of the ratio of the current carried by electrons and that carried by ions is given by equation [2,3]:

$$\frac{j_e}{j_i} = \sqrt{\frac{m_i}{m_e}} \quad (10)$$

in which:  $j_e$  = electron current density  
 $j_i$  = ion current density  
 $m_e$  = electron mass  
 $m_i$  = ion mass

For argon, the ion contribution amounts to about 0.4 % of the total current, for hydrogen this fraction is about 2.3 %. Thus, it can be concluded that the electron current density is much more important than the ion current density.

## 2.6. Ignition of the arc

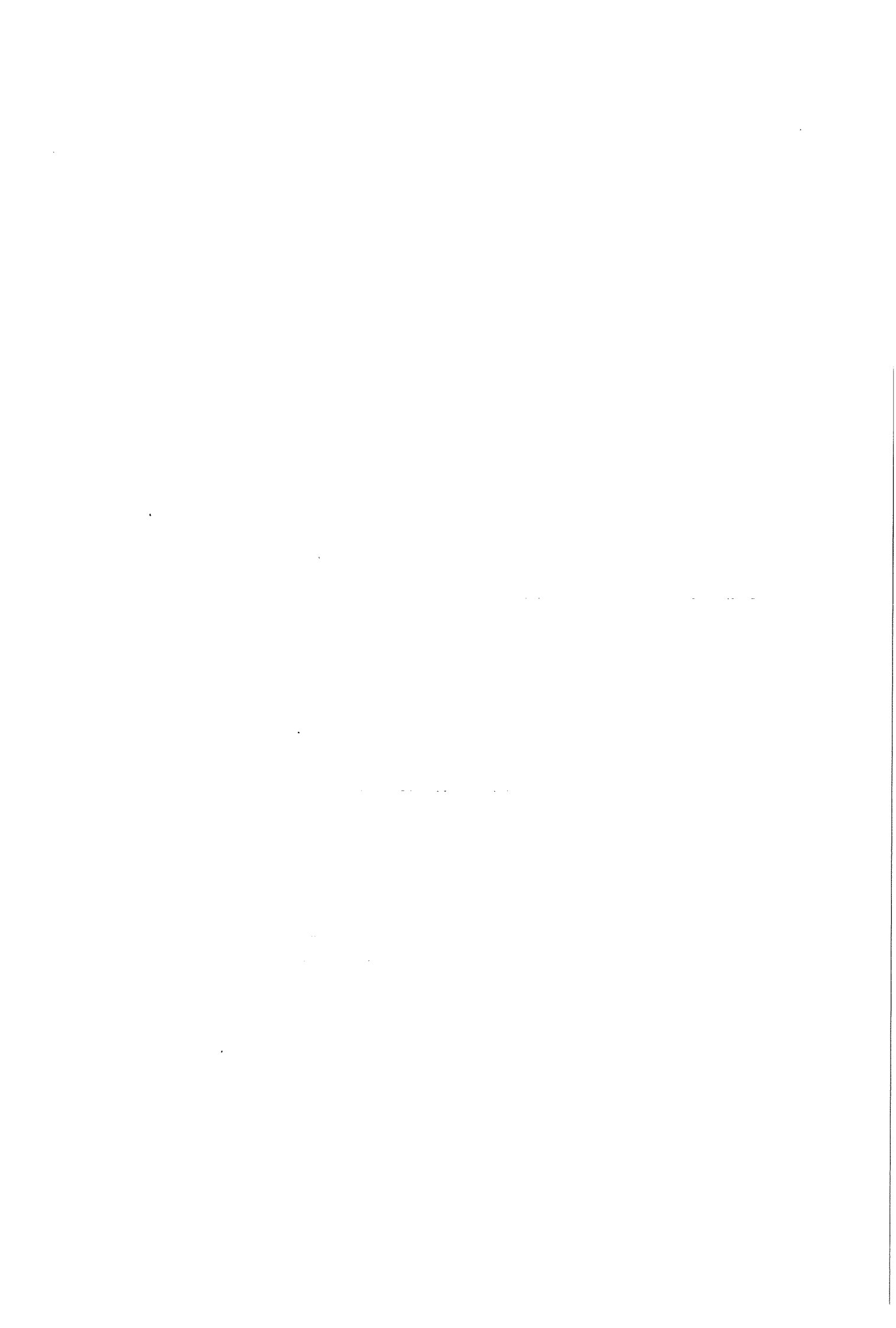
With respect to chapter 4 where an experiment dealing with the ignition of the arc with help of the laser is mentioned, it is necessary to briefly say a few words about the ignition.

There are various ways of igniting the arc. Ignition can take place for example by direct heating of the cathode, ignition by break-down and ignition by high-frequency voltage. All these methods have in common the self-emission of electrons by the local heating of the cathode. The ignition technique used in the experiments described in the following is ignition by a high-limited voltage pulse [7]. High voltage ignition (unlike direct heating) is a non-contacting technique for starting the arc. The high voltage (in this case 12 kV) creates a bridge of limited in time sparks between the electrode and the workpiece. In this way, the path between the electrode and the workpiece is being pre-ionised. When the open voltage of the power source is high enough, around 70 V, the TIG arc will be ignited.

Once the arc is established, the high voltage starting device will automatically shut off.

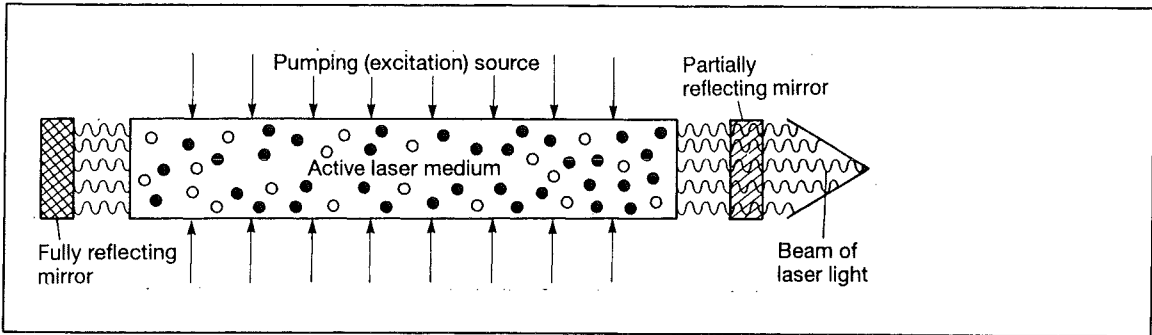
## 2.7. Arc welding process

In this section a short description of the arc welding process used in the experiments described in the following is given. This arc welding process is called TIG welding, which is the abbreviation of Tungsten Inert Gas welding. Figure 4 shows a schematic view of this arc welding process. The anode and cathode are formed by the workpiece and a non-consumable tungsten electrode. In order to enhance the electron emission an amount of 1-2 % of a special oxide (in most cases a rare earth metal is used) is usually added to the tungsten. The increase in electron emission will stabilise the arc and leads to improvement of the ignition and decrease of electrode erosion. The electrode and the weld pool are protected by an inert gas, usually argon. Filler material can be added if necessary.

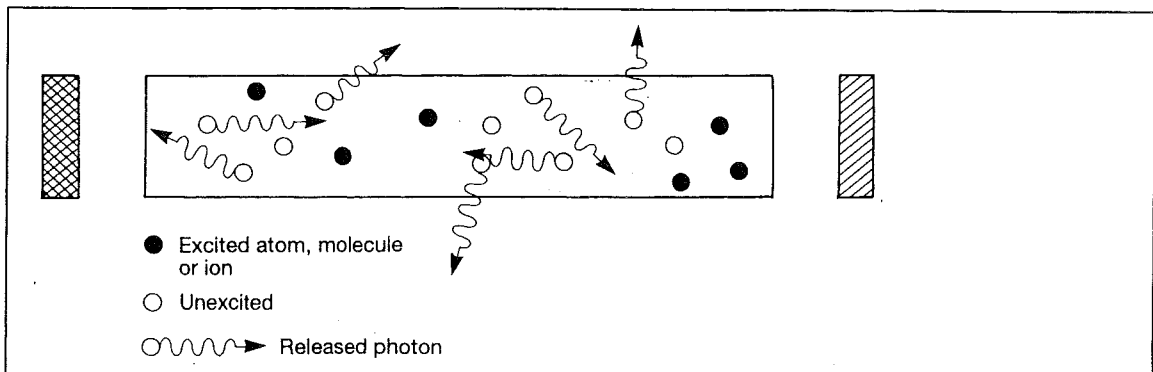


When using the TIG welding process in the next experiments the arc is ignited with a high voltage start supply. It is common to use direct current with negative electrode when using TIG welding.

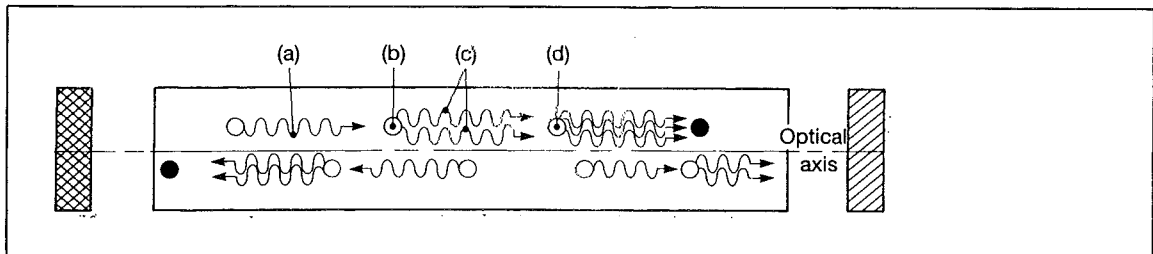
The shape of the arc and the shape of the weld pool are strongly dependent on the tip angle of the electrode. The smaller the tip angle, the wider the arc and the wider and more shallow the weld pool. All metals can principally be welded by TIG welding. It is especially suited for thin sheet and small metal parts.



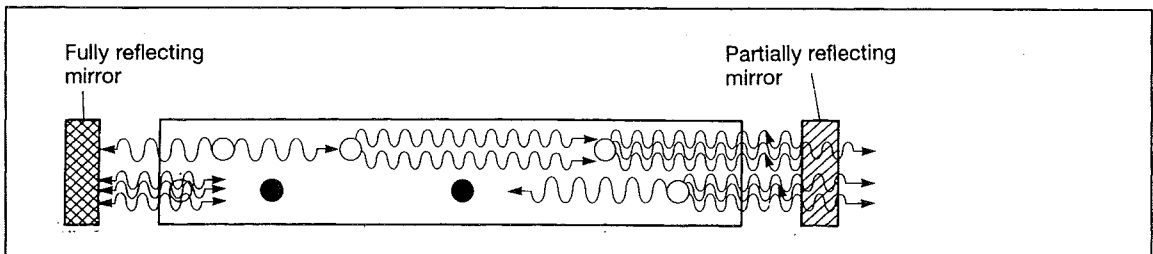
a. The basic elements of a laser.



b. Spontaneous emission of photons from the excited active medium. There are billions of excited atoms, molecules and ions and they release their photons in all directions.



c. Stimulated emission of photons. A photon (a) which collides with an excited atom, etc. (b) will cause it to release its photon before spontaneous emission can occur and thus two photons (c) will travel on in phase until the next collision (d). By stimulated emission photons which travel parallel to the optical axis build up a powerful laser beam.



d. Optical feedback of photons by mirrors to increase the path length for stimulated emission and thus amplify the laser power.

Figure 5: Schematic view of laser [9].

### 3. LASER WELDING

This study deals with the influence of the laser on the arc welding process. Therefore it is necessary to discuss a few laser properties. In the experiments the laser power was kept as low as possible, but it is inevitable that small laser welds will be made, in order to release enough particles/electrons from the workpiece (see § 5.4).

First the basic principle of how the laser works will be discussed [8-12]. After this, the welding with the laser will be presented and here the emphasis will be on the Nd:YAG laser (in particular the spot welding process), since this type of laser will be used in the experiments reported later on [8-12]. Finally some details of the welding phenomena will be discussed [9,10,11,12].

#### 3.1 The laser

The laser produces a collimated, monochromatic and coherent beam of light. The almost parallel light rays which make up the collimated laser beam have a high power density and can be focused to very small spot sizes (several hundred  $\mu\text{m}$ ) [8-12].

The word LASER is an acronym, it stands for: Light Amplification by the Stimulated Emission of Radiation, which refers to the way in which the light is generated [9]. All lasers are optical amplifiers which work by pumping (exciting) an active medium placed between two mirrors, one of which is partially transmitting ( $\pm 99.999\%$ ), see figure 5. This active medium is a collection of specially selected atoms, molecules or ions which can be in a gaseous, liquid or solid form. When the medium is excited by a pumping action they emit radiation as light waves (photons). The pumping of liquids and solids is achieved by flooding them with the light from a flash lamp and gases are pumped by applying an electrical discharge.

When atoms, molecules or ions are pumped, they absorb energy which they hold for a short life time. When their life time expires, they release the extra energy in the form of a photon (spontaneous emission). If a photon collides with another energised atom, it causes it to release its photon prematurely and they travel along in phase. This process is repeated many times and this builds a stream of photons of increasing density.

The photons which travel along the optical axis of the laser have their path length considerably extended by the optical feedback provided by the mirrors, before leaving the laser through the partially transmitting mirror. This is the amplification for photon generation by stimulated emission and it provides the highly collimated coherent light beam that makes the laser so useful (figure 5d).

The currently used welding lasers which are also used for material working, can be divided in-to two groups, depending on their active medium [9-12]:

- solid-state lasers
- gas lasers

The gas lasers which are used currently are almost all  $\text{CO}_2$  lasers. From the solid-state lasers the most applied one is the Nd:YAG laser. The  $\text{CO}_2$  laser, which gives the highest output power, is used in particular for steel cutting and seam welding in heavy engineering. The Nd-laser is used for welding and cutting small parts for the electronics industry.

In figure 6 a diagram of a laser head of an Nd:YAG laser is given. The laser rod exists of an Yttrium Aluminium Garnet (YAG) crystal, in which the Neodymium atoms are implanted in a special way. The output wave length of the Nd:YAG laser is  $1.06\ \mu\text{m}$ .

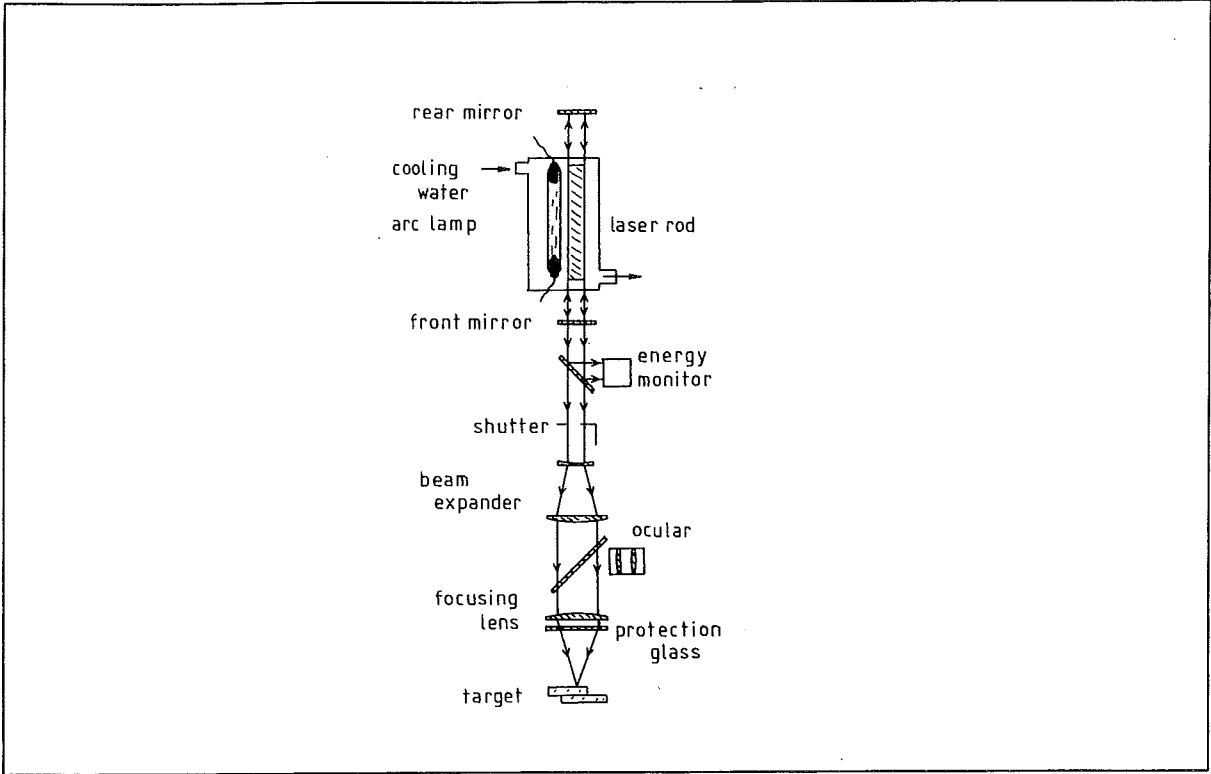


Figure 6: Diagram of laser head [10].

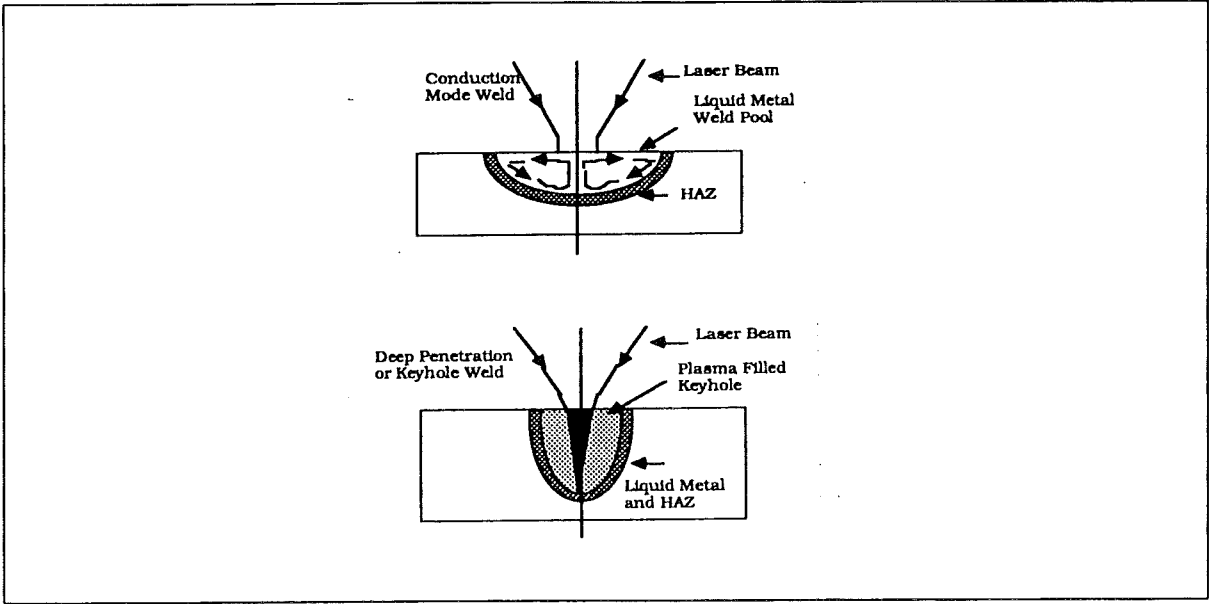


Figure 7: Conduction limited and keyhole type welds [11].

### 3.2 Laser welding

The focused laser beam is one of the highest power density sources available to industry today. It is similar in power density to an electron beam. Both solid-state and gas lasers operating in the continuous or pulsed mode can function as welding sources.

Because of the high energy density of a laser during welding and the small area ( $< 1$  mm for micro spot welding) the energy is deposited on, the bulk of the molten metal is small, the dimensions of the metal effected by the heat are insignificant (certainly compared to arc welding), the rate of heating is high and the rate of cooling near the weld is small. A small heat input results in a very slight distortion of the weldment.

Laser welding covers a large variety of techniques capable of producing welds in various metals ranging from a few hundred micrometers to tens of millimetres in thickness.

The welding process is easy to control by adjusting the beam energy parameters. The laser beam is unaffected by the magnetic field of a workpiece.

To form a laser weld, the laser beam is brought to focus on or very near the surface of the workpieces to be joined. This can be achieved with the use of several (focusing) lenses.

There are two modes of welding with the laser:

- conduction limited welding;
- keyhole welding.

These are illustrated in figure 7. Conduction limited welding occurs when the power density is insufficient to cause boiling, the heat penetrates the metal purely by conduction. The melt pool is usually shallow. The weld pool has strong stirring forces, driven by Marangoni type forces resulting from the variation in surface tension with temperature.

The alternative mode is "keyhole" welding. Here there is sufficient energy (high laser intensities) and the high temperatures causes evaporation of the metal. The vapour pressure of the vaporising metal produces a dent or even a hole in the molten metal pool. At the end of welding, the molten metal flows back into the hole. The result is a penetration or deep weld. The weld pool is much deeper than that from conduction. During this keyhole welding process, a vapour plume is created above the surface of the melt pool.

In micro spot welding with a pulsed Nd-laser the metal is heated until vaporisation occurs. The melt pool diameter usually lies under 1.0 mm. The laser system delivers pulses with an energy of 1 to 5 J and a duration of 1 to 20 ms. For welding, a power density of  $10^9$  to  $10^{11}$  W/m<sup>2</sup> is needed. The laser delivers only  $10^6$  to  $10^8$  W/m<sup>2</sup>, therefore lenses have to be used. Also the use of optical fibres (mostly of the step index type) has proven to be very beneficial to the application of lasers for spot welding. In figure 8 the laser, fibre and focusing head are shown schematically. With optical fibres the laser can be removed from the welding machine. The accessibility on the machine is thereby greatly enhanced. Further, one laser may now serve several welding sites on the same or different machines.

In laser spot welding, the boiling point is reached very early in the pulse. The heat diffuses very rapidly into the bulk under the influence of a very steep temperature gradient. The surface becomes warmer as the temperature gradient decreases until the boiling point is reached. Then vaporisation sets in and the temperature gradient (melt thickness) is kept constant from then onwards. Molten metal flows out of the hole (keyhole mode) from under the recoil pressure. At the end of the pulse the recoil pressure disappears and the molten metal that was stored at the periphery of the weld hole flows back in.

In the following section, some spot welding phenomena will be discussed. This will be the conduction of heat in the melt and surroundings, the plume and the absorption/reflection of the laser beam.

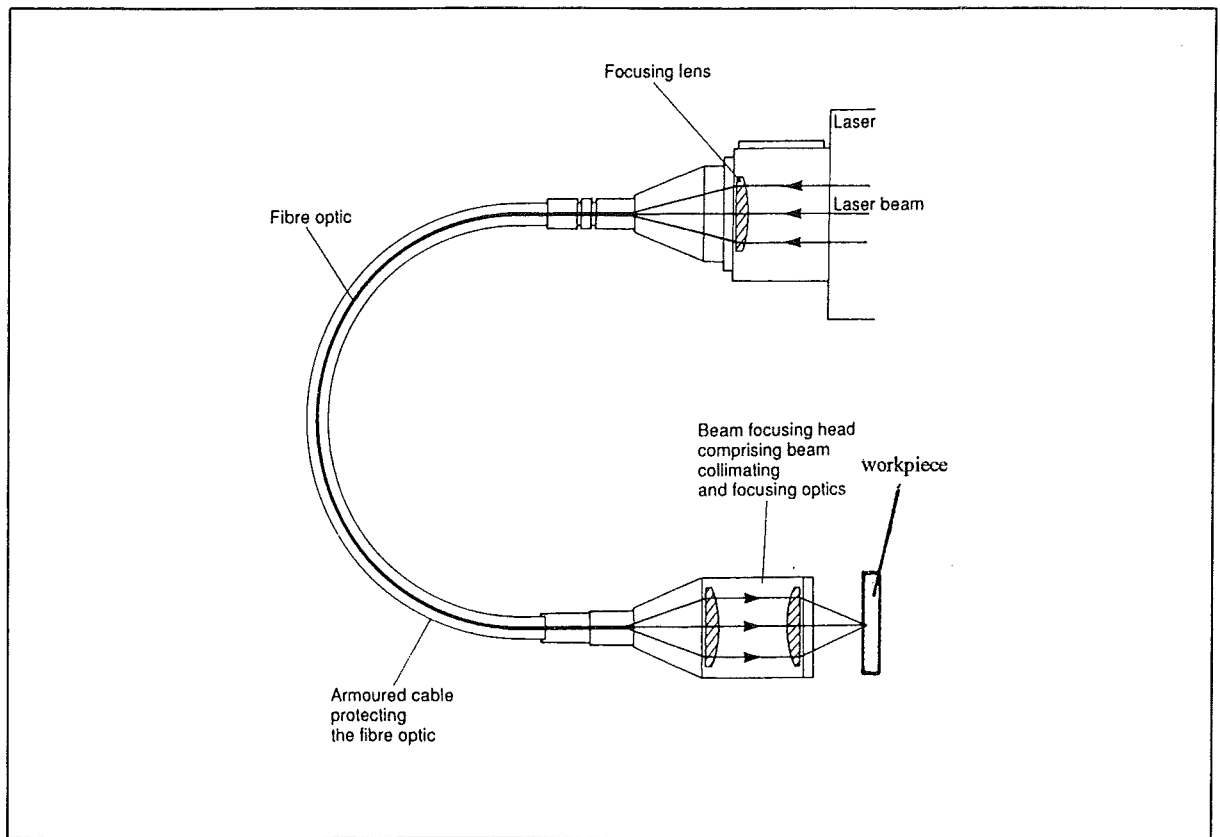


Figure 8: Schematic view of laser, fibre and workpiece [9].

Table 4: Energy that is needed to heat a mole of metal atoms or a cubic metre of a metal to its boiling point for some metals [10].

metal	$T_m$ (K)	$T_b$ (K)	$\Delta H_m$ (J/mole)* $10^3$	$\Delta H_{298-T_b}$ (J/mole)* $10^3$	$\Delta H_{298-T_b}$ (J/m <sup>3</sup> )* $10^9$
Al	933	2793	10.7	81.10	8.11
Cu	1356	2833	13.2	89.56	12.64
Fe	1809	3133	15.4	134.86	19.02
Sn	505	2898	7.20	88.26	5.43
W	3637	5828	35.3	176	18.48

In the following section, some spot welding phenomena will be discussed. This will be the conduction of heat in the melt and surroundings, the plume and the absorption/reflection of the laser beam.

### 3.3 Laser spot welding phenomena

#### *Heat conduction during laser spot welding*

The energy that is needed to heat a mole of metal atoms to its boiling point, assuming that  $T=298$  K is the room temperature, can be obtained from [10]:

$$\Delta H_{298-T_b} = (T_b - 298)C_p + \Delta H_m \quad (11)$$

in which:  $T_b$  = boiling temperature  
 $C_p$  = specific heat at constant pressure  $\approx 32 + 2$  J/mole for all metals  
 $\Delta H_m$  = enthalpy of fusion =  $T_m * \Delta S_m \approx 10 T_m$  J/mole for all metals  
 $T_m$  = melting temperature  
 $S_m$  = entropy of fusion

In table 4 the heat needed for melting a mole/cubic metre of some metals is given.

The theory of heat conduction does not contain general methods for the accurate solution of non-linear heat transfer problems. Researchers commonly resort to different approximate methods to search for the solution on the basis of analytical statements, numerical analysis, simulation modelling, statistical methods and other approaches. The simplest way of defining the temperature fields is to solve analytical expressions derived from linear differential heat conduction equations under linear boundary conditions. This means that the thermal coefficients are thought to be independent of temperature.

Consider a linear heat source that uniformly heats a thin plate across its thickness  $\delta$ . The temperature at point O is given by [12]:

$$T(r,t) = \frac{Q}{4\pi k\delta t} \exp\left(-r^2/4kt - \alpha't\right) \quad (12)$$

in which:  $Q$  = heat given by heat source  
 $k$  =  $K/c\rho$  = thermal diffusivity  
 $K$  = thermal conductivity  
 $c\rho$  = volume specific heat  
 $r^2$  =  $x^2 + y^2$  (square distance from heat source to a point (x,y))  
 $\alpha'$  =  $2\alpha/c\rho\delta$  = factor accounting for the surface heat transfer to the environment  
 $\alpha$  = heat transfer coefficient

Now, the temperature fields of the zones lying at a distance from the source that is 3 to 5 times the laser spot diameter  $d_s$  can be considered. The heat transfer in these zones depends on the characteristic of power density distribution over the cross section of the beam. Consider a simple case of a circular beam with its energy uniformly distributed over the hot spot of radius  $r_s$ . For surface treatment with short pulses of duration  $t_p < r_s^2/k$ , the heat transfer problem can be reduced to a uni-dimensional problem, with the main heat flux assumed to propagate along the Oz axis normal to the target surface.

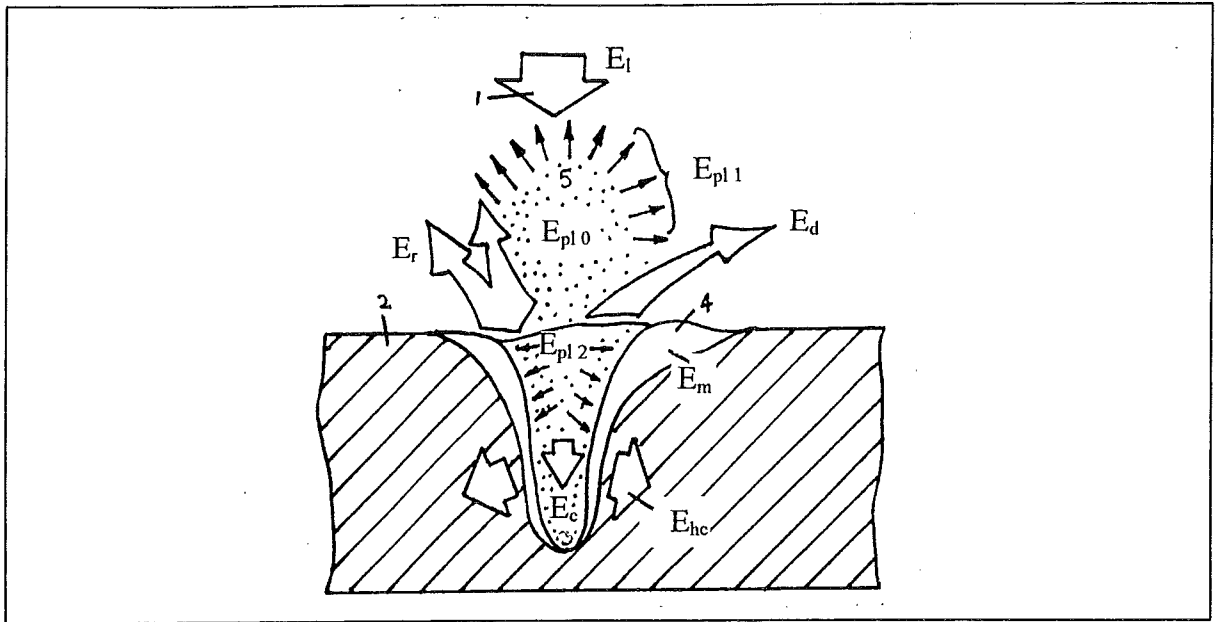


Figure 9: Laser energy distribution in steady conditions of metal melting [12].

(1) focused beam; (2) base metal; (3) keyhole (4) liquid metal; (5) plasma plume;

$E_l$  = laser energy of focused beam;

$E_{pl0}$  = energy of plasma-vapour plume;

$E_{pl1}$  = radiant energy emitted from the plume into the environment;

$E_{pl2}$  = fraction of plume energy absorbed by cavity walls through convection and radiant exchange;

$E_r$  = fraction of laser energy reflected from base metal and cavity bottom;

$E_d$  = energy of disintegration particles blown off by the vapour-gas jet;

$E_c$  = fraction of laser energy absorbed by cavity walls in the process of electron-photon collisions;

$E_m$  = energy of heat of the molten metal pool;

$E_{hc}$  = energy of heat delivered to the base metal by way of heat conduction.

Table 5: Complex refractive index and reflection coefficient of some metals at  $1\mu\text{m}$  irradiation [10]

material	$k_e$	$n$	R
Al	8.50	1.75	0.91
Cu	6.93	0.15	0.99
Fe	4.44	3.81	0.64
Sn	1.60	4.70	0.46
W	3.52	3.04	0.58

This is also the case for spot welding where  $0 < t < t_p$ . Then the uni-dimensional temperature field produced can be given by [12]:

$$T(z,t) = \frac{2q}{K} \sqrt{kt} \operatorname{ierfc}(z/2\sqrt{kt}) \quad (13)$$

in which:  $q = P_p/\pi r_s^2 =$  power density delivered to the hot spot of radius  $r_s$   
 $P_p = E_p/t_p =$  pulse power  
 $E_p =$  energy of the pulse of length  $t_p$

With this equation the surface temperature as well as the temperature profile in the bulk can be calculated.

Various similar analytical expressions are given [10,12] for as much different situations. However, the results obtained from the solution of these experiments sometimes poorly agree with experimental data because thermal properties actually vary with temperature. So, changes in the thermophysical properties of the material with fast heating and cooling should also be taken into account. Therefore so far only estimations of the actual temperature profile can be given.

#### *Laser plume*

During laser welding, including spot welding, a vapour plume is formed within and above the weld pool. This is shown in figure 9 where also the energy distribution in the steady conditions of the metal melting is given.

When the laser beam interacts with the metal surface, first the conduction electrons gain energy and collide with each other. Energy is transferred to the crystal lattice and with time the temperature in the lattice is above the melting temperature. The metal vaporises. This vapour is seen as a plume above the melt pool. Now the question is if this vapour is turned into a plasma when still under the influence of the laser energy. Various theories are given [9-12] on the subject whether the plume is or is not a plasma.

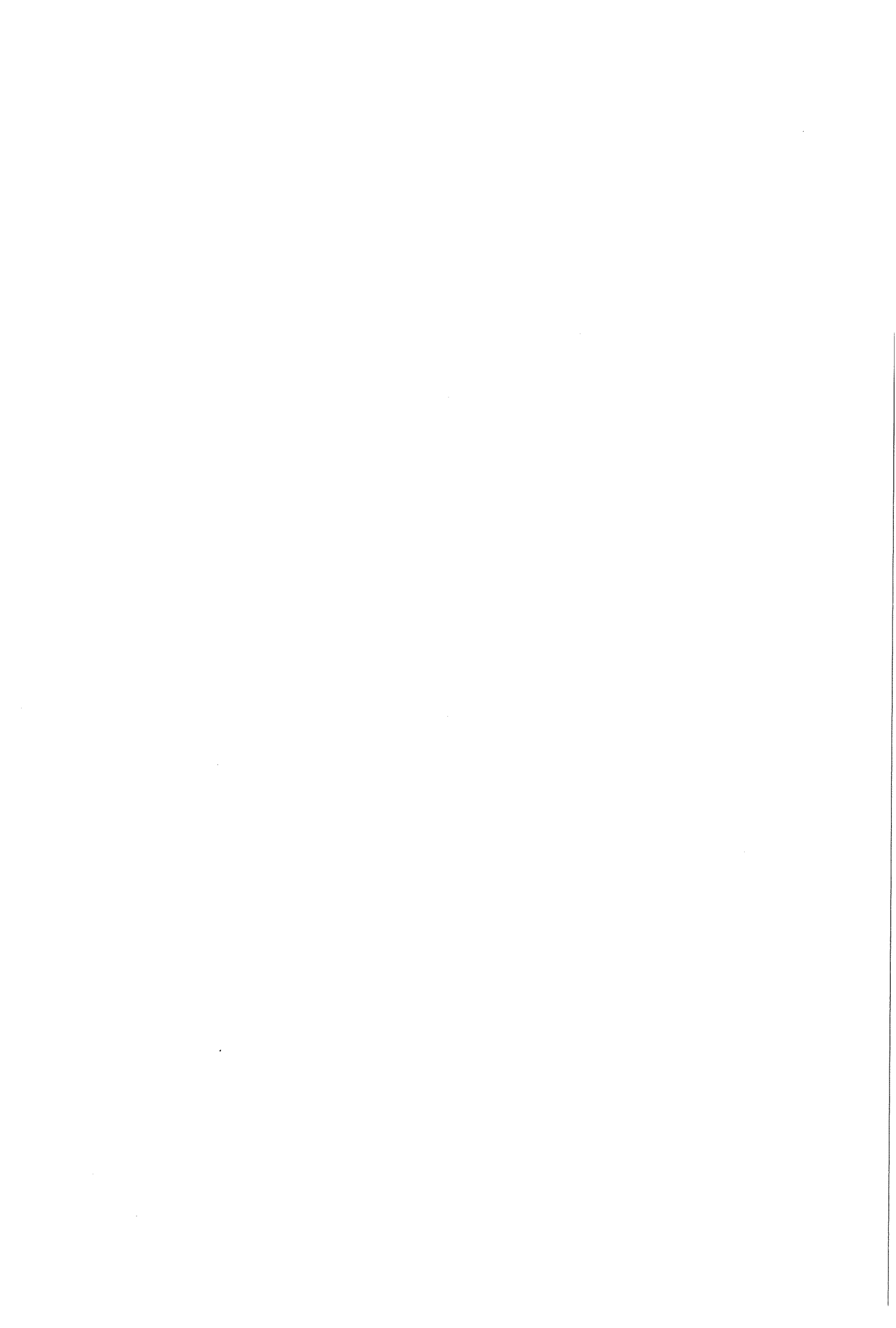
Certainly, part of the metal vapour will be ionised under influence of the lasers high energy. Considering the short pulse times used during (micro) spot welding there may not be time enough to fully ionise the vapour plume. It is for certain that the plume contains various neutral and electrically charged particles.

#### *Absorption/reflection*

The absorption and reflection of the laser energy at the material surface and in the laser plume play an important role in the energy transfer. The intensity with which a material reflects the laser radiation is defined by the material reflectivity that varies with the wave length of radiation.

The reflection coefficient from a metal surface in air ( $n=1$ ) may be calculated from the refractive index ( $n$ ) and the extinction coefficient ( $k_e$ ), in case of perpendicular angle of incidence, for room temperature ( $T = 298$  K) [10]:

$$R = \frac{(1-n)^2 + k_e^2}{(1+n)^2 + k_e^2} \quad (14)$$



In table 5 some reflectivity's are listed, calculated from data on the complex refractive index. From formula 14 it may be observed that large extinction coefficients (or large absorption coefficients) automatically lead to large reflections. The problem with metals does not lie in a low absorption coefficient but in a high reflection coefficient giving rise to a high reflection because of which the actual absorption is low.

It is generally accepted that the reflection of the metal surface remains high until the boiling point is reached. The metal vapour which is formed after the boiling point has been reached is also partially absorbing and hence capable of becoming hotter and forming a plasma. As a consequence, laser intensity can be lost in the plume by three absorption mechanisms:

- absorption in the metal vapour;
- absorption and scattering on the metal clusters;
- absorption and scattering at the plasma.

Under the circumstances prevailing in welding with a pulsed laser, absorption and scattering in the plasma that is formed above the melt may be neglected [10,12].

So in this case, spot welding with pulsed laser, there are no problems with "plasma" or the "plasma shielding effect" which may block a big part of the laser energy [10-13].

The use of a shielding gas is not only to protect the melt pool from the oxidising atmosphere, but according to A. Grigoryants [12] also enhances the absorptivity of the metal.

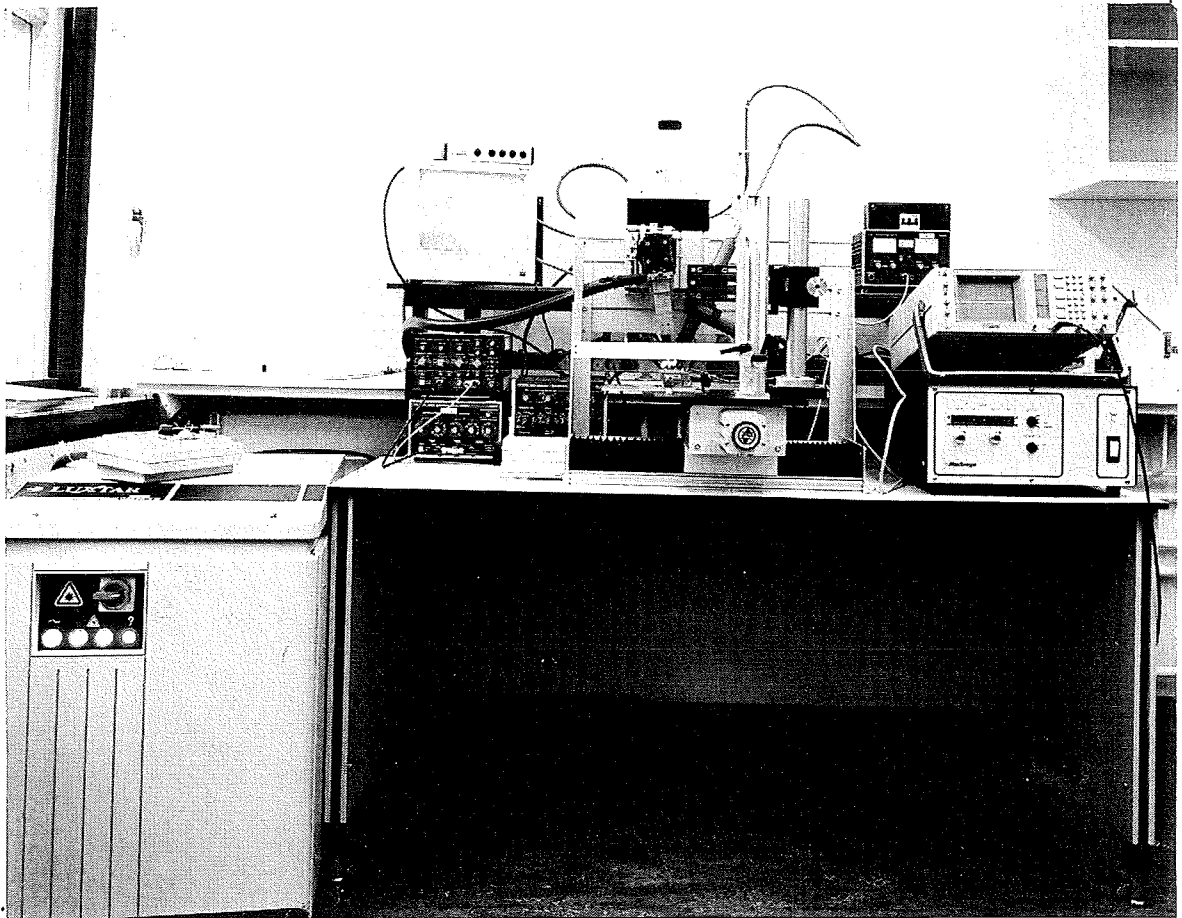
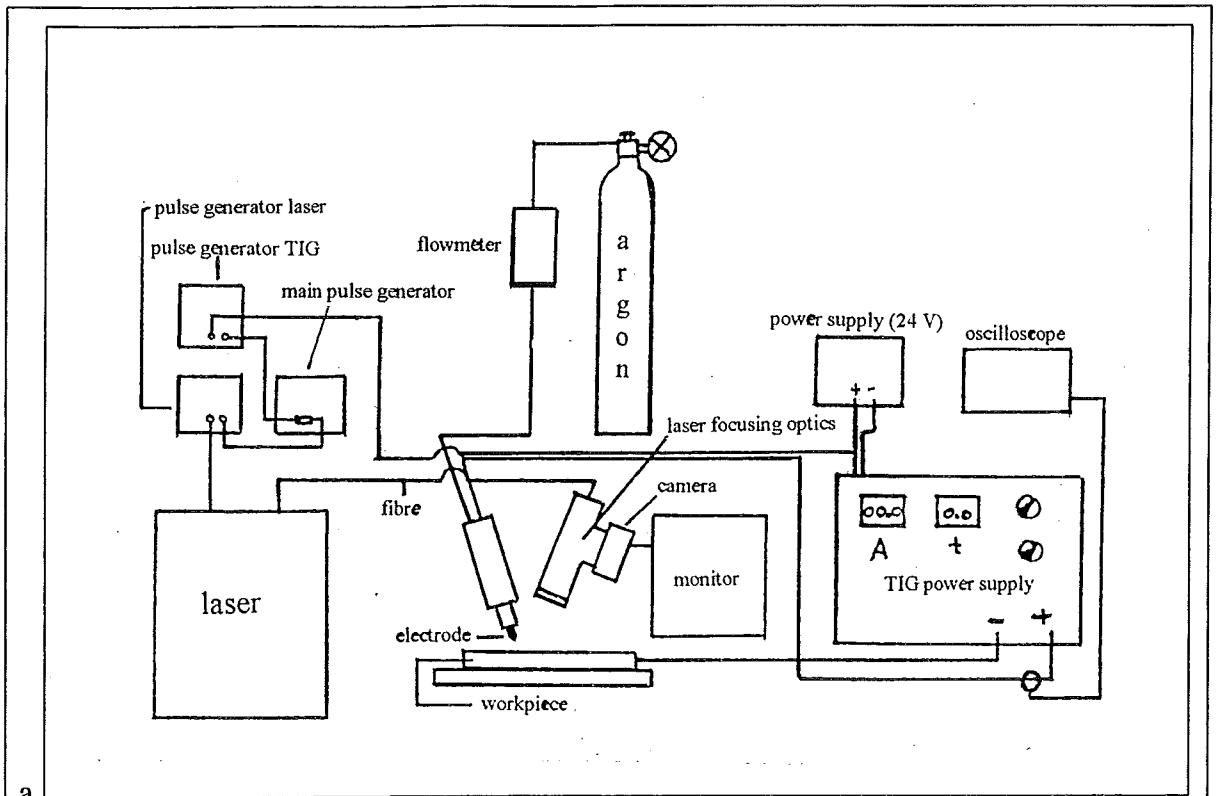


Figure 10: a. Schematic view of experimental set-up.  
 b. Photograph of actual experimental set-up.

## 4. EXPERIMENTAL CONDITIONS

This chapter deals with the experimental conditions. In § 4.1 the experimental set-up is discussed. Next, in § 4.2, the materials which are used in the experiments are briefly described, whereas § 4.3 focuses on the experimental procedure.

### 4.1 Experimental set-up

Figure 10a shows a schematic view of the experimental set-up, whereas figure 10b shows a photograph of the actual set-up.

The two most important parts in the set-up are the TIG welding system (①) and the laser (②). The power source of the arc welding system is specially designed (Mac Gregor) for short pulsed arc welding (maximum 9.9 ms). The rise time of the arc pulse is relatively short,  $\pm 50 \mu\text{s}$ , with an overshoot in the beginning of the pulse of around 10-20 A. Thus the requested stable arc current is reached very quickly within 0.5-1.0 ms. The used TIG electrode is a WS 2 Witstar special electrode of 1.6 mm diameter.

The used laser system is a Lumonics Nd:YAG laser for pulsed spot welding. The laser beam is transported through a step index fibre of  $\rho 600 \mu\text{m}$  to the workpiece. The outlet of the fibre is focused on the surface of the workpiece using optics. With the help of a CCD camera and a monitor the position of the welding spot can easily be seen. Figure 11 shows a schematic view of the laser focusing head. At the end of the optics a so called focusing lens is located. With this lens the magnification factor can be varied between 10:10, 10:7 and 10:5, depending on the focal length of the focusing lens, and in this way the spot size can be manipulated. As the wave length of the laser light is  $1.06 \mu\text{m}$ , the beam is not visible to the human eye. Thus the CCD helps in determining the position of the laser spot. Thus, the optics and camera are adjusted in such a way that the laser spot lies always in the focal plane of the laser and in the middle of the cross-hairs. This means that whenever the image on the monitor is sharp, the spot lies precisely in focus.

Figure 12 shows a detailed view of the configuration of the workpiece and the arc welding torch and laser headpiece. The workpiece is placed on a table which is in X-Y direction moveable. The TIG welding torch is mounted in a X-Y-Z manipulator. It is also possible to rotate the torch around the normal.

In the following experiments both the TIG welding torch and the laser optics are placed at a fixed inclination angle, while the workpiece is being moved.

The shielding gas which is used during these experiments is argon (99.99 % purity). The gas flow is controlled by a mass flow-meter.

In order to manipulate the starting pulses of the laser and of the arc separately, three pulse generators are being used. One main pulse (starting pulse) gives the trigger signals to the two other pulse generators which trigger the laser pulse and the arc pulse. The pulse generators are adjusted in such a way that after the main pulse the laser is being triggered at first and after a delay (several milliseconds) the arc. The delay between the two trigger pulses can be adjusted.

### 4.2 Materials

Most tests are performed on Cr/Ni-steel (N 286) plates. The size of these plates is 35 x 30 x 0.25 mm. This type of material is primarily used because it is applied very often as construc-

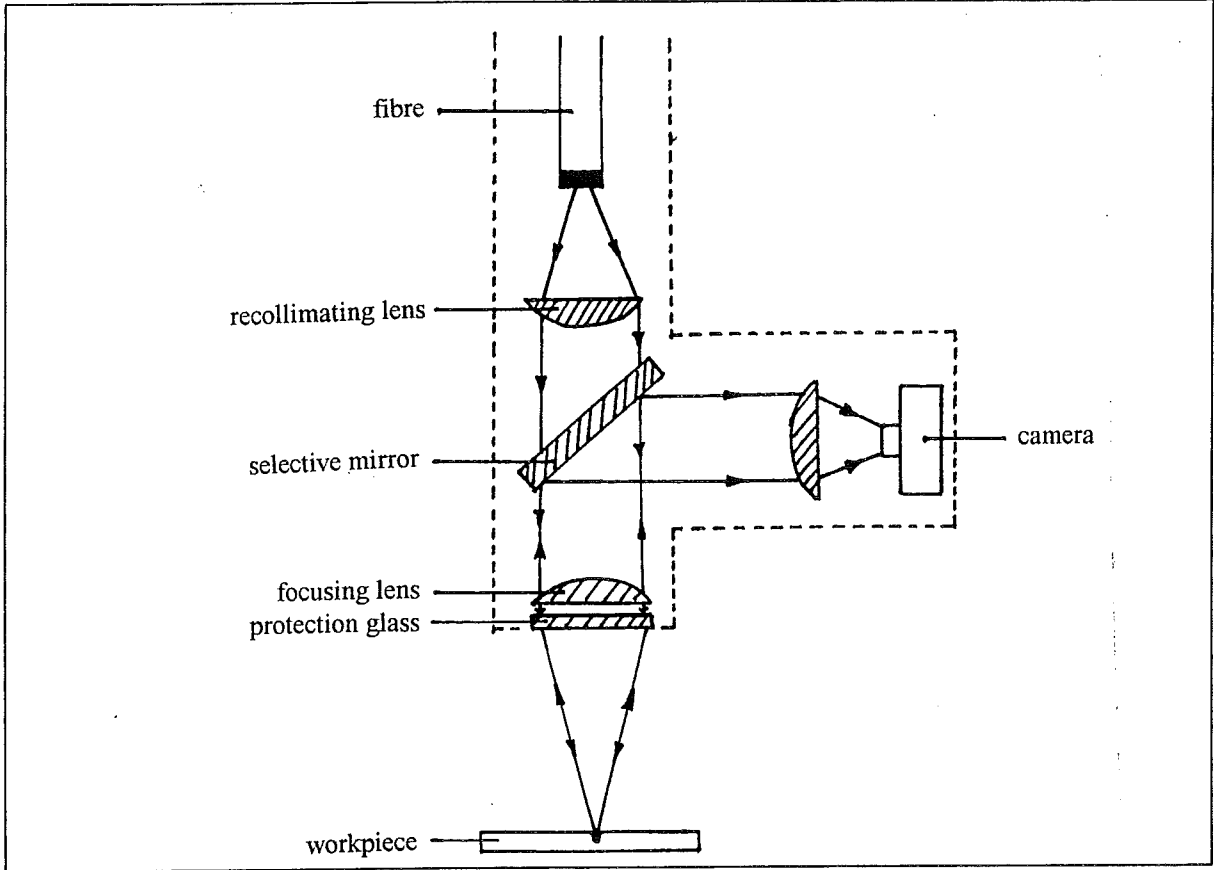


Figure 11: Schematic view of laser head.

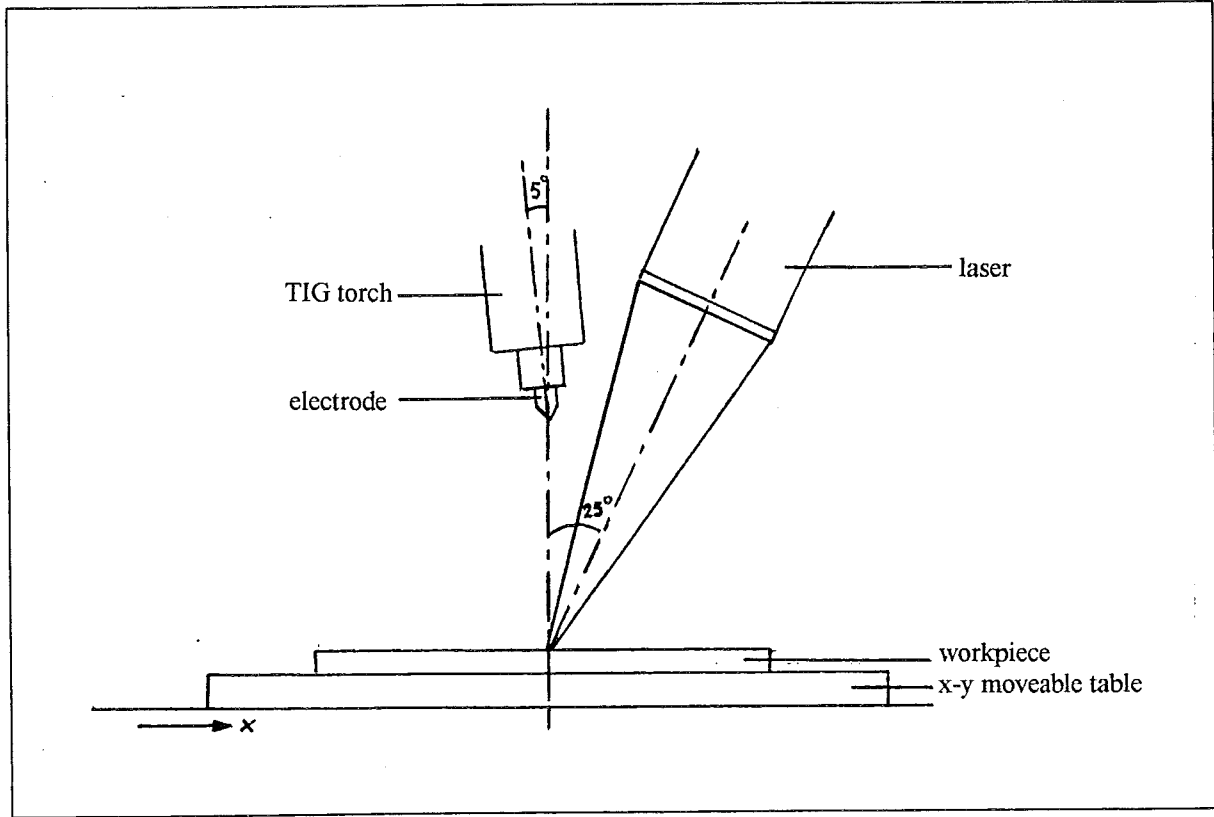


Figure 12: Detailed view of configuration of TIG torch, laser head and workpiece (front view).

Table 6: Composition of Cr/Ni steel plates (N 286). Iron with:

element	%	analysis
Cr	17	min
Cr	19	max
Ni	11	min
Ni	13	max
C	0.1	max
Mn	2	max
P	0.03	max
S	0.01	max
Si	1	max

Table 7: Composition of phosphor bronze plates (R 1178). Copper with:

element	%	analysis
Sn	5.5	min
Sn	7.5	max
P	0.01	min
P	0.4	max
Fe	0.1	max
Pb	0.05	max
Ni	0.3	max
Zn	0.3	max

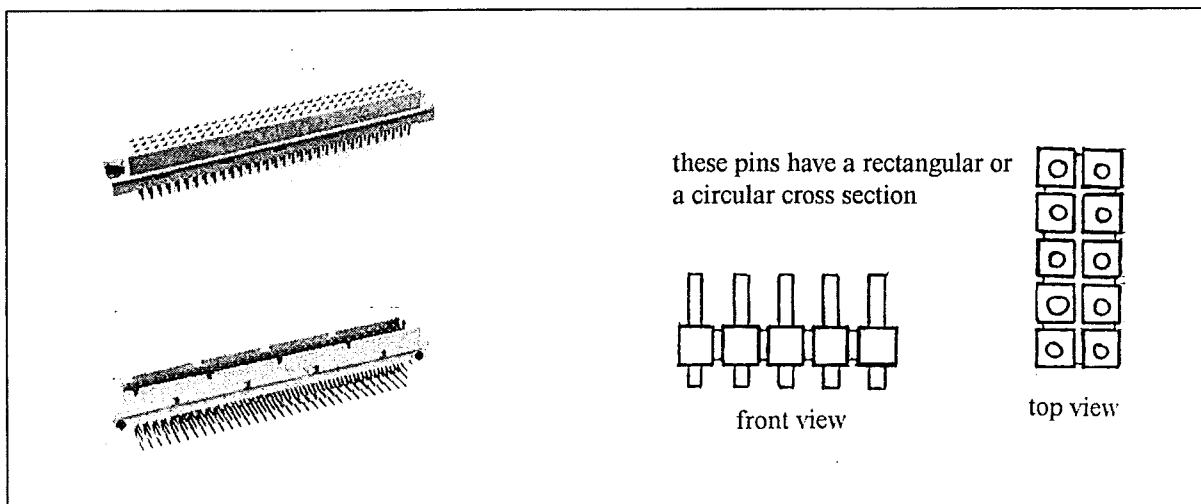


Figure 13: Electrical components with pins.

Table 8: Composition of phosphor bronze pins (R 1179). Copper with:

element	%	analysis
Sn	7.5	min
Sn	9.0	max
P	0.01	min
P	0.4	max
Fe	0.1	max
Pb	0.05	max
Ni	0.3	max
Zn	0.3	max

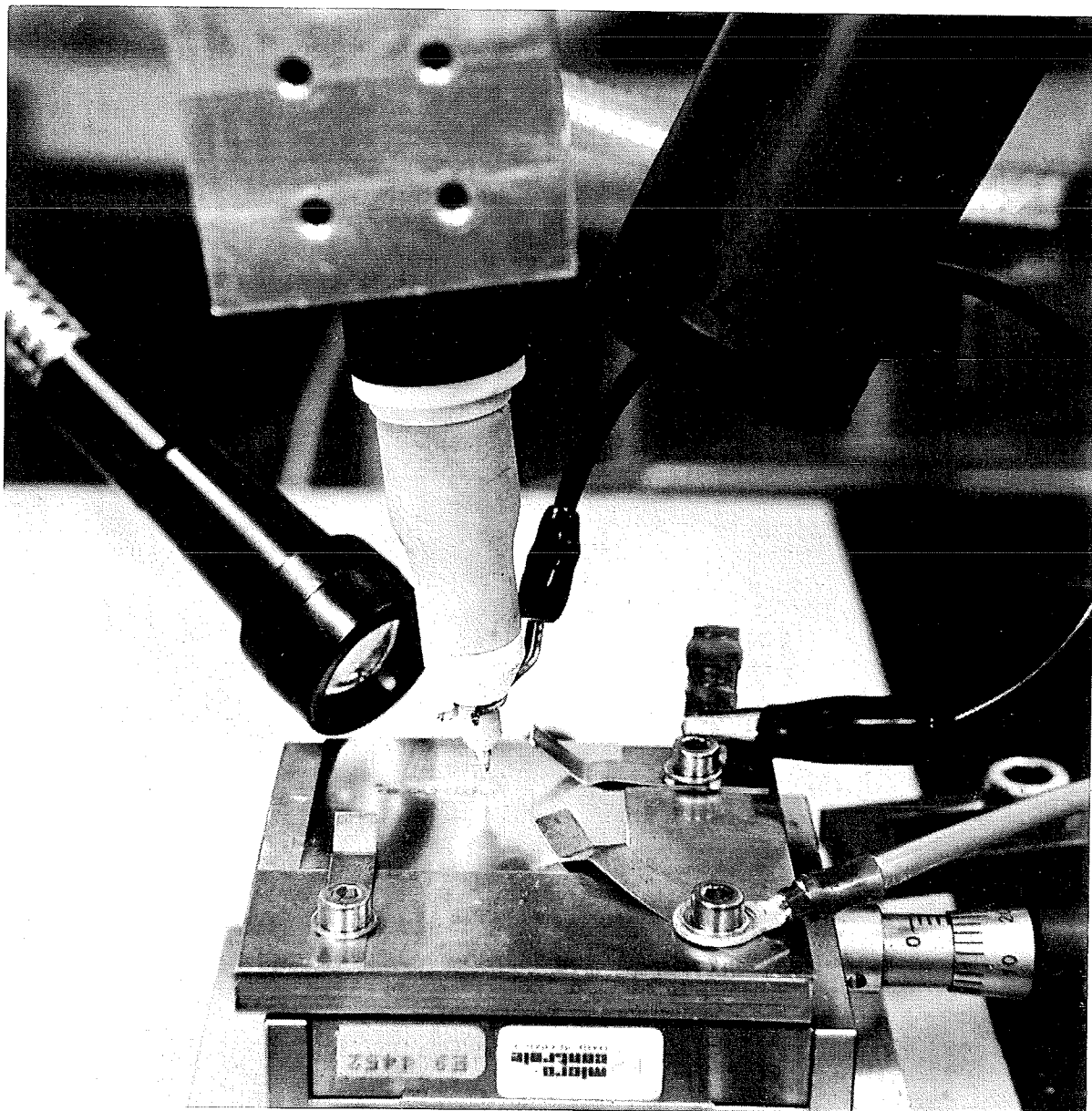


Figure 14: Detailed photograph of welding set-up.

tion material in Philips products. It can easily be spot welded with the laser (reflection is low), whereas also arc welding is possible. The composition of these plates is given in table 6. Experiments were also carried out with phosphor bronze (R 1178) plates. The composition of these plates is given in table 7. The size of these plates is 40 x 30 x 0.3 mm. The reason for testing these type of plates is that the application of the combined welding process (if successful) will probably be on phosphor bronze pins, which are part of electrical components (connectors). These components are shown in figure 13. There are two types of shape and two types of protective layer. The pins consist of phosphor bronze (R 1179) with either a gold or tin layer. In order to obtain contact with the phosphor bronze at the top of the pins, they will be grinded. The composition of the phosphor bronze in the pins is given in table 8. Before the spot welds were made on the plates and pins the surfaces were cleaned with alcohol.

### 4.3 Experimental procedure

As mentioned earlier, a literature search [1] on laser/arc interaction has been carried out. This search yielded several influencing parameters, the most important being:

- arc current
- laser power
- material type
- arc length
- travel speed

The investigation which will be dealt with in this report concerns the possibility of positioning the arc with help of the laser. Most attention will be given to pulsed TIG welding combined with a pulsed laser.

#### 4.3.1 Initial tests

First, some initial tests were conducted in order to check if the arc is attracted to the laser spot. The investigations which are discussed in the literature search [1] are all based on continuous welding with relatively high (mostly around 100 A) arc currents and with a laser power varying from 100 W to 4 kW.

The arc welds produced in the present work are spot welds made by pulsed TIG welding with a pulse duration of several milliseconds.

The inclination angles of the laser and TIG electrode in the experiments are 25° and 5° respectively. When using a standard gas cup for the TIG electrode, the inclination angle of the laser has to be at least 50°, otherwise the laser beam will partially hit the gas cup. Therefore a gas cup with an extended ceramic tube is used, see figure 14.

Having completed these initial tests, the following parameters appeared to be of the utmost importance, see also figures 15 and 16:

- horizontal distance between electrode and centre of laser spot (critical distance  $l_c$ )
- arc length ( $l_a$ )
- arc current ( $a$ )
- pulse duration TIG pulse ( $t_1$ )
- pulse duration laser pulse ( $t_2$ )
- laser pulse power ( $b$ )

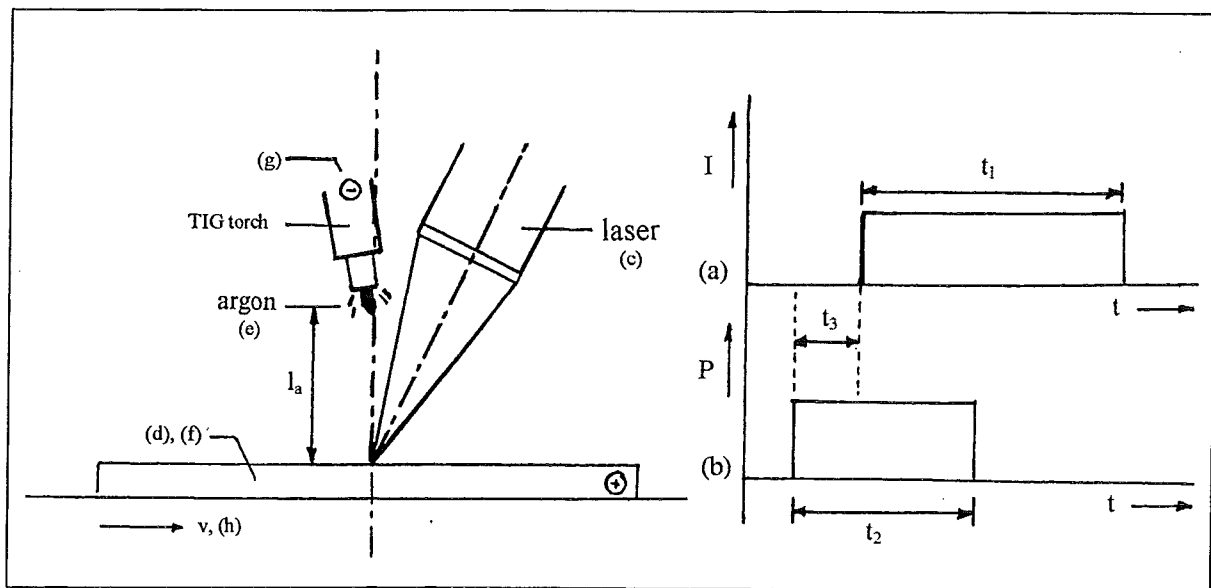


Figure 15: Overview of influencing parameters.

Table 9: Overview of experimental procedure.

STANDARD CONDITIONS		VARIATIONS
<b>LASER</b>		
power	500 W	100/200/300/750 W
pulse duration	3 ms	1/2/5 ms
intensity (spot size)	420 $\mu\text{m}$	300/600 $\mu\text{m}$
<b>ARC</b>		
current	20 A	25/30/40/50 A
arc length	2 mm	0.5/.../4.5 mm
pulse duration	4 ms	1/2/3/5/6/7/8/9/9.9 ms
delay	1 ms	0/0.2/0.4/0.6/0.8/1.0/2.0 ms
geometry	plate	pin
shielding	air	argon

- laser intensity (c)
- type of material (d)
- delay between triggering laser pulse and triggering TIG pulse ( $t_3$ )
- welding environment (e) (air or argon)
- workpiece geometry (f)
- polarity of TIG electrode (g)
- travel speed (h)

Knowing which parameters determine the attraction, their influence can be analysed more thoroughly. Unfortunately, it is not possible to investigate the influence of the travel speed, because the arc discharge strongly interferes with the Isel x-y-z software of the power unit.

#### 4.3.2 Standard

For examining the influences of the before mentioned parameters, a standard needs to be determined at first. This is done as follows.

A standard is made on thin rectangular steel plates (Cr/Ni-steel, N 286), under “standard conditions”. These standard conditions are listed in table 9. The welding environment in which these tests are conducted is air. Argon, which is normally used as shielding gas during TIG welding, is also taken as an influencing parameter, because the initial tests revealed that specific changes occur when argon is used instead of air (i.g. higher arc lengths, “double spots”).

Under standard conditions the TIG electrode is the cathode and the workpiece is the anode. Furthermore, the value of the arc pulse current is 20 A with 4 ms pulse duration. The laser parameters are 0.5 kW pulse power, a pulse duration of 3 ms and a spot size of  $\pm 420 \mu\text{m}$ . The delay between the trigger pulses is 1 ms.

The attraction is being determined by increasing the distance between the electrode tip and the centre of the laser spot while keeping the other parameters constant. From these data the critical distance  $l_c$ , which is the maximum distance where there is still successful attraction, can be determined, see figure 16. First, a laser spot weld alone and a TIG spot weld alone are made, see figure 17, in order to have a reference (to determine if attraction has occurred when the combined spot welds are made). Then the combined spot welds are made, 5 per varied parameter, to obtain reliable results. When the standard is completed, the influence of the other parameters relative to this standard can be examined systematically (influence on  $l_c$ ).

#### 4.3.3 Variations

In table 9 the variations which will be used to examine the parameter influences on the attraction are given. Only one parameter will be varied at a time, while the values of all other parameters are kept constant. The experimental program includes the measurement of the influence of the following parameters:

- polarity of the electrode;
- arc length; the variations will be 0.5 to 4.5 mm according to occurrence of attraction;
- arc current;  
the variations in arc current will be 25-30-40-50 A;
- pulse duration of TIG pulse;

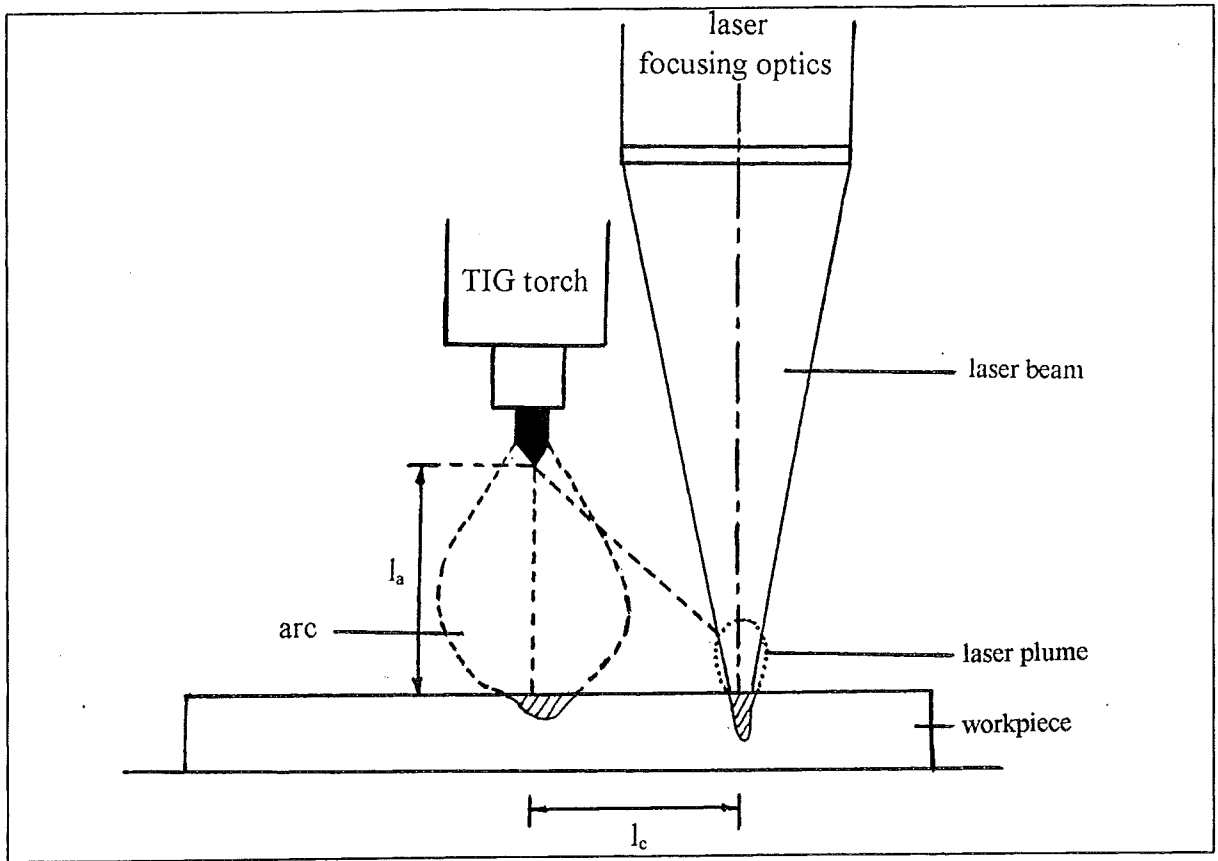


Figure 16: Schematic view of laser plume and electrode.  
 $l_a$  = arc length;  $l_c$  = critical distance

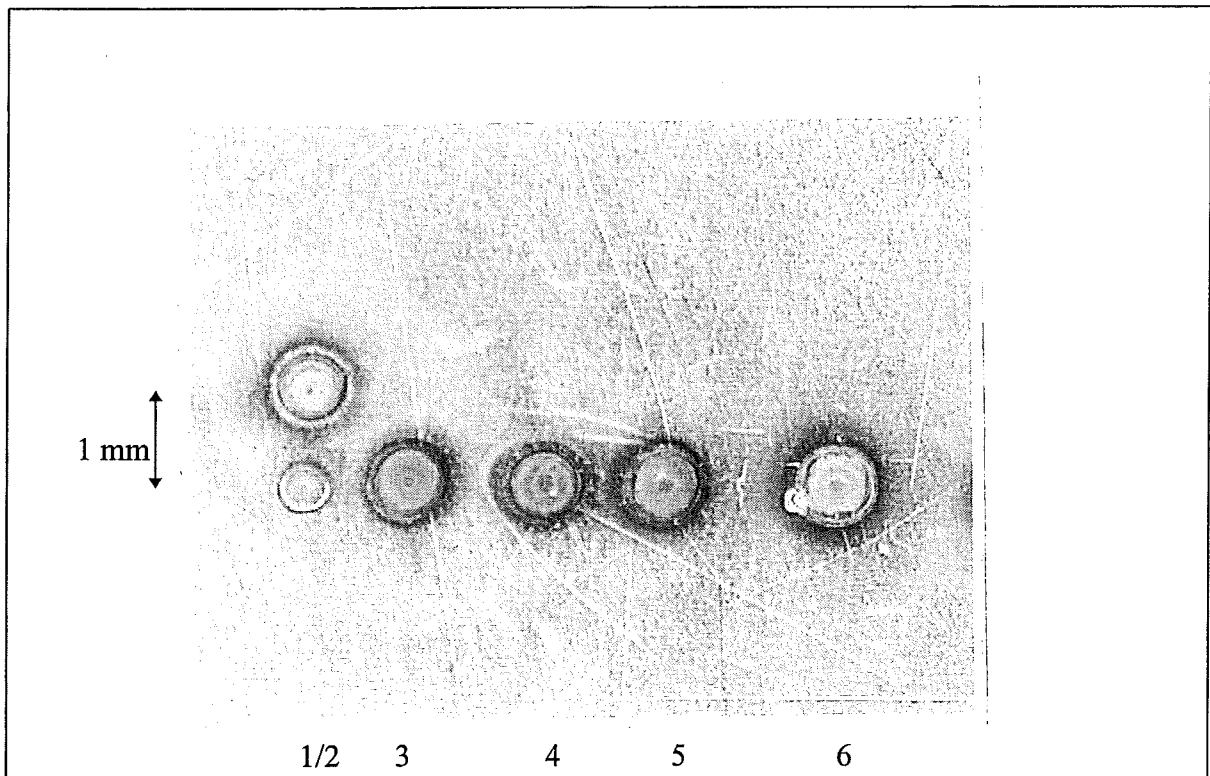


Figure 17: Example of experimental sequence for one series of tests (standard conditions,  $l_c=1.0$  mm). Spot 1 and 2 are the spots obtained by resp. arc alone and laser alone. Spots 3 to 6 are obtained by combined pulsing, 4 times after each other under the exact same conditions.

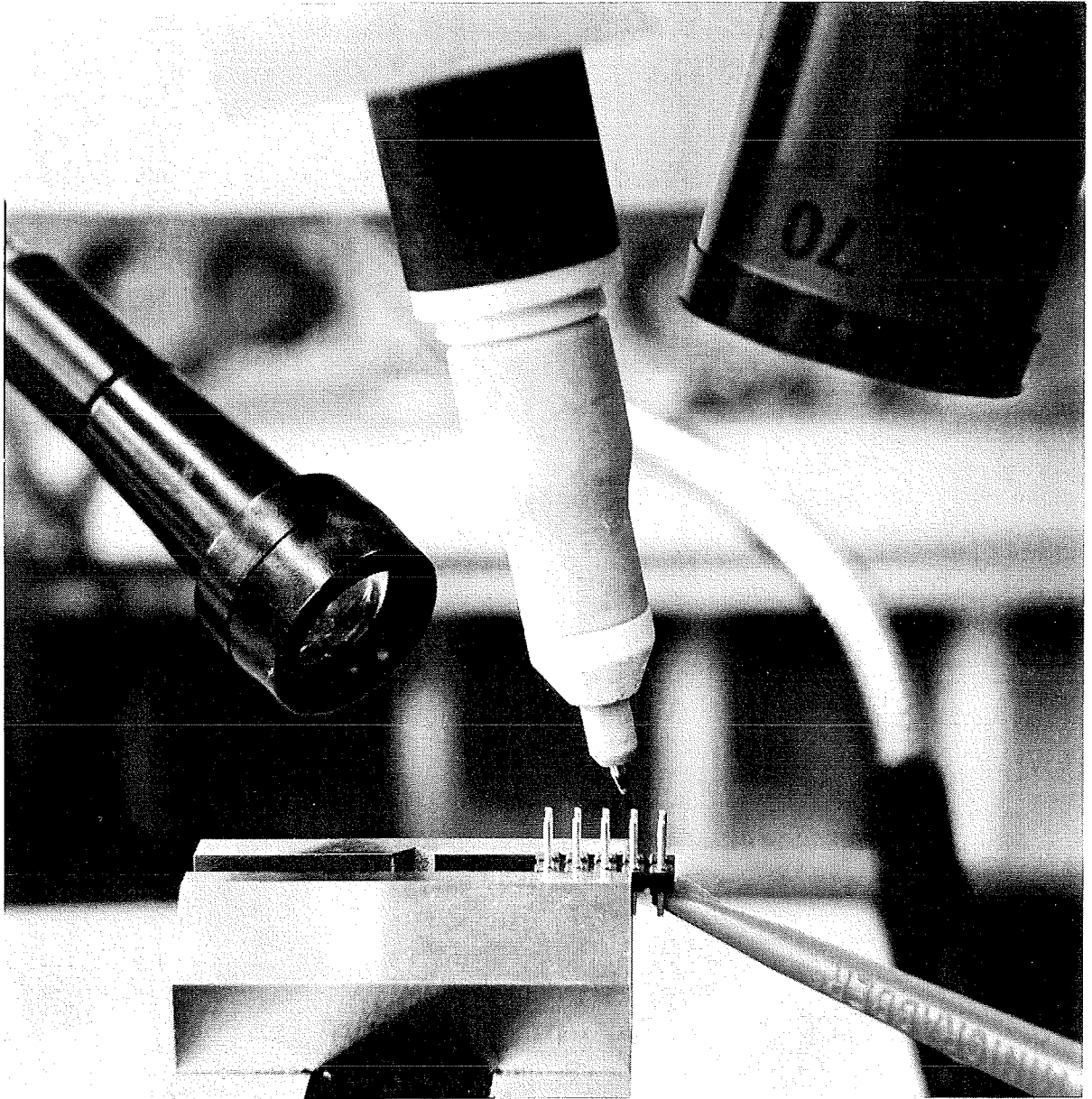


Figure 18: Actual set-up for experiments on phosphor bronze pins.

- the variations in pulse duration will be 1-2-3-5-6-7-8-9-9.9 ms;
- laser power;
  - the variations in laser power will be 100-200-300-750 W;
- pulse duration of laser pulse;
  - the variations will be 1-2-5 ms;
- delay between starts of laser and TIG pulse;
  - the variations are 0-1-2 ms and step-like with steps of 0.2 ms from 0 ms to 1.0 ms;
- shielding gas (argon);
  - flow: 1 l/min.

As mentioned before, TIG welding is normally performed in argon. Because the initial tests showed changes in the attraction behaviour when argon is used (as compared to attraction in air) the parameters which are examined in air are also examined in argon. Thus a standard in argon will be made, similar to the one in air. This standard not only gives information of the influence of argon (as a parameter variation which will be compared to the standard in air), but it also functions as the standard for the parameter influences examined in argon. The parameter influences in argon will not be examined as thoroughly as in air. Only a rough idea of their individual influence will be acquired.

Another parameter that needs to be considered is the type of material. In this study only two types of material are examined, which are Cr/Ni-steel (N 286) and phosphor bronze (R 1178/1179). Most of the tests will be conducted on the Cr/Ni-steel.

For determining the influence of the geometry of the workpiece, tests are performed on small gold plated and tin plated phosphor bronze pins. The gold and tin surface layers of the pins are removed so that the underlying phosphor bronze comes in direct contact with the surrounding surface. In figure 18 the actual set-up of the laser optics, the TIG torch and the pins is given.

As was mentioned earlier (§ 4.1), the spot size of the laser can be manipulated with the focusing lens (magnification factors). By replacing the focusing lens used during the standard ( $f = 70$  mm) by a focusing lens with focal length of  $f = 50$  mm the laser spot size changes from around  $420 \mu\text{m}$  to around  $300 \mu\text{m}$ . If the laser energy is the same as it was in the standard situation, this means that the same amount of energy is focused on a smaller area, which means that the intensity is changed. In this way the influence of the laser intensity on the attraction behaviour of the arc can be determined.

Finally a totally different kind of test was carried out. Its purpose was to investigate if it is possible to ignite the arc with help of/by means of the laser. The results are mentioned in appendix A.

Table 10: Results of defining the standard.

l (mm)	arc length ( $l_a=2$ mm)
0.5	++
1.0	++
1.5	++-
2.0	+-
2.5	+-

Table 11: Results of  $l_a$  influence on the attraction.

l (mm)	arc length (mm)							
	0.5	1.0	1.5	2.0	2.5	3.0	3.5	4.0
0.5	++	++	++	++	++	++	++	+-
1.0	--	+-	++	++	++	++	++	+-
1.5	--	--	++-	++-	++	++	++	--
2.0	--	--	+-	+-	+-	+-	+-	--
2.5	--	--	--	--	+-	+-	--	--

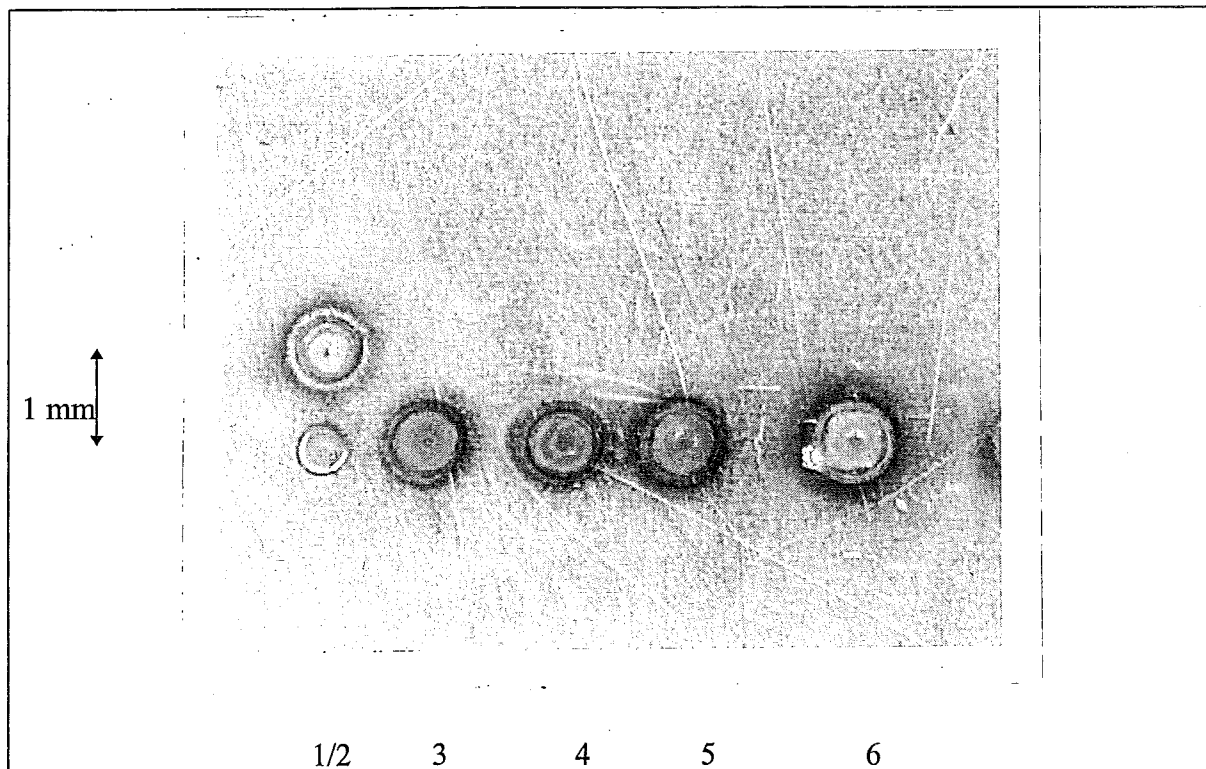


Figure 19: Example of experimental series with successful attraction. Conditions: arc: 20 A/4 ms; laser: 0.5 kW/3 ms;  $I_L = 420$   $\mu$ m; air; delay = 1 ms;  $l_c = 1.0$  ms;  $l_a = 2.0$  ms.

## 5. RESULTS & DISCUSSION

This chapter presents the results of the experiments. In § 5.1 the influence of the main welding parameters on the attraction of the arc to the laser spot will be discussed for the experiments on the plates. The results for the phosphor bronze pins is discussed in § 5.2. The combination process was also filmed with a high speed video camera. The pictures made from this film spread some light on what seemed at first to be unexplainable results. This is discussed in § 5.3. Finally, in § 5.4, modelling of the results will be presented and discussed.

### 5.1 Influencing parameters on the attraction of the arc for plates.

#### 5.1.1 Standard

As was mentioned in § 4.3, a standard was made at first. The standard conditions used during welding are given in table 9. The configuration of the laser headpiece, the TIG torch and the plates is given in figure 12. The results are given in table 10. In this table the attraction behaviour is presented as follows:

- ++ means that of five combined spot welds made under the same conditions, all pulses give successful attraction
- -- means there is no attraction at all
- +- means that half of the five combined spot welds made under the same conditions give successful attraction (two or three times)
- +-- means attraction only occurs one time
- +-+ means only one time there is no attraction

As can be seen, there is no attraction when the arc length exceeds 2.0 mm. In the following the results of the experiments which were mentioned in § 4.3 will be discussed.

#### 5.1.2 Influence of arc length

In figure 19 an example of one series (five combined spot welds made under the same conditions) is given. Spot 1 and 2 are the spots made with the laser alone and the TIG arc alone. Spots 3 to 6 are made with TIG arc and laser combined, according to the standard conditions, with an arc length of 2.0 mm and a critical distance of 1.0 mm. Spot 1 and 2 are made in order to be able to determine the positions of both spots when they are operated separately, which makes it possible to see if attraction has occurred. If they are operated at the same time, there are no longer two separate spots visible in case of successful attraction. The TIG spot is located on the exact position of the laser spot.

When several TIG spots alone would be made right after each other, they would not lie on a straight line. As can be seen in figure 19 the combined spots all lie on the same straight line. In figure 20 examples of unsuccessful attraction next to successful ones are shown.

In table 11 the results of varying  $l_a$  are given. The results are obtained by taking a fixed  $l_a$  and then varying the distance  $l$ . For example, first the arc length is 0.5 mm and  $l$  is being varied between 0.5 and 2.5 mm and the attraction is thus being determined.

As can be seen, there is (almost) no attraction when the arc length exceeds 3.5 mm. This is caused by the impossibility of creating an arc at that distance. When the distance  $l$  is exceeding the 1.5 mm the attraction decreases and from 2.0 mm, there is no attraction at all. When

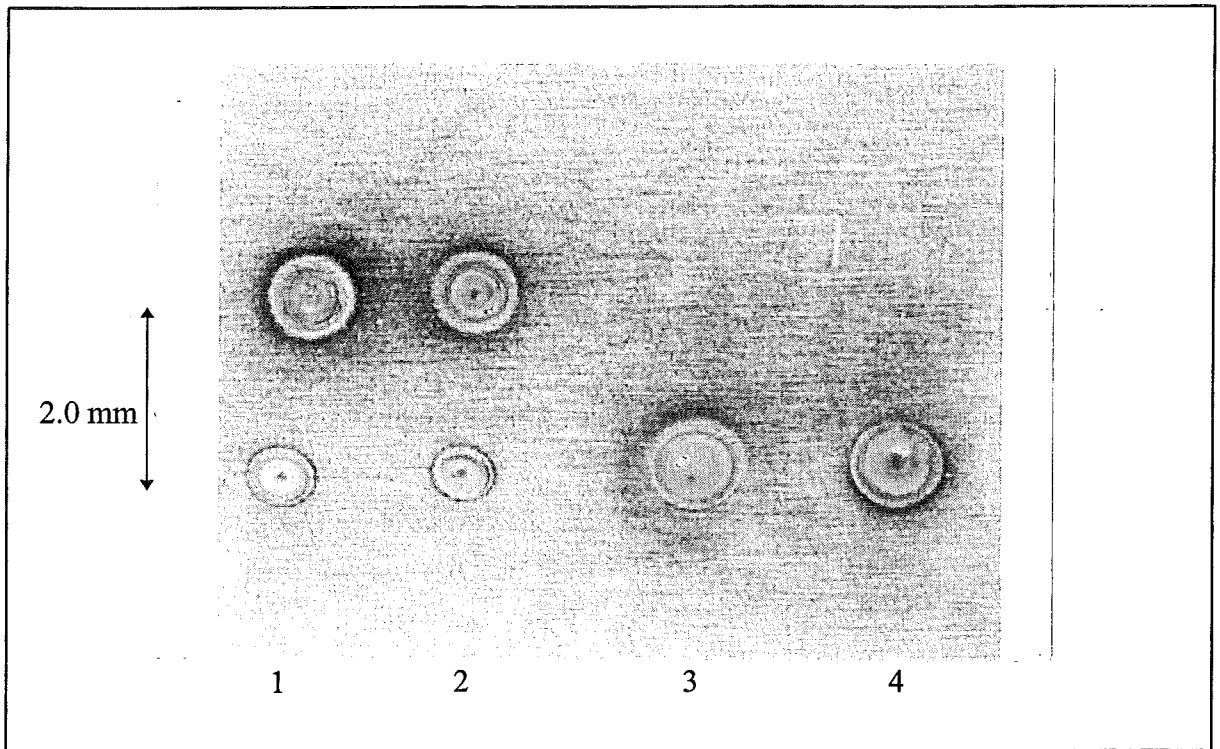


Figure 20: Example of experimental series with unsuccessful and successful attraction. Conditions: arc: 20 A/4 ms; laser: 0.5 kW/3 ms;  $I_L = 420 \mu\text{m}$ ; delay = 1ms; spot 1&2:  $l_c = 2.0 \text{ mm}$ ;  $l_a = 1.5 \text{ mm}$ ; spot 3&4:  $l_c = 1.0 \text{ mm}$ ;  $l_a = 2.0 \text{ mm}$ .

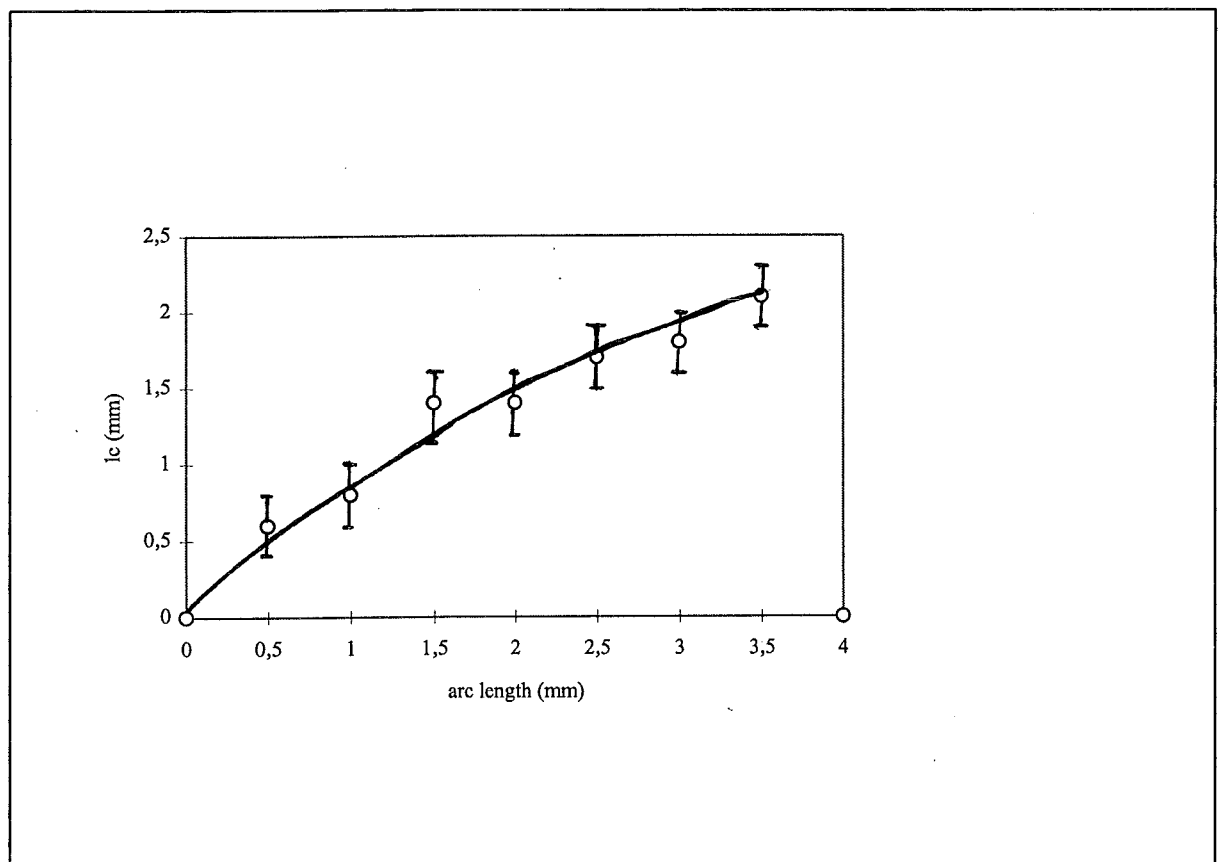


Figure 21: Critical distance as function of arc length.  
Conditions: arc: 20 A/4 ms; laser: 0.5 kW/3 ms; air;  $I_L = 420 \mu\text{m}$ ; delay = 1 ms.

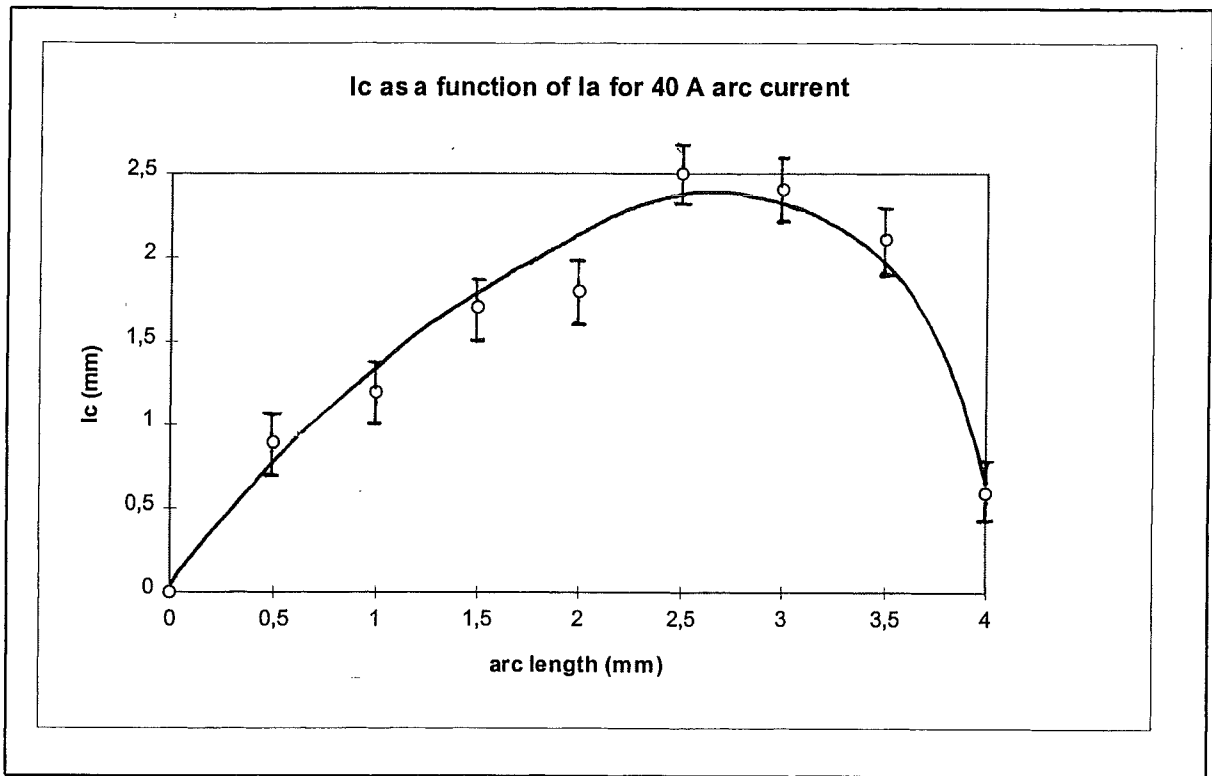


Figure 22: Critical distance as function of arc length for an arc current of 40 A.

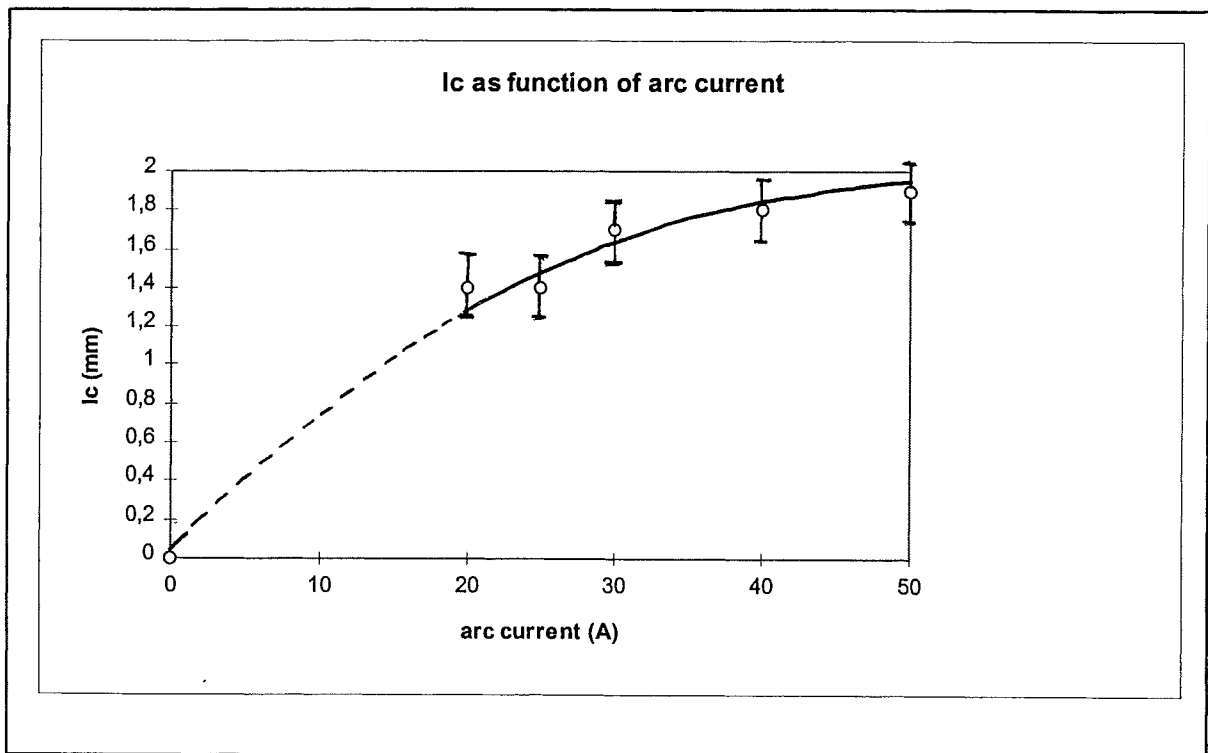


Figure 23: Critical distance as function of arc current. Conditions: arc = 4 ms; laser = 0.5 kW/3 ms; delay = 1 ms;  $I_L = 420 \mu\text{m}$ ;  $l_a = 2.0 \text{ mm}$ .

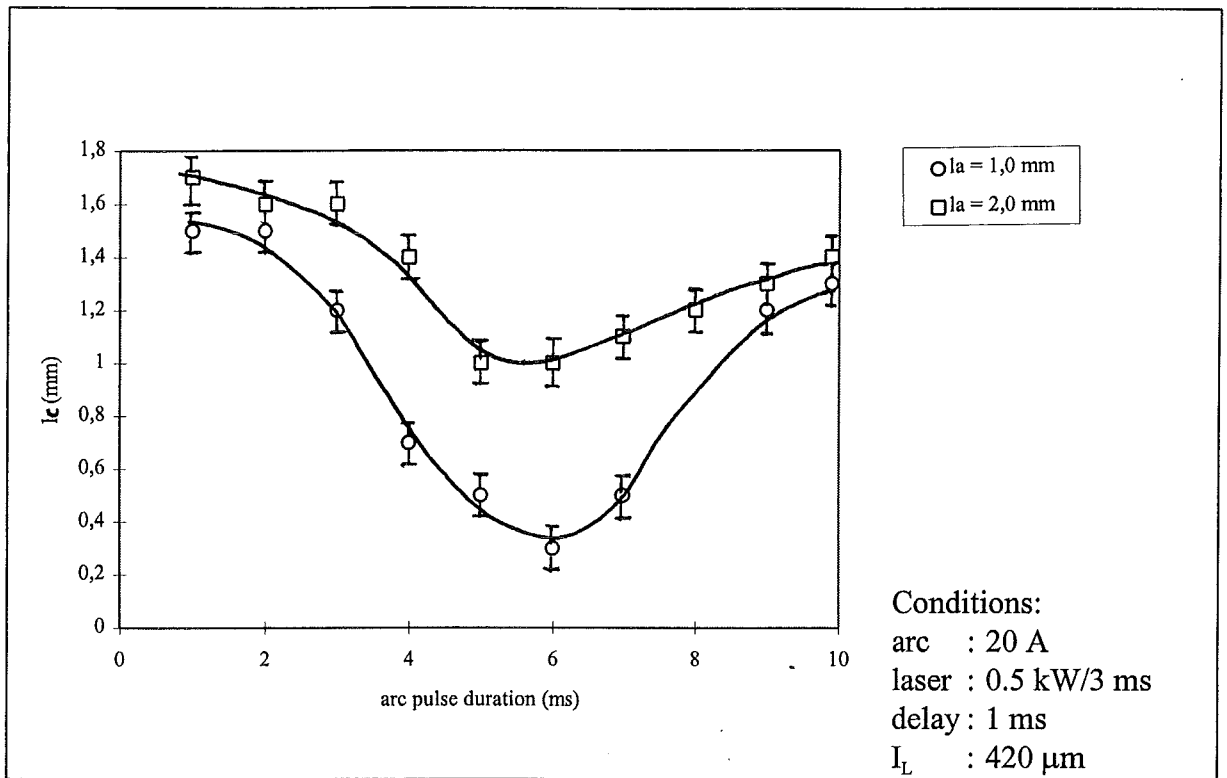


Figure 24: Critical distance as function of TIG pulse duration.

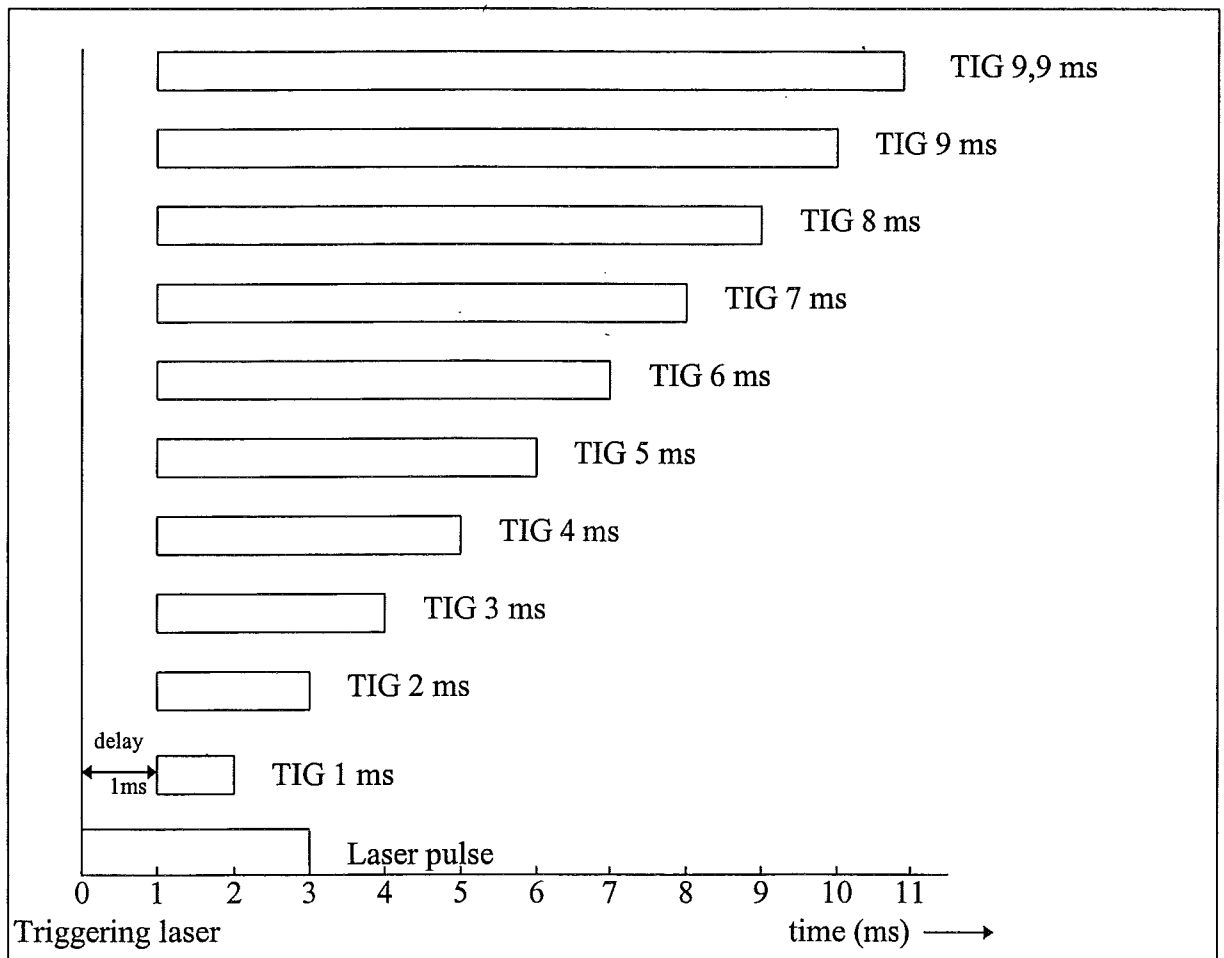


Figure 25: Position of TIG pulse (in time) with respect to laser pulse.

the distance  $l$  also exceeds the arc length there will be no attraction either. In figure 21 the influence of the arc length on the critical distance is given in graphical form. The figure shows that with increasing arc length the critical distance also increases, but after exceeding the 3.5 mm arc length  $l_c$  decreases.

### 5.1.3 Influence of polarity.

In order to examine the influence of electrode polarity, experiments were also carried out with the electrode positive.

Under these conditions several difficulties were encountered. First, there is no sign of any attraction whatsoever. With an arc length of 3.0 mm and lower it was difficult to get the arc started when the laser was turned on as well.

In comparison to the spots made with the electrode negative, the spots made with electrode positive are very irregular and the surface of the spots and their surrounding area are strongly oxidised.

When both laser and TIG arc are operated, the laser has a negative influence on the arc formation. For instance, if the arc length was 3.0 mm and the TIG arc alone is triggered, an arc is formed and a spot is made. But when the laser is triggered together with the TIG arc only a spark is formed instead of an arc. This indicates that the mechanism at the cathode is being negatively influenced by the laser plume.

In view of this it was decided not to look further into this switching influence.

### 5.1.4 Influence of the arc current

In table 1, appendix A, the results of changing the arc current are given. Increasing arc current improves the attraction for the higher arc lengths (3.5-4.0 mm) and this effect can also be seen in the smaller arc length regions (1.0-2.0 mm). The trend that was seen in figure 21, increasing critical distance with increasing arc length, is also seen when different currents are used. This is shown in figure 22, for an arc current of 40 A.

For the standard arc length of 2.0 mm the increase in possible  $l_c$  with increasing arc current is shown in figure 23.

The increasing arc current not only stabilises the arc which results in increasing arc lengths, but the arc also becomes wider. Therefore part of the arc could just yet come within the lasers surrounding attraction region. Thus the critical distance will increase if the arc current is increased.

### 5.1.5 Influence of the pulse duration of the TIG pulse

Figure 24 shows that for small pulse duration the attractions in the small arc length region (< 2 mm) are successful. With increasing pulse duration the attraction decreases (possible  $l_c$  decreases), but from 7.0 mm and up to 9.9 ms the attraction increases again ( $l_c$  increases). The delay between the triggering of the laser and the arc is 1 ms (the laser is triggered 1 ms before the arc). Thus with the laser pulse duration being 3 ms it means that a TIG pulse up to 2 ms is being overlapped entirely by the laser pulse and a TIG pulse of 3 ms and higher has an overlap time in the beginning of the pulse of 2 ms, see figure 25.

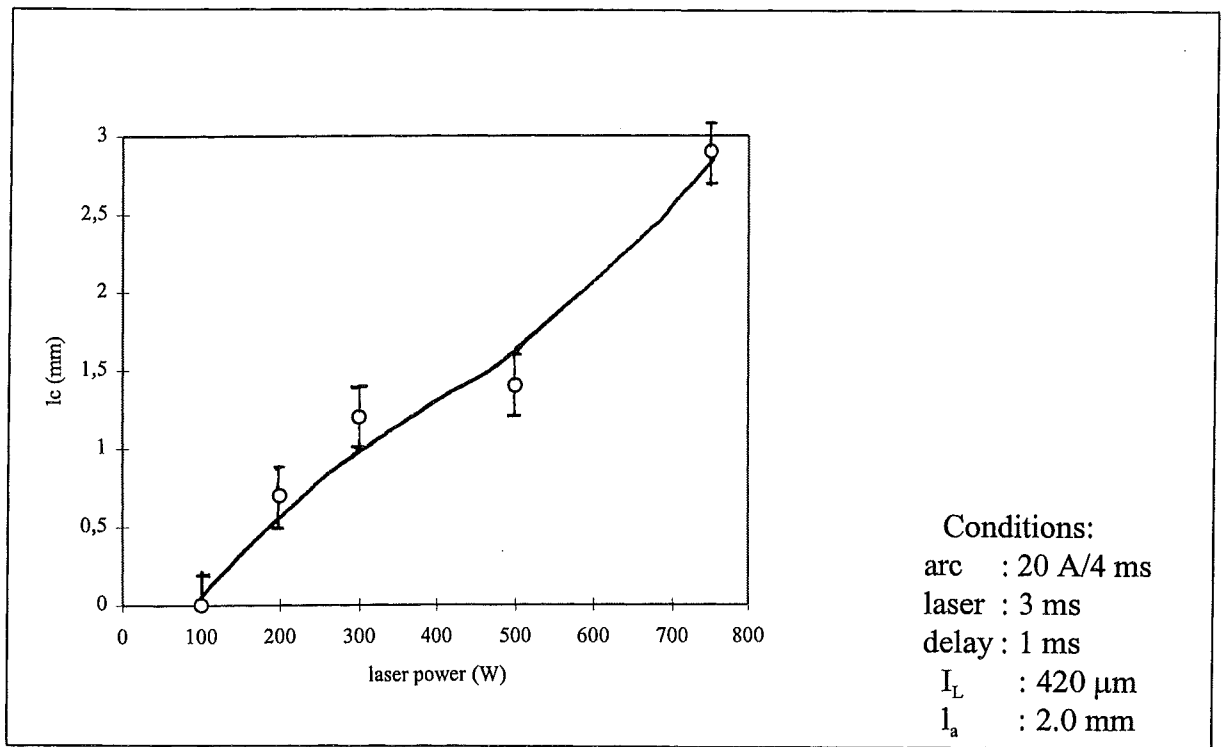


Figure 26: Critical distance as function of laser power.

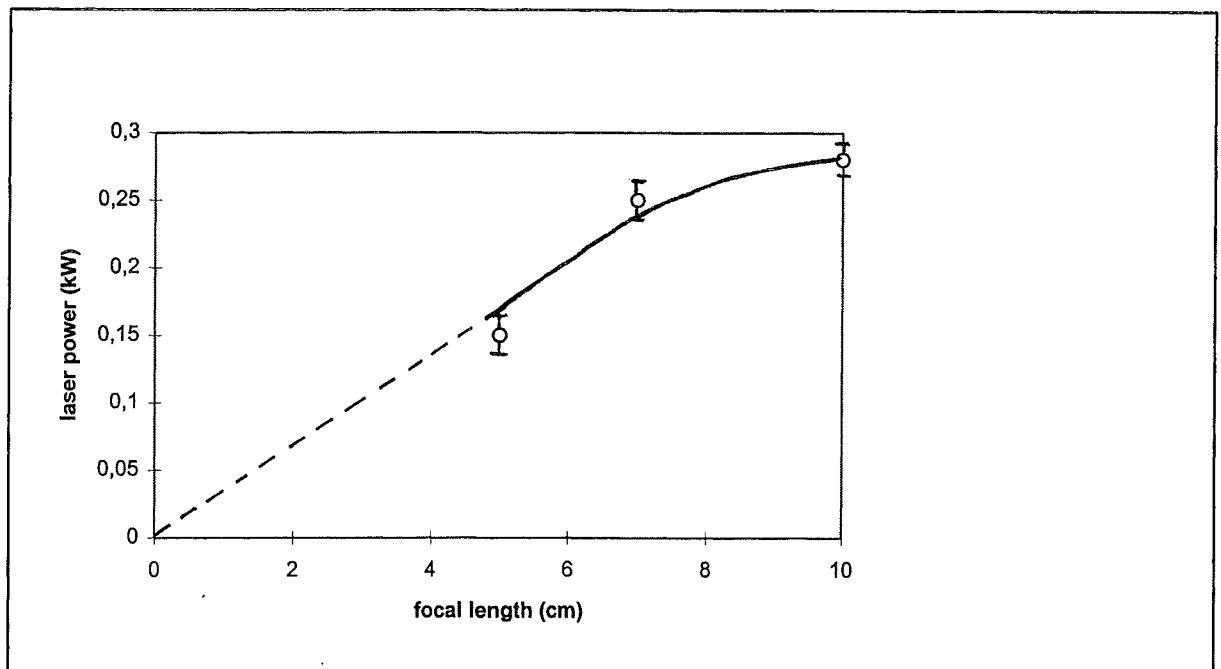


Figure 27: Increase in required laser power versus focal length of focusing lens.

The initial decrease can be explained by the fact that at the short TIG pulse durations the laser pulse overlaps (almost) entirely the TIG pulse and therefore there is still attraction in this critical situation. The improvement for the longer pulse durations of 8.0 or 9.9 ms is probably due to the expanding arc when the pulse duration is increased and thus can just reach the lasers surrounding attraction region. For the medium arc pulse durations (4-7 ms) the laser pulse is shut off too quickly and the critical distance is longer than the arc length causing the arc to impact at the closest workpiece surface, instead of following the laser spot.

### 5.1.6 Influence of laser power and laser intensity

In figure 26  $l_c$  is plotted as function of the laser power. The data of these measurements are given in table 2, appendix A. The figure shows that the critical distance  $l_c$  increases with increasing laser power.

From the data (appendix A) it can be seen that a laser power of 100 W only gives successful attraction one time. With the laser alone (100W/3 ms which equals 0.3 J) there were no spots visible. Apparently, the laser power was not high enough to melt the surface and therefore not sufficient for releasing enough electrons/particles from the surface, which is probably the plume mechanism for conducting the arc to the laser spot position (§ 5.4).

A laser power of 200 W seems sufficient for attraction to occur. When the laser power is increased, the attraction improves in both the higher arc length regions ( $\geq 3.0$  mm) and the lower arc length regions ( $\leq 3.0$  mm).

From the data one could also see that when the laser power is as high as 750 W it results in a considerable improvement on the attraction behaviour in comparison with the standard situation. The critical distance increases and for a fixed critical distance the possible arc length not only increases but the attraction in the lower arc length regions (0.5-2.5 mm) also improves noticeably (compare with results of influence of  $l_a$ , table 11). This is caused by the increase in freed particles (charged as well as neutral) from the workpiece surface. In consequence, the laser plume becomes higher and wider, by which the attraction region of the laser increases (see § 5.4 model).

The data show also that higher arc lengths are possible compared to the arc lengths in the influence of  $l_a$  experiments (table 11). This indicates that the ignition and starting of the arc is facilitated by the lasers presence.

However, the laser power can be expressed in terms of laser intensity. As the intensity is defined as  $W/m^2$ , increasing the laser power and keeping the spot diameter constant means, that the intensity is increased. But, when the spot diameter is kept constant the variation in laser intensity is easier manageable on the machine as the variation in laser power. Thus, the result obtained by varying the laser power reflects the influence of the laser intensity on  $l_c$ .

Another test involving the laser intensity was conducted. This test examined how changing the spot diameter affected the laser intensity and if there are differences with respect to the influence of laser intensity by changing the laser power. The laser spot diameter can be changed by using focusing lenses with different focal lengths. The other lenses used here have a focal length of 5.0 cm (f 50) and 10.0 cm (f 100). The focal length of the lens used during the standard is 7.0 cm (f 70). Thus their magnification factors are 10:5, 10:10 and 10:7 respectively. This means that the laser beam of 600  $\mu m$  in diameter will be reduced to 300  $\mu m$ , 600  $\mu m$  and 420  $\mu m$  respectively after leaving the fibre.

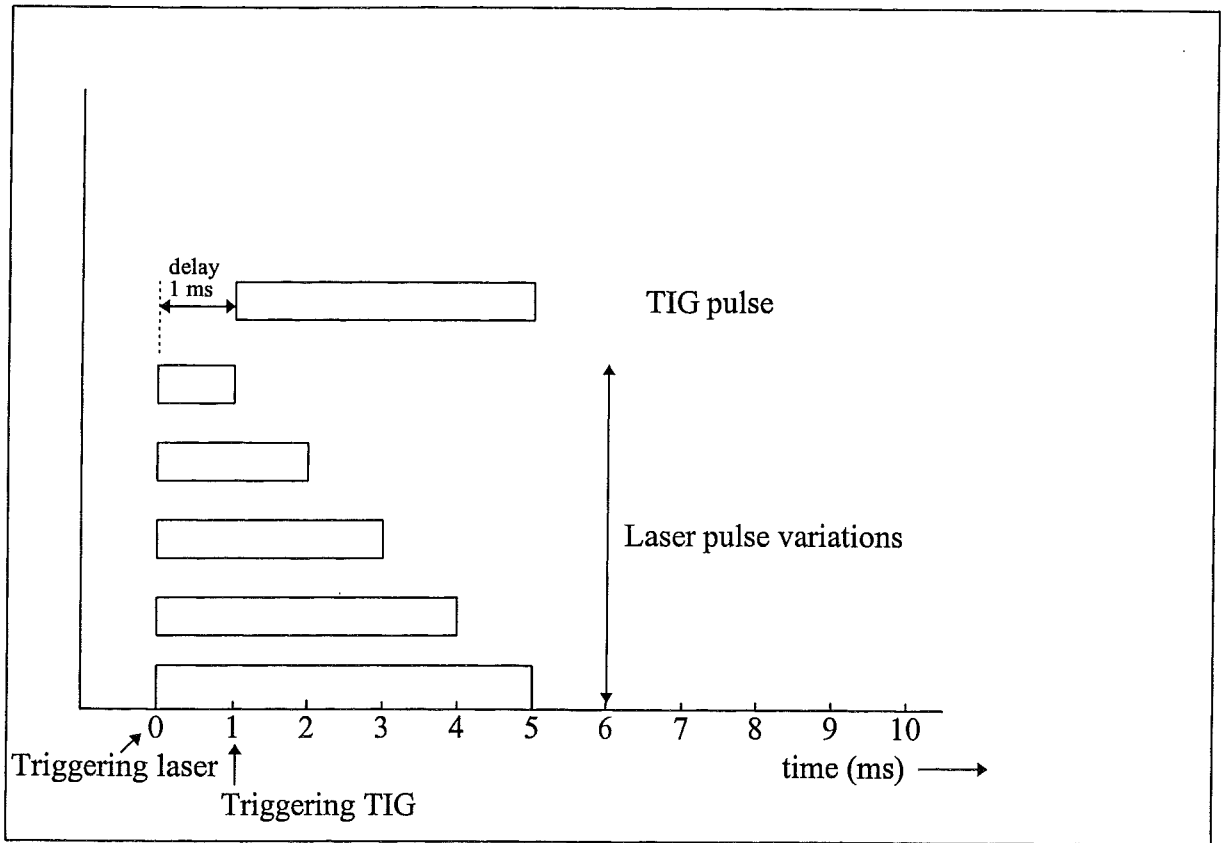


Figure 28: Variation of laser pulse duration.

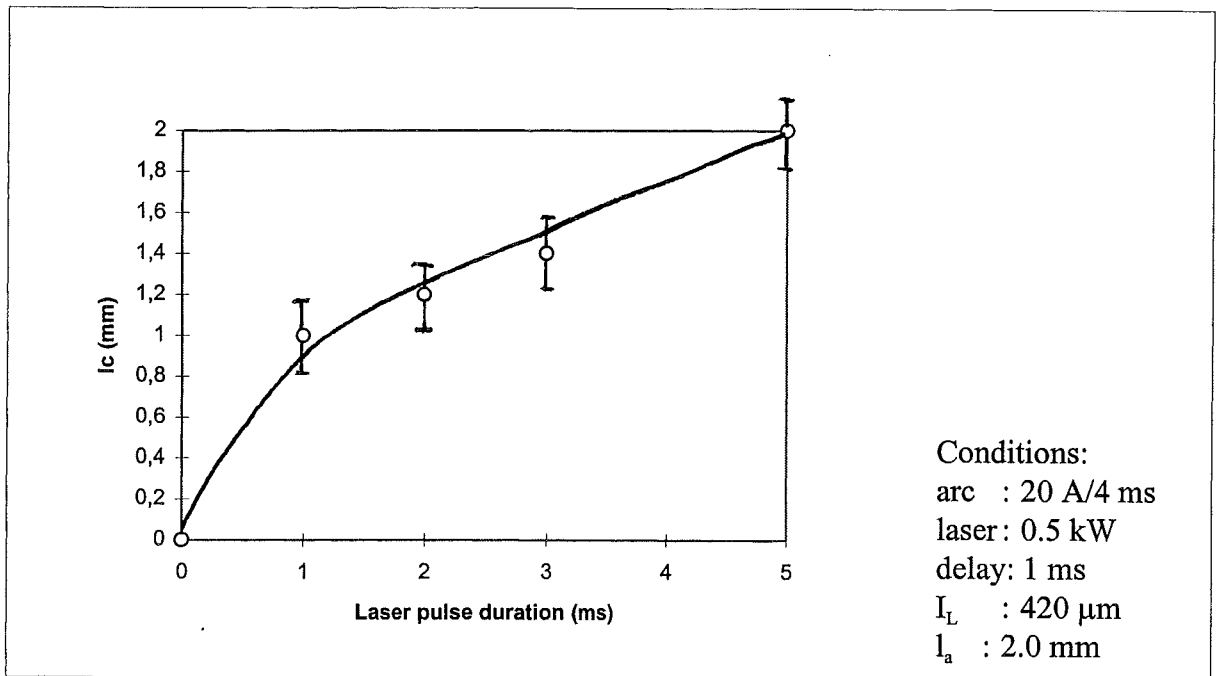


Figure 29: Critical distance as function of laser pulse duration.

The tests show that with the f 50 lens the successful attraction at the same settings of the other parameters as in the standard is already reached at 0.15 kW. While for the f 70 lens, this result is only just met at 0.25 kW. Using the f 100 lens results in an power of 0.28 kW. In figure 27 the increase in required laser power as a function of the focal length of the focusing lenses is shown. It is interesting to compare this figure with figure 26, because the laser power and the laser intensity examined as described here are related.

A focusing lens of f 50 will, in comparison with a f 70 focusing lens and with the same settings of the laser, deliver the power on a smaller surface area. As a result more particles are released from the workpiece surface when using the f 50 lens instead of the f 70 lens. When the data are converted into laser intensity it results in:

- f 50: intensity=  $531 \times 10^6 \text{ W/m}^2$

- f 70: intensity=  $451 \times 10^6 \text{ W/m}^2$

- f 100: intensity=  $248 \times 10^6 \text{ W/m}^2$

Here it can be seen that the intensity of the laser with f 50 lens is somewhat higher than with the f 70 lens at the same settings .

Using a f 100 lens should mean that a higher (around 500 W) laser power is needed in order to have the same result of attraction at  $l = 1.0 \text{ mm}$  and  $l_a = 2.0 \text{ mm}$  (because the spot diameter increases). But from the data above one can see that the required laser power lies lower (~ 50%). Apparently, at a larger spot size other factors are involved. Maybe, the temperature gradient at larger spot sizes is lower, which results in a lower heat transport. Another possibility may be the increase of the width of the laser plume, which increases the attraction region and may be just sufficient.

### 5.1.7 Influence of laser pulse duration

The pulse duration of the laser has also influence on the attraction behaviour of the arc. In figure 28 is shown how the pulse duration is varied.

The experimental results are listed in table 3, appendix A. From these data the influence of the lasers pulse duration can be plotted in graphical form, which is shown in figure 29. This figure shows that the critical distance  $l_c$  (at a fixed arc length) increases if the laser pulse duration increases. The delay between the triggering of the laser and the arc was kept constant at 1 ms.

When the laser pulse lasts for only 1 ms, there is no overlap of both pulses. But still there is attraction. When the influence of the delay time is discussed (§ 5.1.8) it is shown that at a delay of 1 ms and a laser pulse duration of 1 ms there is no attraction in case of  $l = 1.0 \text{ mm}$  and arc length = 2.0 mm. But in the experiments which are under discussion in this section there actually is attraction for the same  $l$  and arc length. This could be explained by variations in the starting time of the pulse. To check this the pulses were monitored with a oscilloscope. It appears that there is no variation in the main trigger pulse and in the start of the arc pulse. The starting time of the laser pulse however, sometimes jumps back and forth. This difference in starting time varies between 0.2 and 0.4 ms. This could account for the difference which determines whether there is (a conducting laser plume has already been formed) or isn't any attraction.

The longer the laser pulse duration, the more particles will be evaporated from the workpiece surface (weld pool). As a result the plume expands with longer durations and thus becomes higher. Thus the attraction region surrounding the laser increases (§ 5.4). Therefore not only  $l_c$

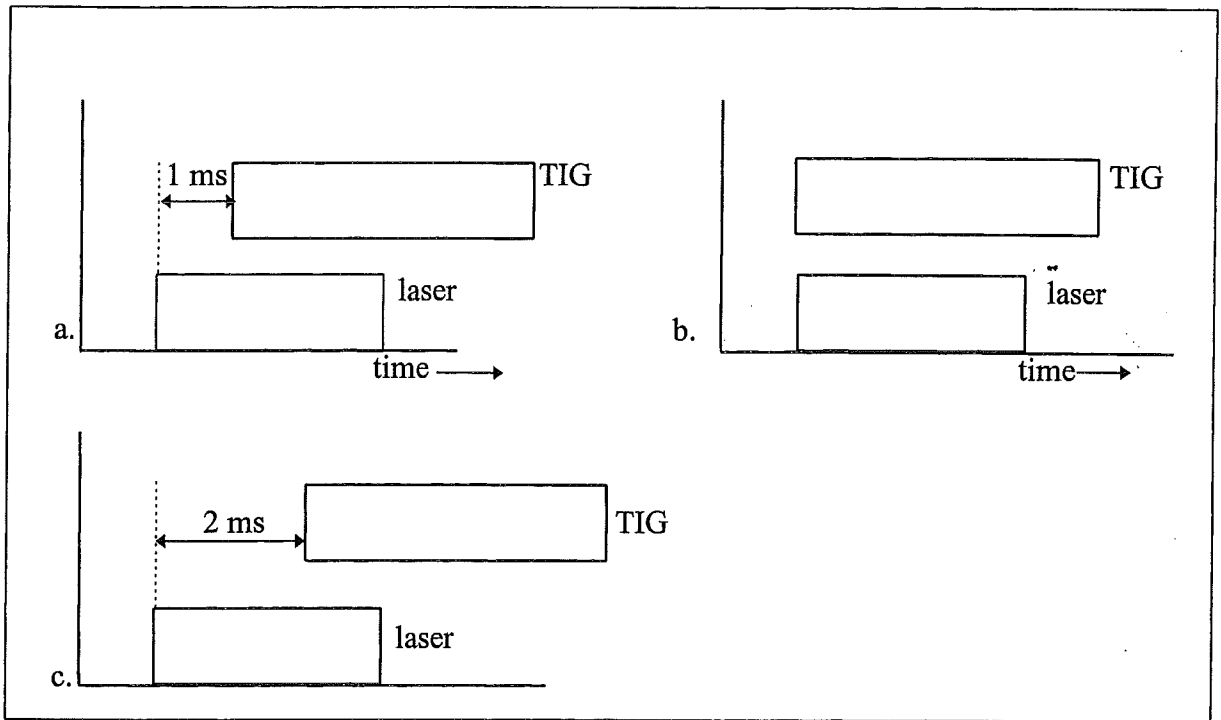


Figure 30: Variations in delay time.  
 a. delay 1 ms (standard);  
 b. delay 0 ms;  
 c. delay 2 ms.

increases, but the attraction in the low ( $< 2.0$  mm) and high ( $> 3.5$  mm) arc length regions is also improved.

### 5.1.8 Influence of delay time

The influence of the delay time on  $l_c$  was also studied. The experimental results are given in table 4, appendix A. In figure 30 it is shown how the delay is changed in order to determine its influence.

First, the delay of 0 ms is investigated. With this delay the laser and TIG are triggered at the same time, see figure 30b. If all other values remain the same as during the standard, there is no attraction. The distance  $l$  tested here is 1.0 mm. Changing the laser pulse duration to 1.0, 2.0 and 5.0 ms (total overlap) made no difference. In figure 31 a photograph of the tests with a delay of 0 ms and a laser pulse duration of 3.0 and 5.0 ms is shown. Here one can see that the “laser spot” (the lowermost row) expands in size with increasing laser pulse duration. This indicates that part of the arc is drawn to the laser spot and the other part still chooses the shortest path to the surface (see § 5.3, high speed camera).

Next, the laser pulse duration remains 3 ms and the TIG pulse duration is changed, see figure 32. The arc pulse durations are 1.0, 4.0 and 9.9 ms. Testing under the same conditions as in the standard and for  $l = 1.0$  mm, resulted in the following, see table 5, appendix A. When the TIG pulse (1.0 ms) falls entirely within the laser pulse there is no attraction. A TIG pulse of 4.0 ms results in the “double spot” attraction, i.e. part of the arc energy is drawn to the laser spot position and the other part goes to the nearest place on the workpiece surface (normal path). If the pulse duration is 9.9 ms, then most of the time there are “double spots” and a few times there are successful attractions. The successful attractions are caused by the expanding arc when the duration increases and therefore the arc reaches the attraction region of the laser.

Increasing the delay to 2 ms (figure 30c) results in successful attraction for all tested arc pulse durations. The laser plume has had enough time to be fully developed and be at its utmost height, so the attraction region of the laser is optimal. In comparison to the standard (delay = 1 ms) and the results of the influence of  $l_a$  the attraction region has increased (optimum).

Tests have also been conducted to see how long the minimum delay should be. The data are given in table 6, appendix A. Under the same conditions as during the standard, the minimum delay time proved to be at least 0.4 ms in order to have successful attractions for  $l = 1.0$  mm and arc length = 2.0 mm. In order to determine what the minimum overlap time should be, tests were carried out with increasing the delay time in steps of 0.2 ms and determining the attraction for each delay for 1.0, 2.0 and 3.0 ms laser pulse duration. From these tests (table 6, appendix A) it could be concluded that the minimum overlap time lies between 1.2-1.4 ms for these conditions. This overlap time is also sufficient if the TIG pulse duration is increased (in this case max. 9.9 ms). Should the distance  $l$  or arc length be changed, then the overlap time and delay time (probably) must be changed too. The laser plume needs time to grow and the attraction region of the laser needs to exist long enough for attraction of the arc to occur.

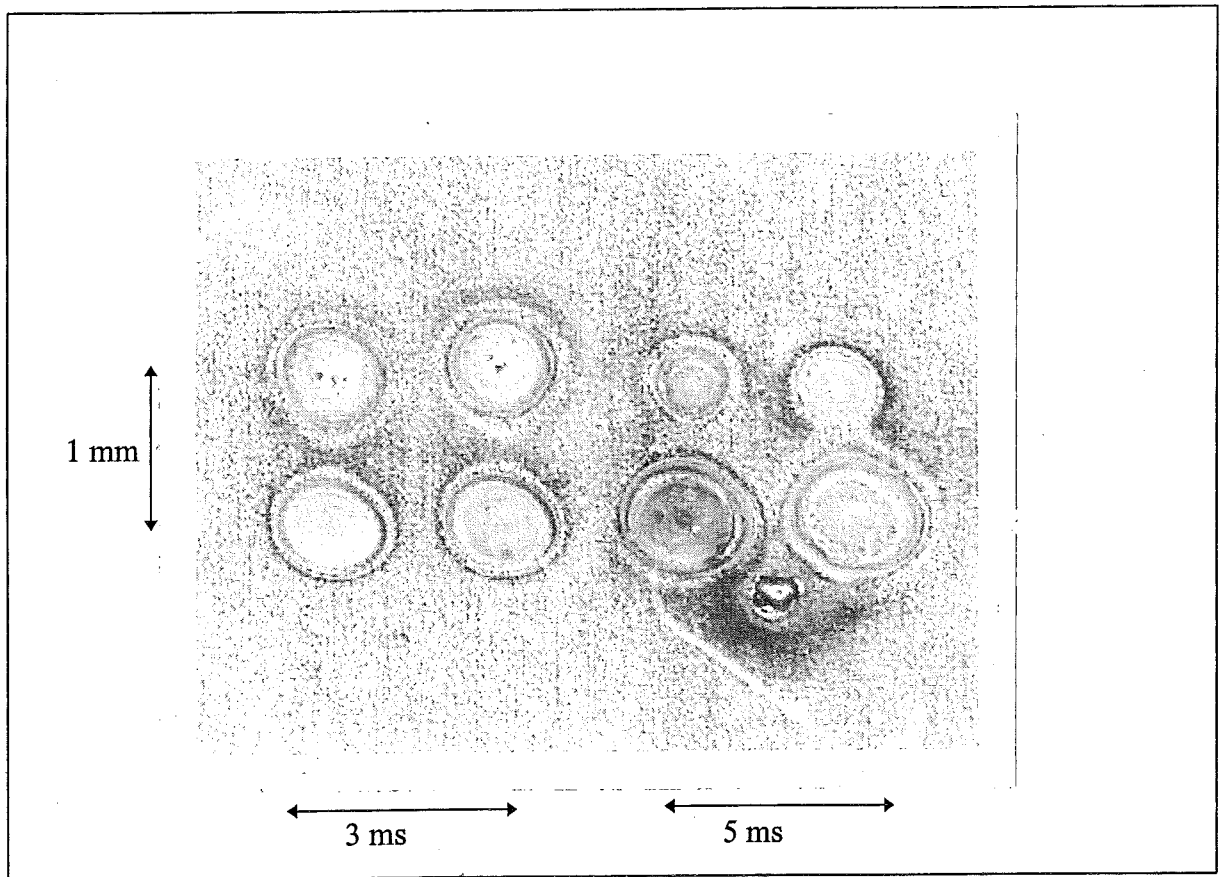


Figure 31: Photograph of test result delay time experiments. Conditions: arc: 20 A/4 ms; air; delay: 0 ms ; laser: 0.5 kW/ 3 & 5 ms;  $I_L = 420 \mu\text{m}$ ;  $l = 1.0 \text{ mm}$ ;  $l_a = 2.0 \text{ mm}$ .

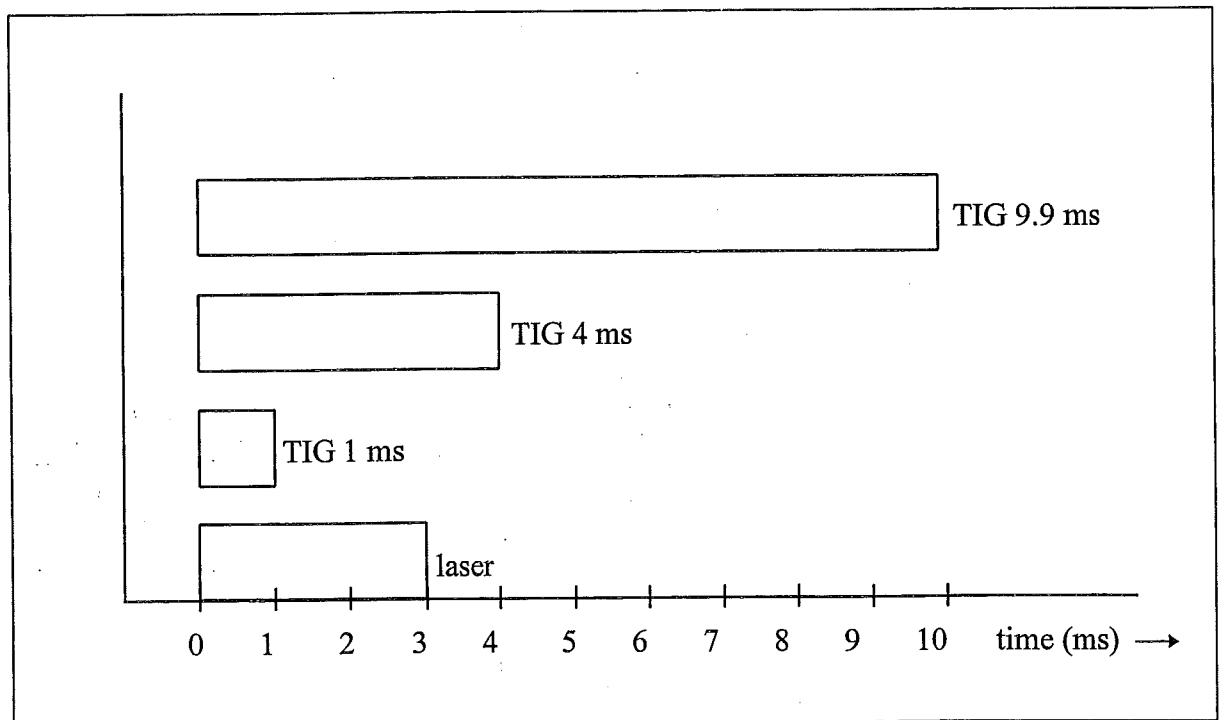


Figure 32: Delay time experiments with variation in TIG pulse duration.

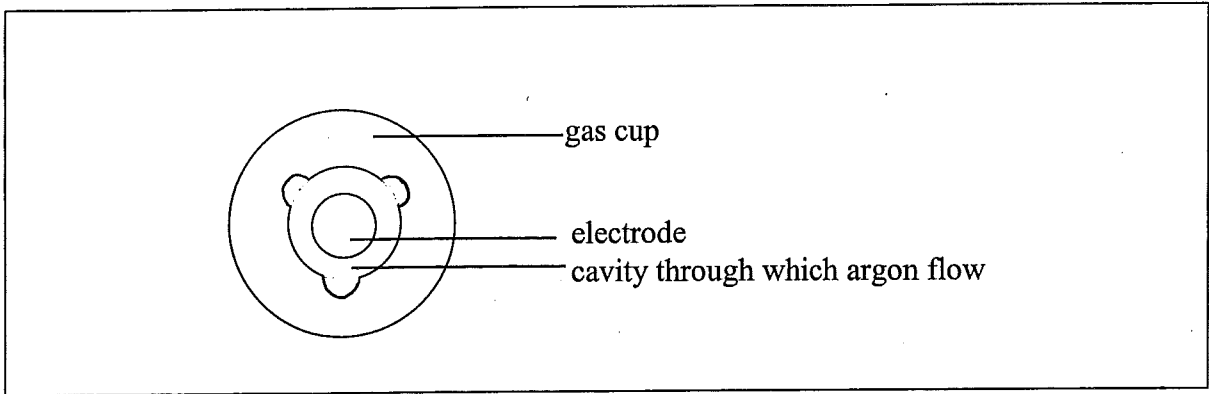


Figure 33: Schematic view of cross section of gas cup.

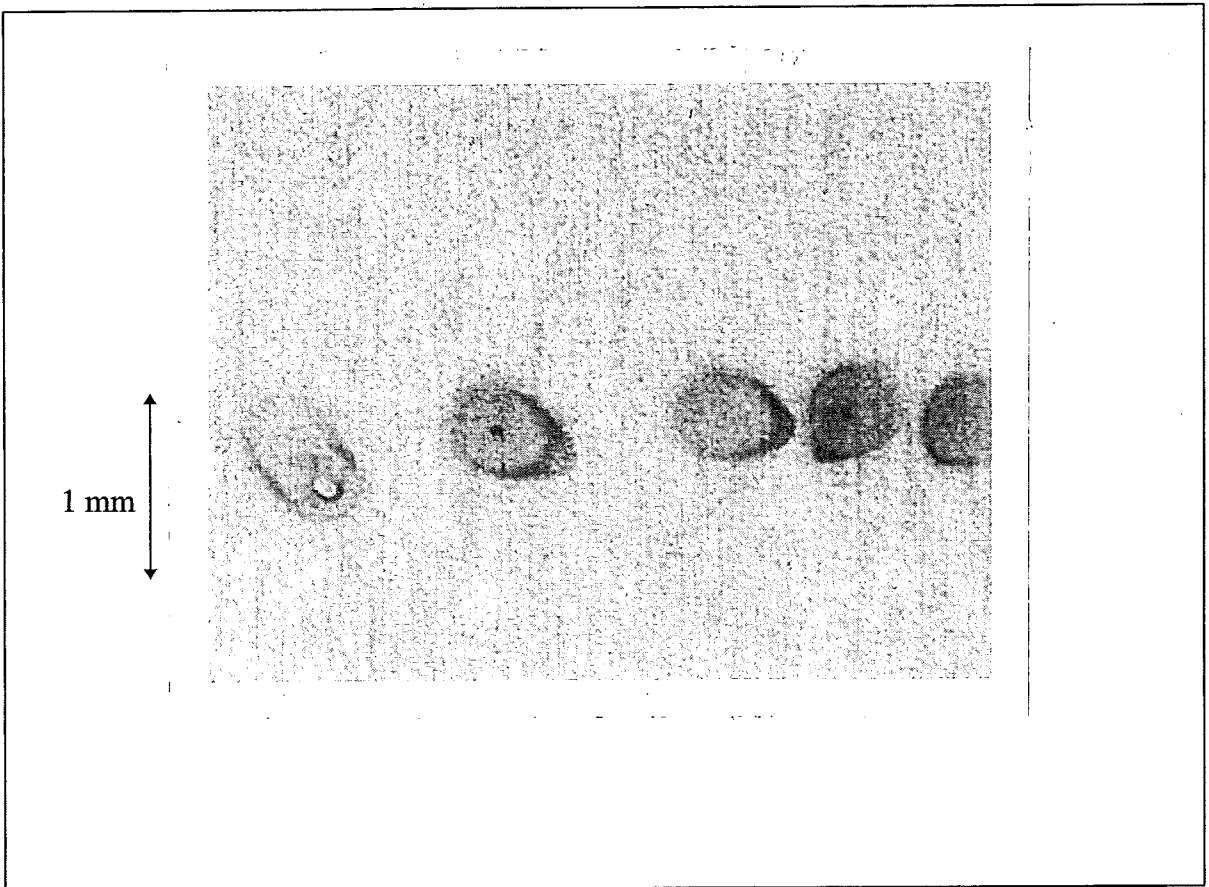


Figure 34: Photograph of TIG spot welds. Conditions:  $l_a = 2.0$  mm; arc: 20 A/4 ms; argon.

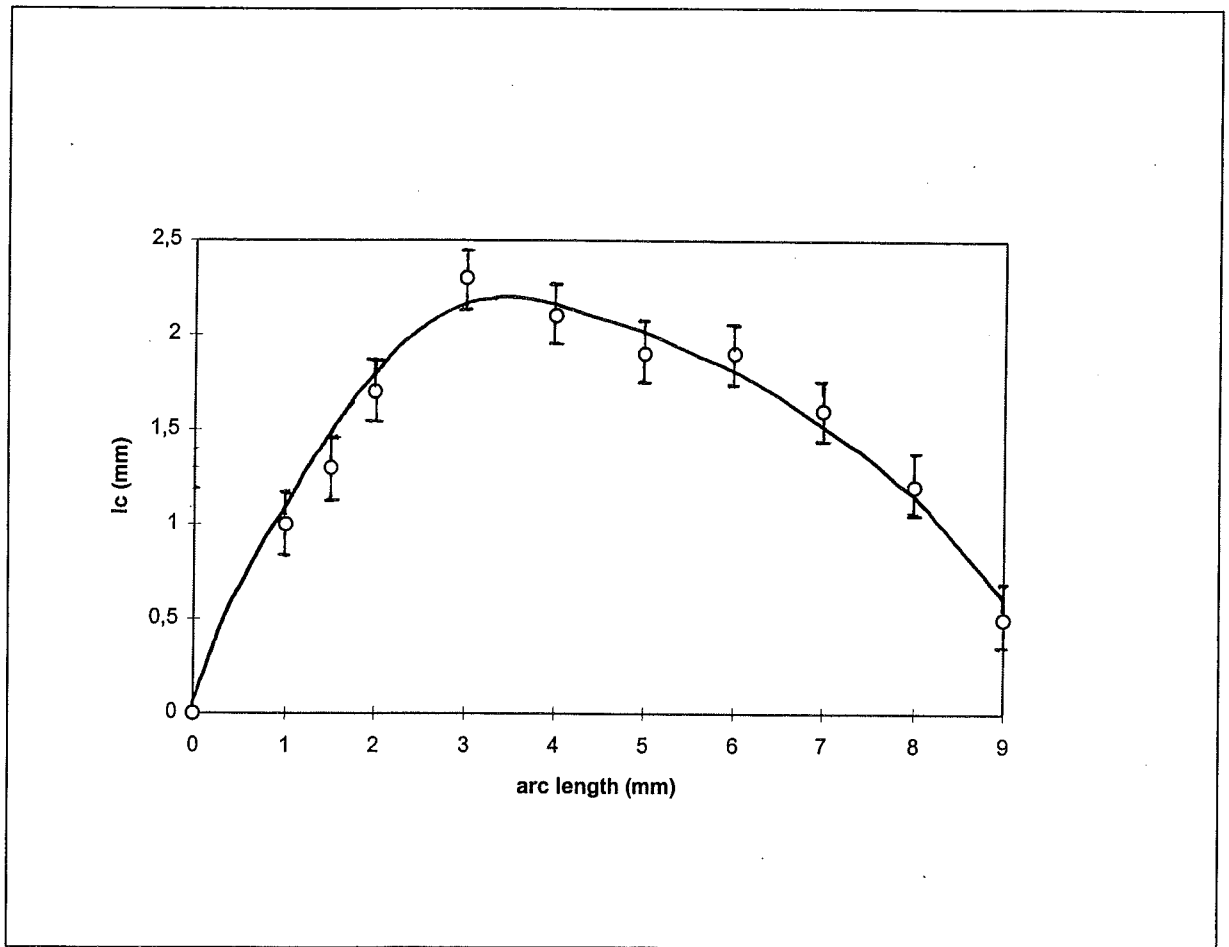


Figure 35: Critical distance as function of arc length in argon. Conditions: arc: 20 A/4 ms; laser: 0.5 kW/3 ms; argon flow: 1 l/min; delay = 1.0 ms;  $I_L = 420 \mu\text{m}$ .

### 5.1.9 Influence of shielding gas

As was mentioned earlier, § 4.3 experimental procedure, it is necessary to examine if and how the shielding gas influences the attraction behaviour of the arc. First, a standard was made in argon in a similar way as the standard in air (same conditions, but now there is an argon welding environment, table 7, appendix A). These measurements are needed in order to have a general idea of the changes in the attraction behaviour of the arc, in comparison with the standard in air. It also serves as the reference for all tests performed under the influence of argon. These are tests which are conducted to see if the influencing parameters discussed in the previous paragraphs behave the same as in air if there is an argon atmosphere. The argon flow is 1 l/min. In figure 33 the cross section of the end of the gas cup is shown. In the centre is the electrode, the gas flows past it through the specially constructed cavity.

In argon the arc welds are much cleaner, they are almost produced without spatter and a larger arc length is possible compared with arcs in air (see table 8, appendix A). However, in the lower arc length region (0.1-4 mm), the TIG spots do not look like real melts (see figure 34). At the back of the plates there are prints visible. From 4 mm and up (tested up to 9.0 mm) there are melts (spots) formed. In table 8 (appendix A) the results of  $l_a$  as parameter are listed. Here one can see that at a critical distance of 1.0 mm there always is attraction for all arc lengths up to 9.0 mm. Like the measurements in air there seems to be a similar trend in increasing critical distance with increasing arc lengths, see figure 35. But when the arc length exceeds 4.0 mm, the critical distance decreases with increasing arc length.

Above an arc length of 5 mm there are also "double spots" visible, see figure 36. At first sight the arc seemed to go entirely to the laser spot position, but after the pulses there was still a very small spot visible where the TIG spot would have been if there were no attraction. What happens here is discussed in § 5.3 where the use of the high speed video camera is discussed. In comparison to the measurements in air the attraction in the low arc regions (1.0-1.5 mm) for critical distances of 1.0-1.5 mm is better, which can be seen in table 8, appendix A. Why this happens is discussed later on in this section when the delay time experiments will be discussed.

Next, the influence of the other parameters in the case of argon shielding will be considered.

#### *Arc current*

The arc current is set on 10 A and the critical distance is determined for several arc lengths (2-8 mm). Then the arc current is increased to 40 A. Then too, the critical distance is determined for the same arc lengths. The results are shown in figure 37. As can be seen, the trend is the same as in air: increasing the arc current results in increasing critical distance. Still there are sometimes "double spots" formed. Most of the time they are very small, but at 40 A,  $l = 2.0$  mm and arc length = 7.0 mm the arc is attracted to the laser spot but still a part of the arc goes to a position on the workpiece surface right under the electrode. This is shown in figure 38. This figure also shows that the part of the arc which is not attracted by the laser plume, does not precisely go straight to the workpiece surface (shortest path), but it is deposited in a direction away from the laser plume. This also applies for the other arc lengths at which the double spots were also observed (5.0-9.0 mm). The distance over which the non-attracted part of the arc is moved from the electrode position lies between 0 and 1.0 mm. Interesting to note is that the direction and the position of the double spots is always the same, see figure 38.

#### *TIG pulse duration*

Tests are conducted for two distances  $l$ , namely:  $l = 1.0$  mm and  $l = 2.0$  mm. The arc lengths

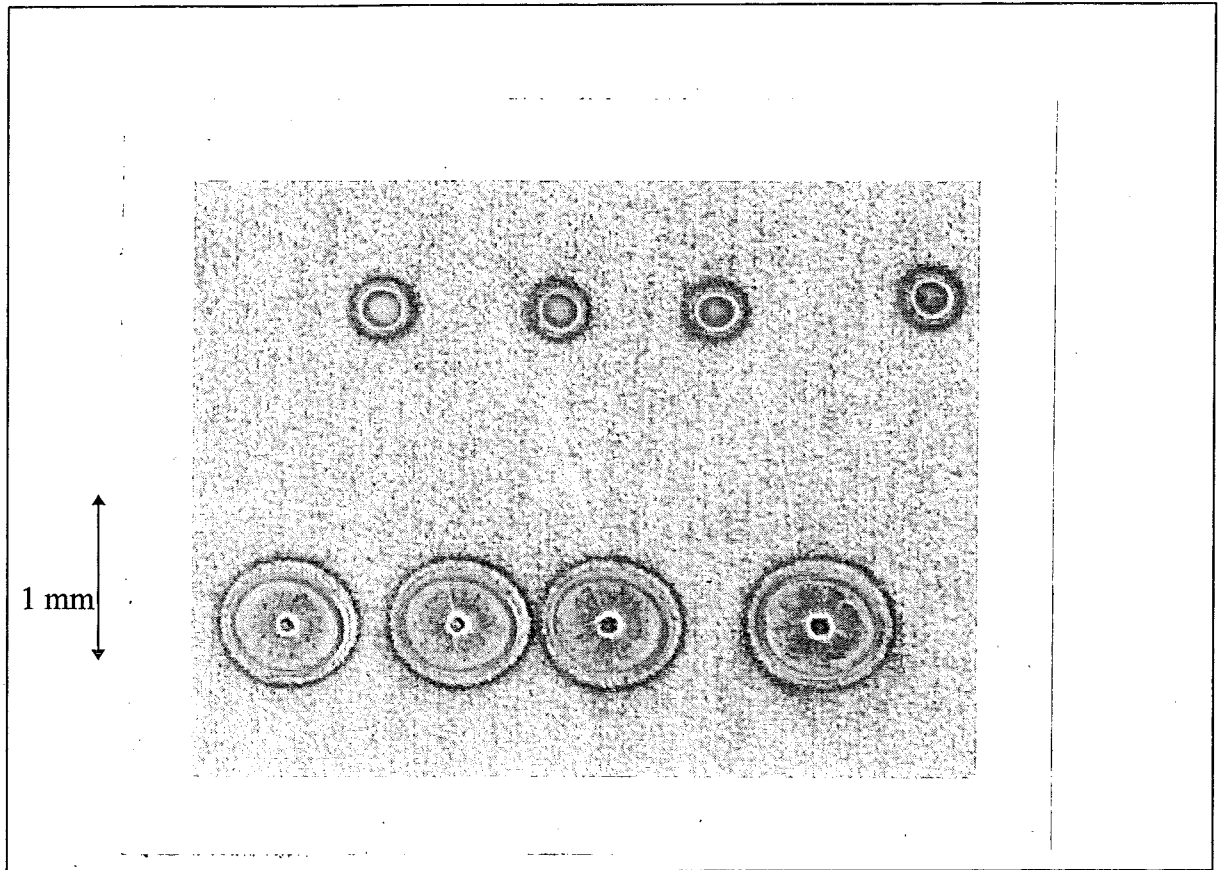


Figure 36: Photograph of 'double spots' in argon. Conditions: arc: 20 A/4 ms; laser: 0.5 kW/3ms; delay = 1.0 ms;  $I_L = 420 \mu\text{m}$ ; argon;  $l = 1.0 \text{ mm}$ ;  $l_a = 7.0 \text{ mm}$ .

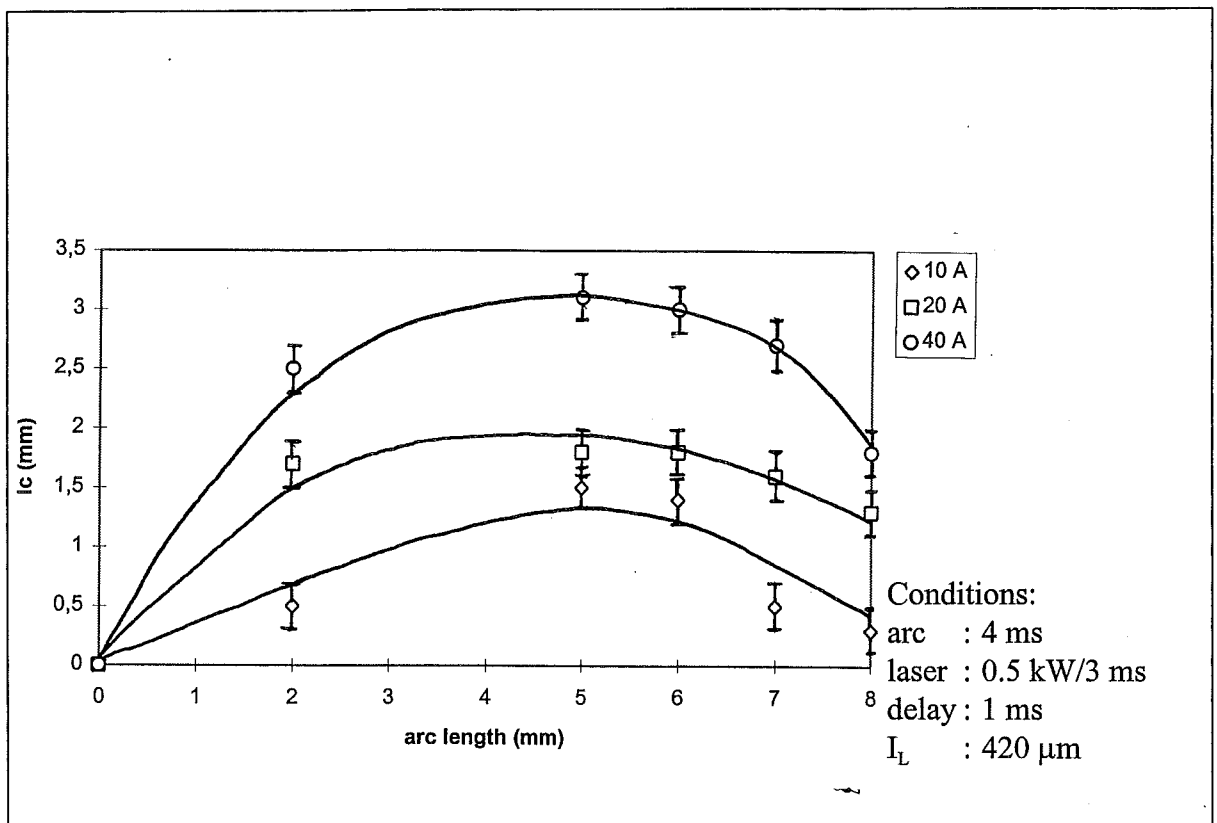


Figure 37: Critical distance  $l_c$  as function of  $l_a$  for different arc currents in argon.

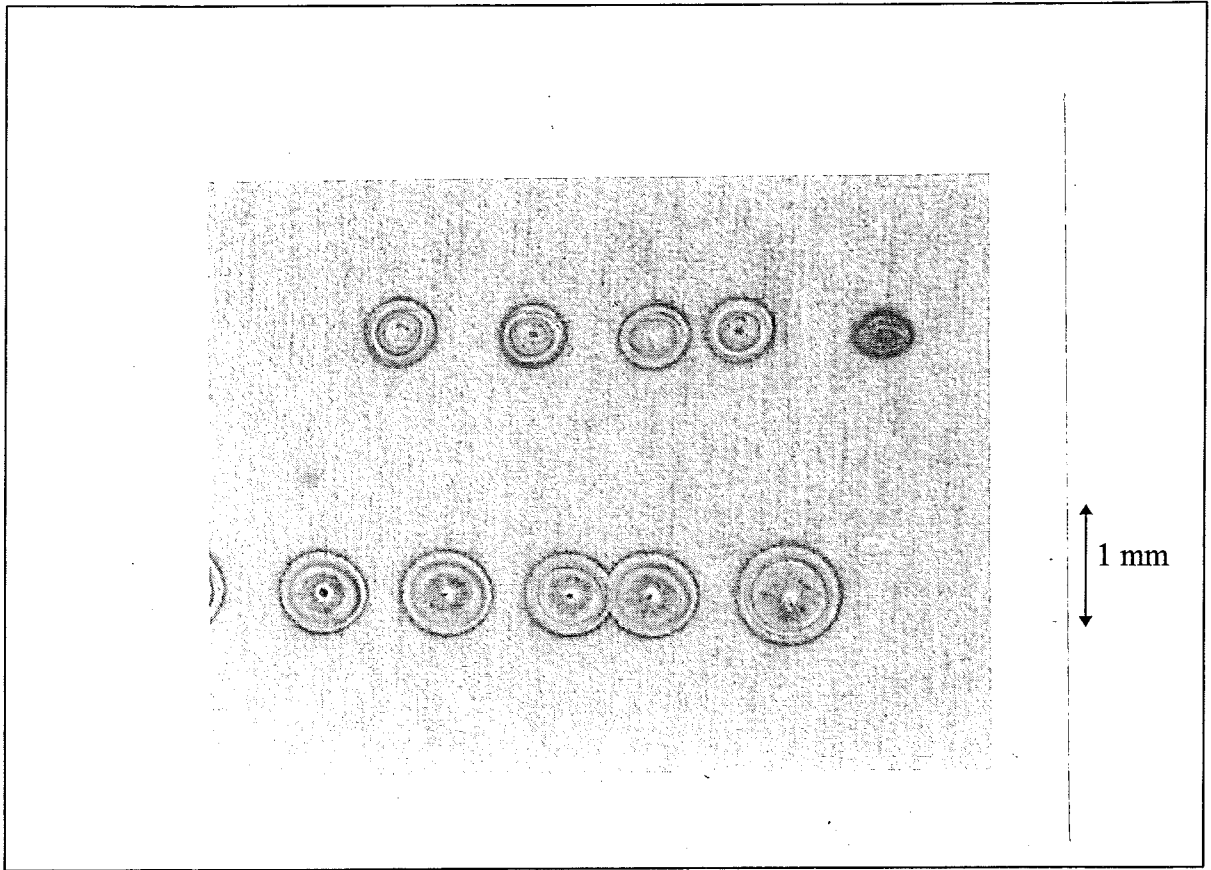


Figure 38: Photograph of experiment in argon resulting in double spot. Conditions: arc: 40 A/4 ms; laser: 0.5 kW/3 ms; argon; delay = 1.0 ms;  $l = 2.0$  mm;  $l_a = 7.0$  mm;  $I_L = 420$   $\mu$ m.

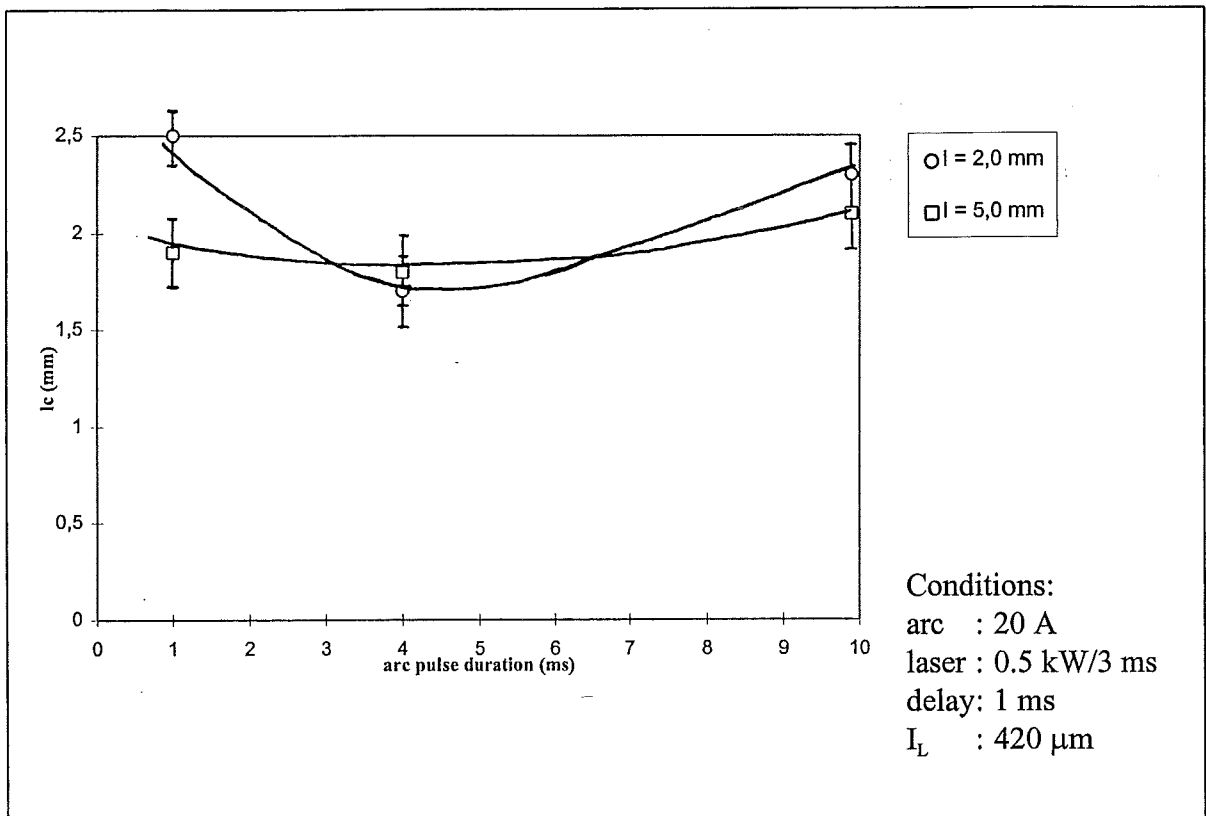


Figure 39: Critical distance  $l_c$  as function of TIG pulse duration in argon .

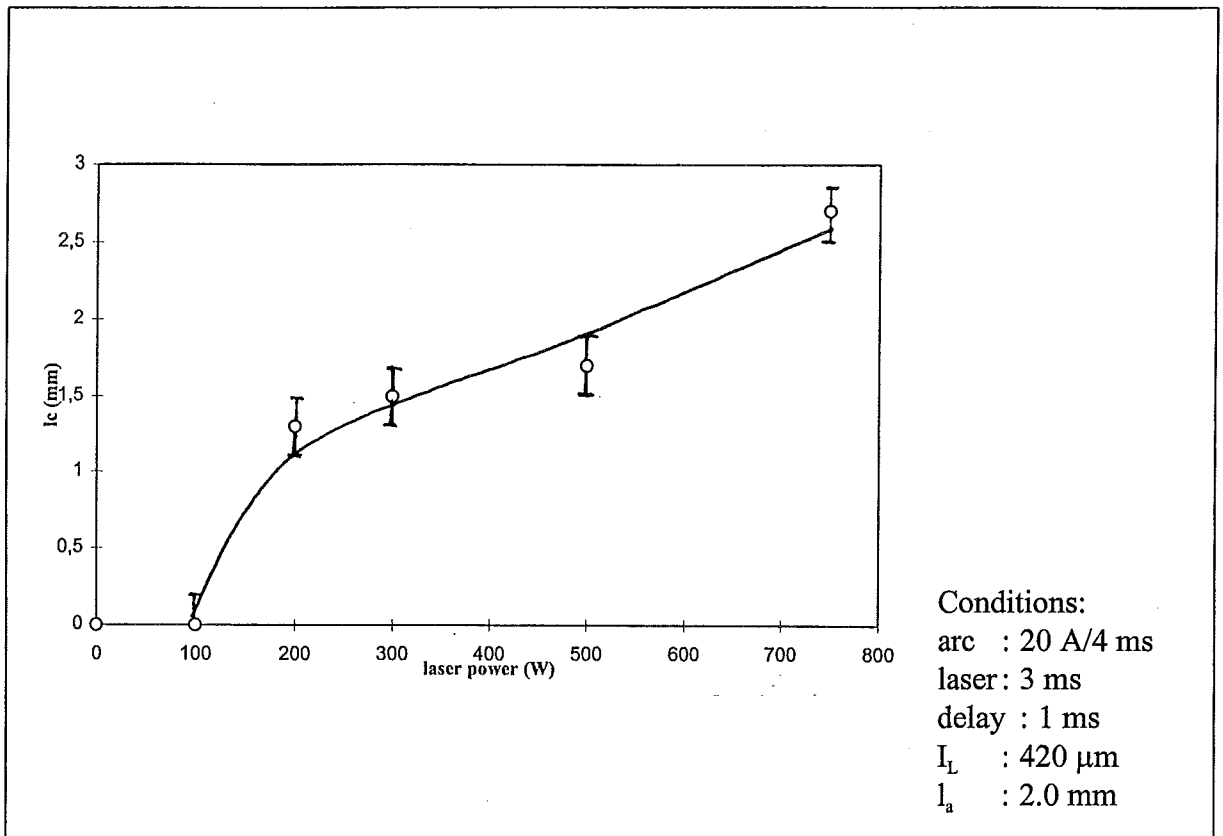


Figure 40: Critical distance  $l_c$  as function of laser power in argon (estimation).

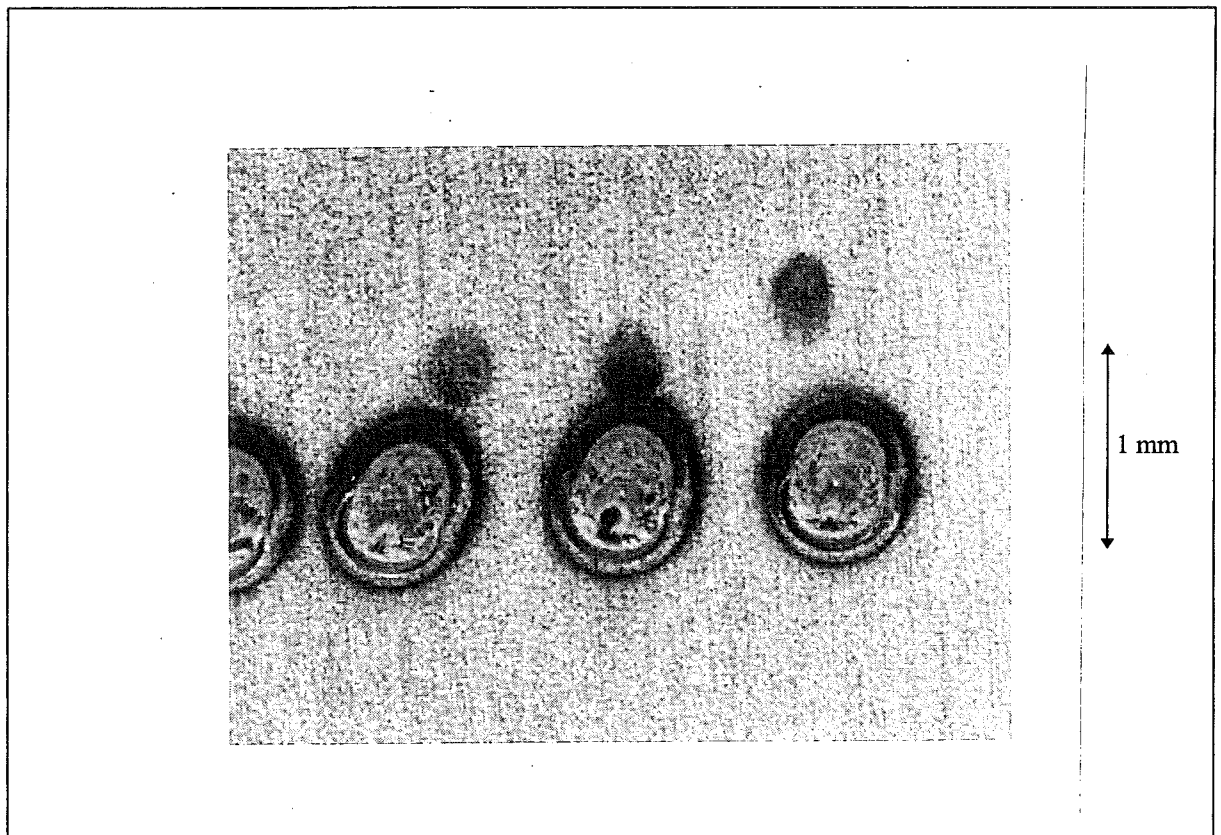


Figure 41: Photograph of delay time experiment in argon. Conditions: arc: 20 A/9.9 ms; laser: 0.5 kW/3 ms; argon; delay = 0 ms;  $l = 1.0$  mm;  $l_a = 2.0$  mm;  $I_L = 420 \mu\text{m}$ .

tested for each of the two  $l$ 's are 2.0 and 5.0 mm. The TIG pulse durations examined are 1.0 and 9.9 ms. The data for 4.0 ms are already available (afore mentioned standard in argon). Here too the attraction ( $l_c$ ) is decreasing at first with increasing TIG pulse duration, but increasing slightly again after a certain pulse duration. This is shown in figure 39. However only an estimation of the path of the graph can be given because the in-between pulse durations were not examined. An explanation for this relationship of  $l_c$  and  $t_a$  is already given in section 5.1.5.

#### *Laser power and intensity*

After testing the influence of the laser power in argon and comparing the results with the results obtained in air, it became clear that in argon the laser power has to be about 100 W higher to reach the same attraction as in air (tested for arc lengths of 2.0 mm). Comparing the laser spots in air and in argon one could see that with the same power, the spots in argon are smaller. Thus in air the laser energy is used more effectively. The trend in argon for increasing laser power is similar to the trend in air: increasing  $l_c$  with increasing laser power. Here no exact relation can be given either, as the influence has not been examined extensively. However, an estimation of the behaviour can be given and is shown in figure 40. As was explained in § 5.1.6, the change in power is actually the change in laser intensity. Thus, the actual relation given in figure 40 is  $l_c$  versus the laser intensity.

#### *Laser pulse duration*

The laser pulse duration in argon has a similar effect on the attraction as in air. An increased duration improves the attraction;  $l_c$  increases.

#### *Delay time*

The delay time tests performed in argon show for  $l = 1.0$  mm and arc length = 2.0 mm (same as delay test in air) that at a delay of 0 ms (both pulses triggered at the same time) the attraction is successful. In air under these conditions the attraction was only medium. For different TIG pulse durations the attraction is as follows (table 9, appendix A):

TIG pulse 1.0 ms  $\Rightarrow$  no attraction. This is the same as in air.

4.0 ms  $\Rightarrow$  successful attractions.

9.9 ms  $\Rightarrow$  successful attractions. A very small double spot is still visible (see figure 41), but this double spot is smaller than in air. In air the double spot is a fully penetrated melt, in argon not.

When the delay is increased with steps of 0.2 ms from 0.0 ms, and for each step the laser pulse duration is changed from 1.0 ms to 2.0 ms and 3.0 ms, there are a few changes in comparison with the same tests performed in air, see table 6 and 10, appendix A. In air there was not hardly any successful attraction (see § 5.1.8) for any of the tested laser pulse durations when the delay was 0.0 ms. In argon however, all tested pulse durations (1.0, 2.0 and 5.0 ms) give successful attractions (same conditions as in air). Looking very close, a double spot is very faintly visible. Now, increasing the delay with steps improves the attraction (no more double spots) just as it is in air. When the delay reaches 1.0 ms the attraction for the 1 ms laser pulse is not successful (just like in air). In air the attraction for a 2.0 ms laser pulse was only medium, but in argon the attraction is still good. In both air and argon a laser pulse of 3 ms still results in successful attractions.

Thus it appears that in argon the laser plume is created more quickly than in air. Therefore the delay time in argon can be smaller than in air (in fact no delay is needed; 0.0 ms delay results

Table 12: Results experiments on phosphor bronze plates (R 1178); delay = 1.0 ms; air;  $I_L = 420 \mu\text{m}$ .

$P_{\text{laser}}$ (kW)	$t_l$ (ms)	$I_{\text{arc}}$ (A)	$t_a$ (ms)	$l_c$ (mm)	$l_a$ (mm)	result
0.5	3.0	20	4.0	1.0	2.0	--
0.7	3.0	20	4.0	1.0	2.0	+--
0.9	3.0	20	4.0	1.0	2.0	+ -
1.0	3.0	20	4.0	1.0	2.0	+ -
0.5	5.0	20	4.0	1.0	2.0	+--
0.7	5.0	20	4.0	1.0	2.0	+ -
0.9	5.0	20	4.0	1.0	2.0	+ -
1.0	5.0	20	4.0	1.0	2.0	++ -

Table 13: Results of experiments on phosphor bronze plates (R 1178); delay = 2.0 ms; air;  $I_L = 420 \mu\text{m}$ .

$P_{\text{laser}}$ (kW)	$t_l$ (ms)	$I_{\text{arc}}$ (A)	$t_a$ (ms)	$l_c$ (mm)	$l_a$ (mm)	result
0.5	3.0	20	4.0	1.0	2.0	--
0.7	3.0	20	4.0	1.0	2.0	+--
0.9	3.0	20	4.0	1.0	2.0	+--
1.0	3.0	20	4.0	1.0	2.0	++
0.5	4.0	20	4.0	1.0	2.0	+ -
0.9	4.0	20	4.0	1.0	2.0	++
0.7	4.0	20	4.0	1.0	2.0	++

already in successful attraction), and the overlap time can also be less (0.2 ms less, for this type of material).

#### 5.1.10 Influence of workpiece material

If the combined process proves to be successful and profitable, it will probably be used for spot welding phosphor bronze pins. Before testing the actual pins, the attraction was examined using small rectangular phosphor bronze plates (R 1178). At the same time information is gained on the changes in the attraction behaviour of the arc when the workpiece material is changed.

At first the welding conditions were chosen the same as the standard conditions. Under these conditions there was no attraction, not even when the arc length and the critical distance were changed. Apparently, the laser intensity is not high enough to make a melt, there is hardly any change on the surface visible. No particles are freed from the surface, which enable the arc to be conducted by means of the laser plume to the laser spot on the workpiece surface (see § 5.4). This indicates that the coupling of the laser energy into the material surface is more difficult as compared to the Cr/Ni-steel, the reflection is higher.

In order to create a plume the laser power was increased (from 0.5 kW) in steps of 0.2 kW to 1.0 kW, see table 12. The results yield only a small increase in attraction (double spots and combined spots). To achieve successful attraction, the laser pulse duration was increased, see table 12. This seemed to be almost successful for 1.0 kW/5 ms.

Because the coupling of the laser energy into these phosphor bronze plates differs from the coupling into the steel plates, it could be possible that the effective laser plume takes a longer time to form when using phosphor bronze. So, maybe increasing the delay time (with respect to the standard conditions) would help. The delay was increased to 2 ms, see results table 13. Initially, there seems to be no change. After increasing the laser power to 1.0 kW, the attraction improved. Of the five times the combined spots were made with 1.0 kW/3 ms for the laser, two times resulted in successful attraction. Now decreasing the laser power to 0.5 kW and increasing the laser pulse duration to 4 ms also improved the attraction. Was it not possible to have any attraction with a laser power of 500 W before (delay 1 ms, see above), now there were two successful attractions, see table 13. Increasing the laser power drastically to 700 W or higher resulted in 100 % successful attractions. With 600 W laser power the attraction became poor, so 700 W/ 4 ms (=2.8 J) at least is necessary to have 100 % good attractions when phosphor bronze is used. Compared to the Cr/Ni-steel, where 0.6 J was sufficient, this is very high. Obviously, the material type (reflection/ absorption, heat conduction etc.) is an important factor for determining the attraction of the TIG arc to the laser spot position.

## 5.2 Results of experiments on phosphor bronze pins

For the experiments on the pins, the inclination angles of the TIG torch and the laser optics need to be changed into 10° and 15° respectively (see figure 42).

From the results on the phosphor bronze plates it came forward that a delay of 2 ms is needed in order to have some attraction. And that for successful attraction to occur the laser power at least must be set at 700 W and 4 ms pulse duration .

First two pins are contacted. The configuration of pins, TIG torch and laser head is also shown in figure 42. The tests are first conducted in air. When the electrode is positioned in the

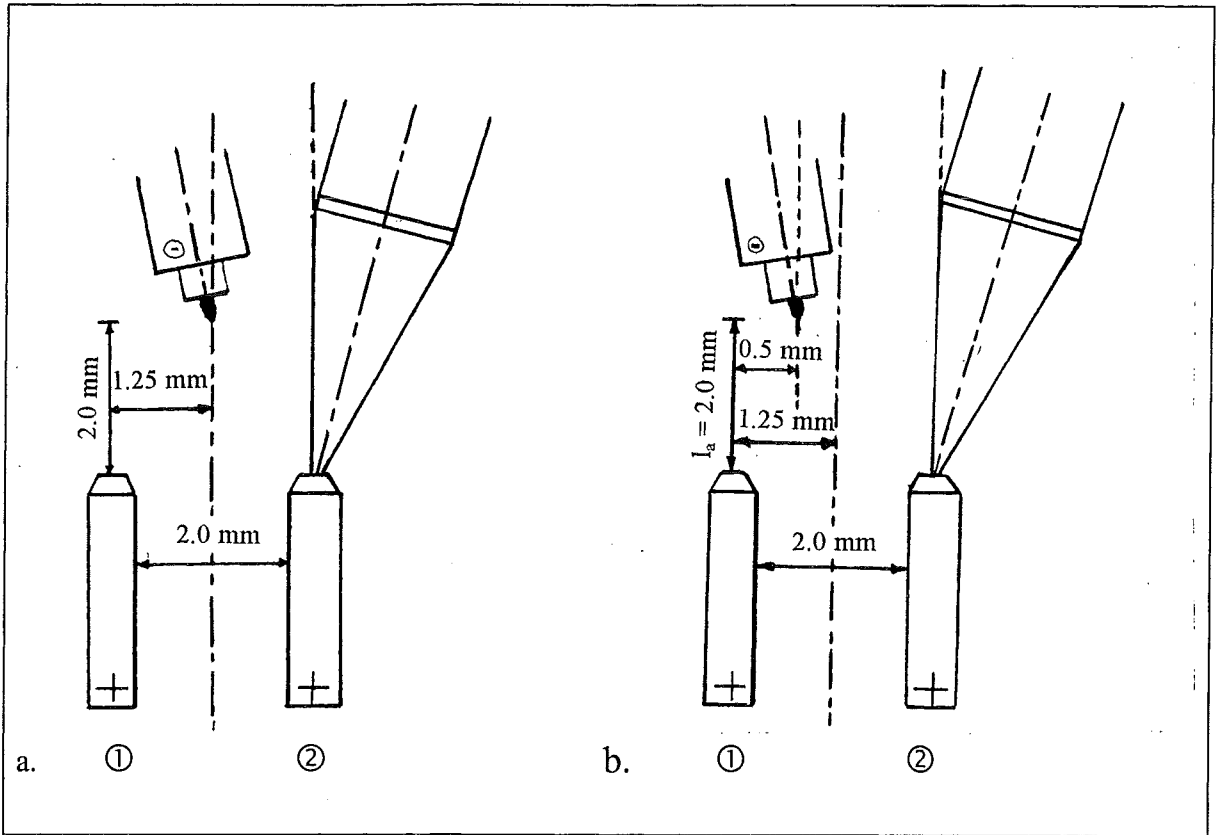


Figure 42: Schematic view of configuration of laser head, TIG torch and pins for experiments on pins.

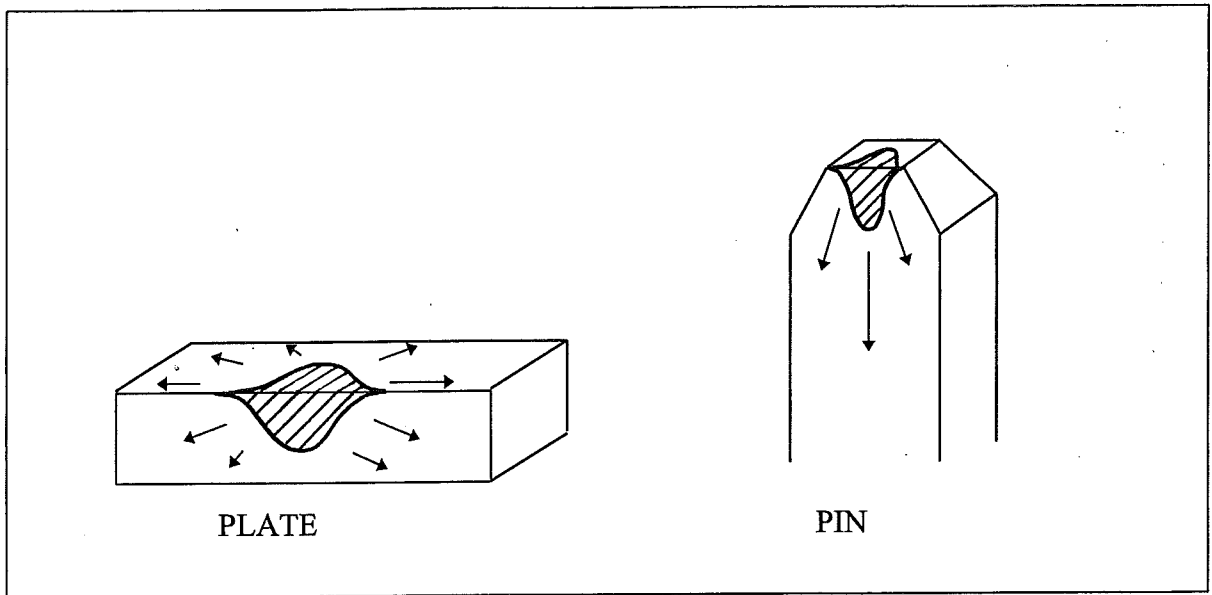


Figure 43: Heat flow in plates and pins.

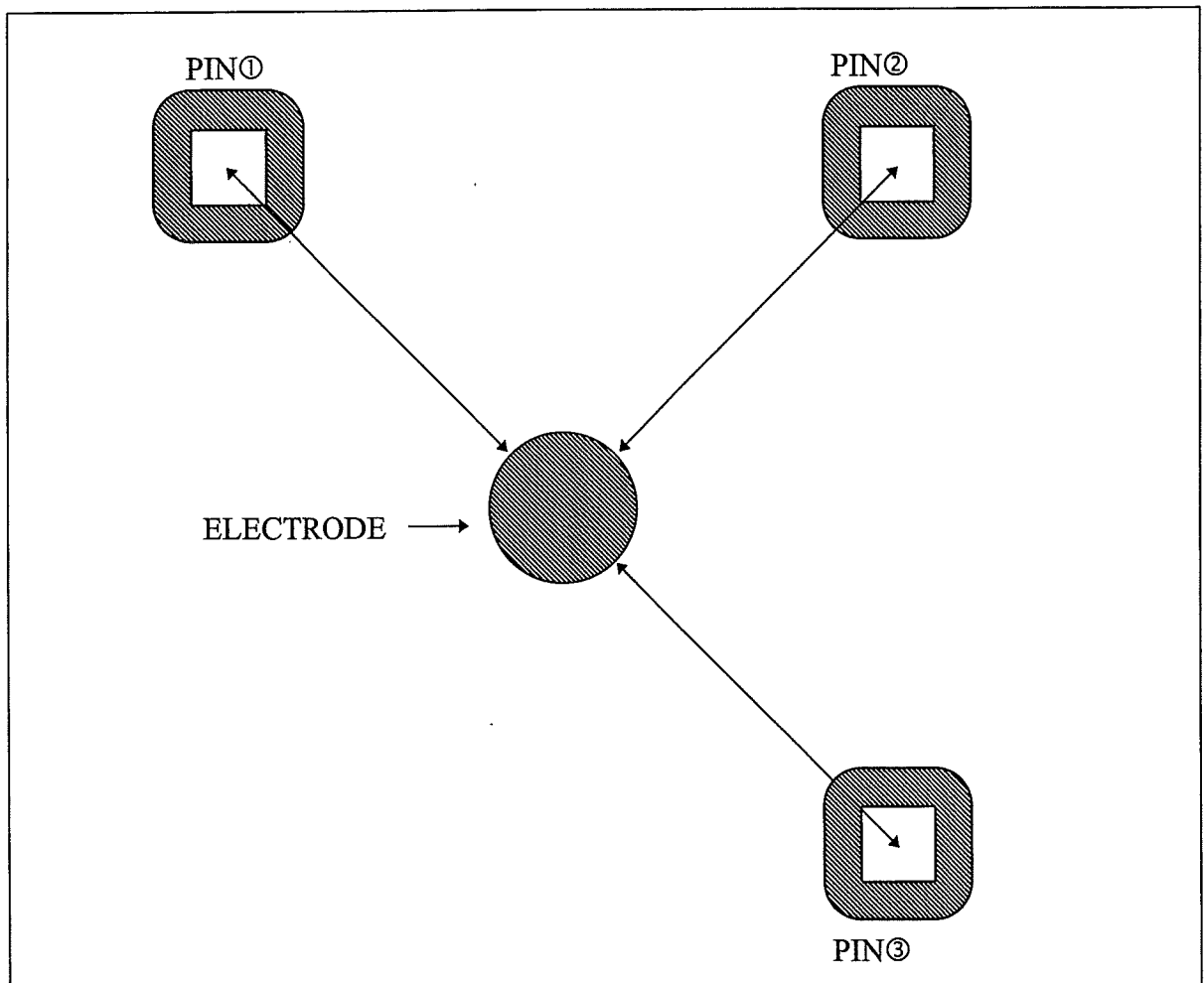


Figure 44: "Jumping" experiment, schematic top view.

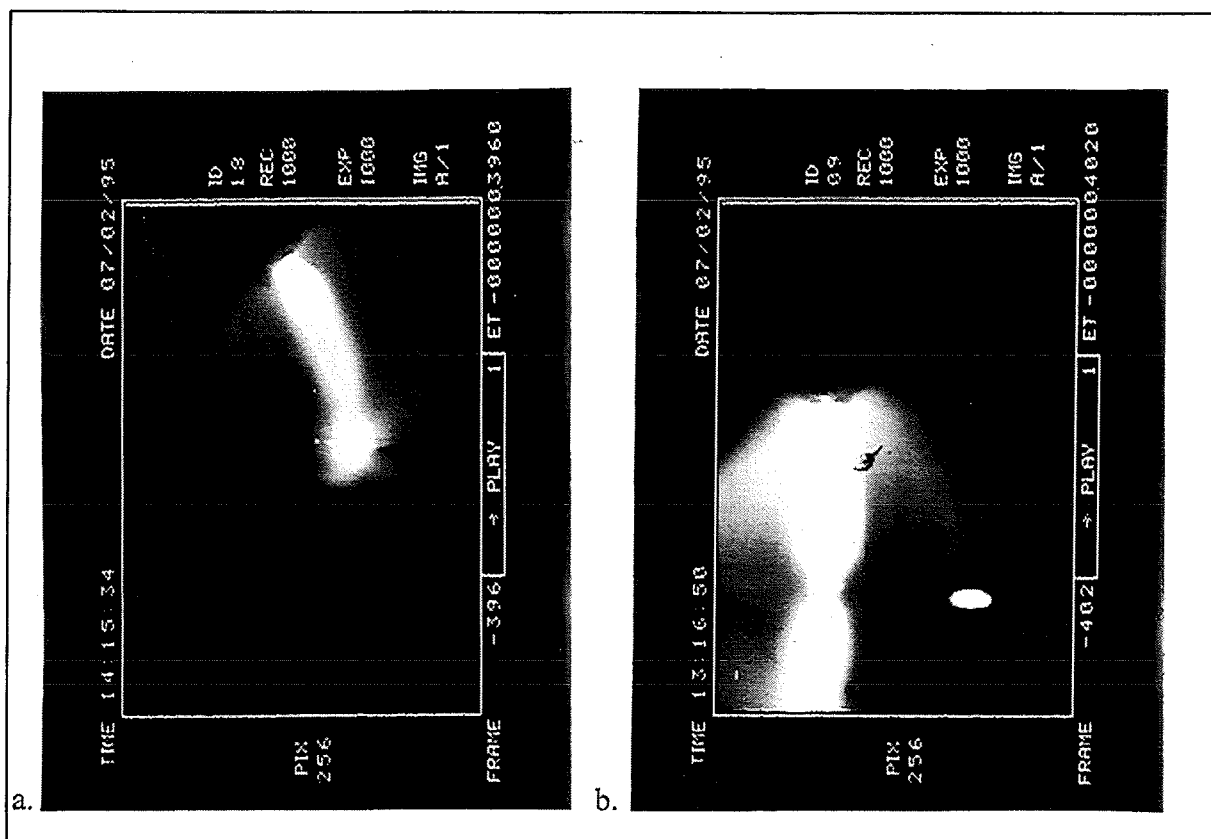


Figure 45: Video print of  
 a. successful attraction (standard conditions,  $l = 1.0$  mm,  $l_a = 2.0$  mm);  
 b. unsuccessful attraction (standard conditions,  $l = 2.0$  mm,  $l_a = 2.0$  mm).

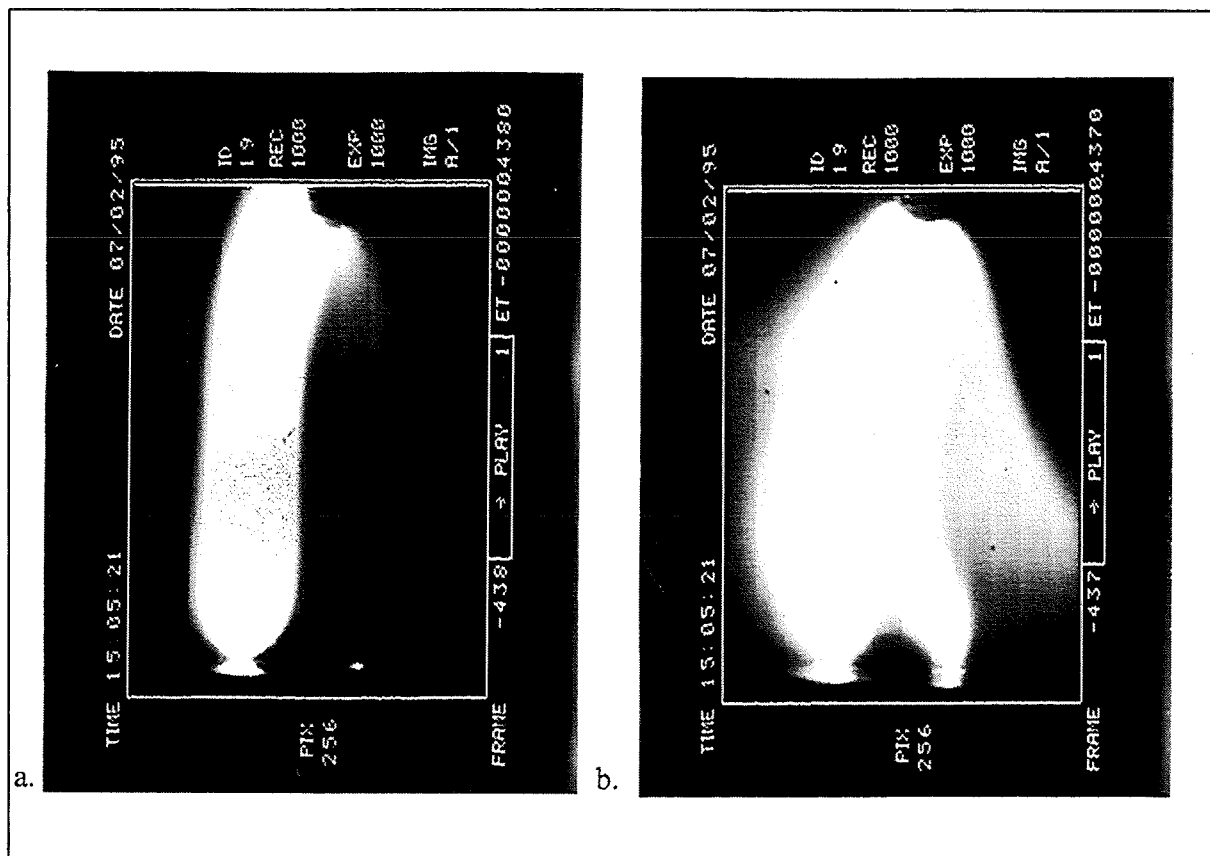


Figure 46: Video print of the creation of the "double spots"(continued on next page).

middle of these two pins (figure 42a), the arc moves arbitrarily to pin ① or pin ② when only the arc is triggered. However, if the laser is directed onto pin ② and both laser and TIG are triggered, the arc moves consequently every time to pin ②. The arc length varies hereby between 1 and 3 mm.

The laser pulse on top of the pin looked more powerful than the same pulse on the phosphor bronze plates. This is caused by the difference in geometry. In the plates the heat of the incoming laser beam can flow away in three directions, see figure 43, whereas the heat of the laser beam in the pin can only diffuse downward. So the heat is used more effectively (faster build up of heat) in a pin-like geometry. Knowing this, it should be possible that a lower laser energy is enough for attraction to occur at the pins and maybe a delay of 1 ms is also sufficient. Therefore first the laser power was reduced to 200 W with a pulse duration of 3 ms, but the delay was held at 2 ms. For the same configuration (figure 42a) this resulted in successful attractions too. So the geometry of the workpiece is definitely of influence on the attraction behaviour.

In a following step the delay was set to 1 ms. The 200 W/3 ms set of the laser pulse was not effective enough in attracting the arc to pin ②. Increasing the laser power to 400 W resulted in the movement of the arc to pin ② and thus successful attraction.

Next, the electrode was positioned 0.5 mm from pin ①, see figure 42b. When the laser power is increased with 100 W, thus now 500 W/3 ms, the arc still moved to pin ②. Positioning the electrode above pin ① and the laser above pin ② did not result in attraction. Even if the power or the delay are increased. The electrode is too close to pin ① to follow the easy path to pin ②.

It was also tested if it was possible to jump between the pins. Hereto the configuration was set as is shown in figure 44. The electrode is positioned at equal distances from pin ①, ② and ③. All three pins are contacted. The laser is directed to pin ① (with laser 500 W/3 ms). When only the TIG arc is triggered, the arc moves arbitrarily to pin ①, ② or ③. There seems to be no preference towards any pin. When both laser and TIG are triggered (standard conditions), the arc is each time attracted to pin ①. Directing the laser to pin ②, and repeating the experiment results in the arc moving only to pin ②. The same result is obtained when the laser is directed to pin ③. Also with lower laser values of 200 W/3 ms the same results are obtained (in spite of the earlier tests performed with these values).

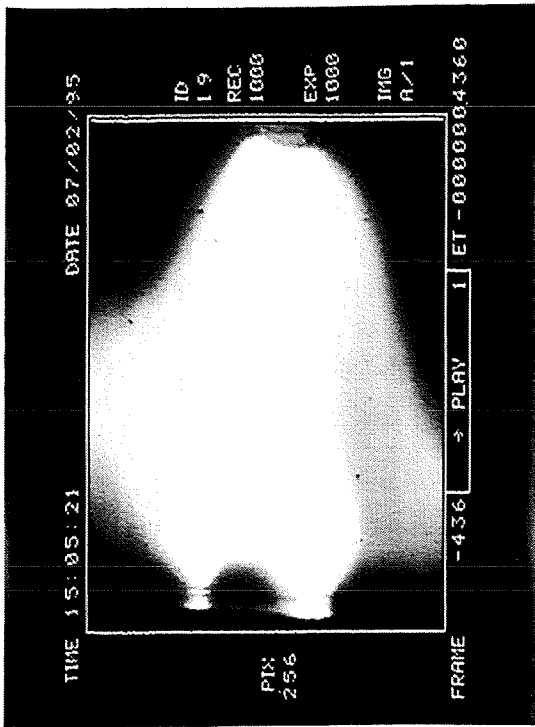
As TIG welding is usually performed with a shielding gas, the tests are also conducted with argon shielding. Larger arc lengths than in air are possible ( $\pm 5$  mm was tested). Testing in argon made it very difficult to actually see to which pin the arc was going. When the same test was done as is shown in figure 41b, which resulted in successful attractions to pin ②, there were spots on both pins visible after pulsing. What happens here is shown in section 5.3, where the results of the use of the high speed video camera is presented.

In air the electrode and pins are very quickly and heavily polluted, as when argon is used, pollution of the electrode and pins hardly occurs.

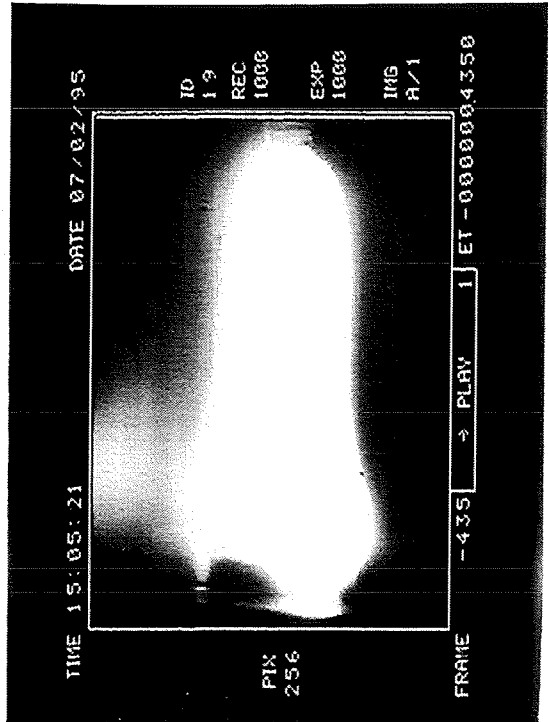
### 5.3 High speed video camera

In order to see what happens when the arc is combined with a laser and for better understand-

c.



d.



e.

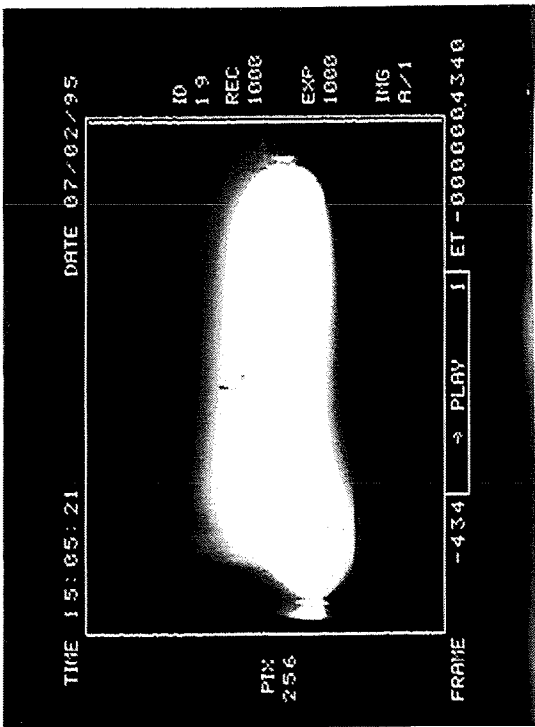


Figure 46: continued. Conditions: arc: 30 A/4 ms; laser: 0.5 kW/3 ms; argon;  $l = 1.0$  mm  
 $l_a = 7.0$  mm; delay = 1.0 ms;  $I_L = 420$   $\mu$ m.

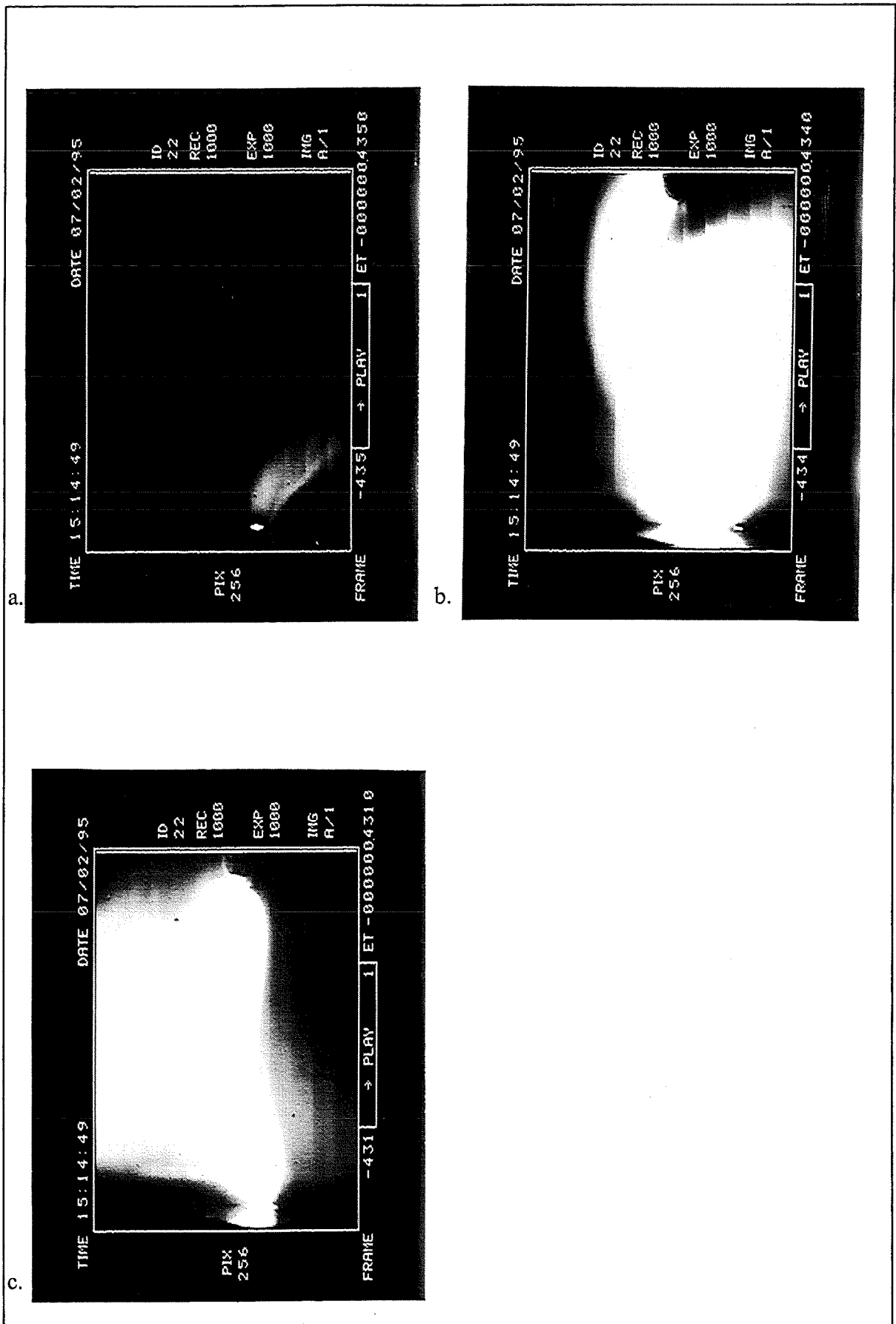


Figure 47: Successful attraction (no double spot) at higher arc lengths. Conditions: arc: 30 A/4 ms; laser: 1.0 kW/3 ms;  $l = 1.0$  mm;  $l_a = 7.0$  mm; delay = 1.0 ms; argon;  $I_L = 420\mu\text{m}$ .

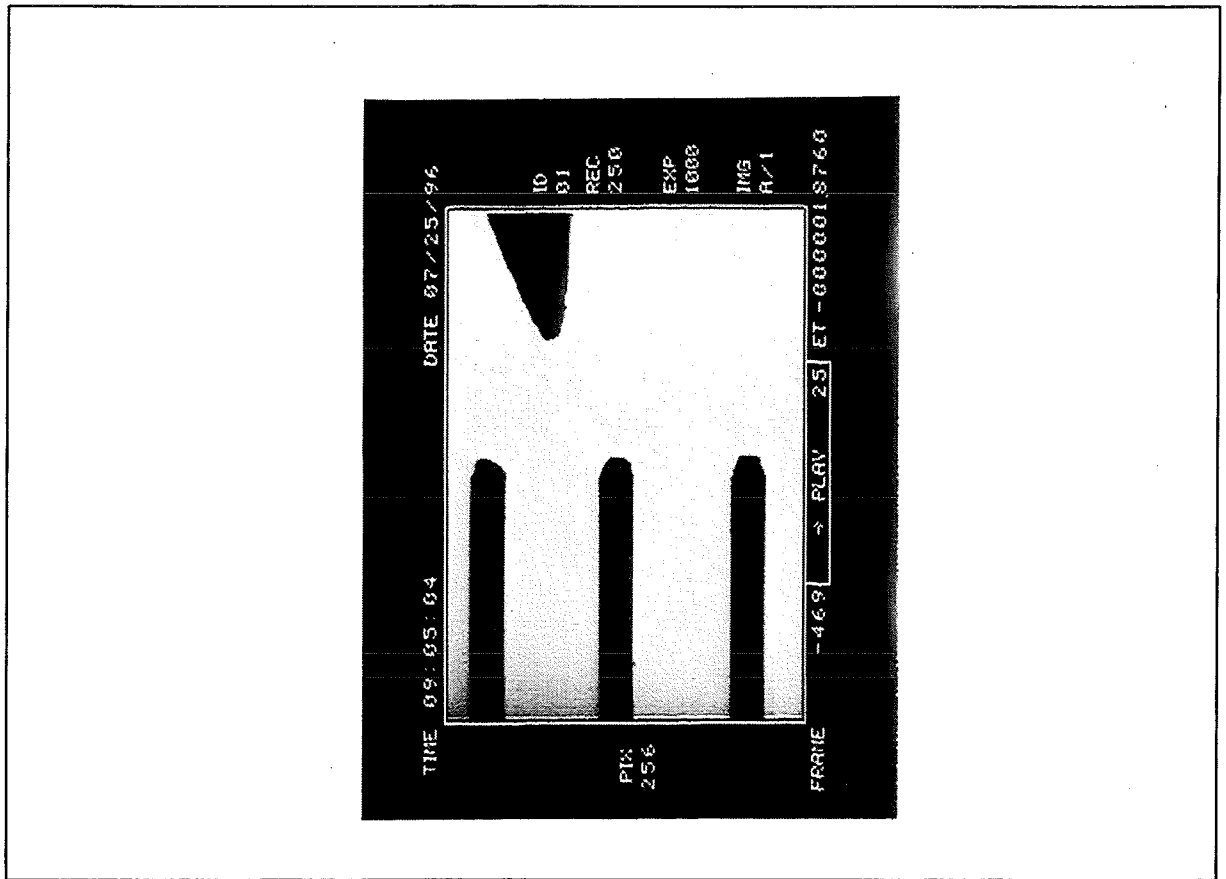


Figure 48: Position of pins and electrodes before pulsing.

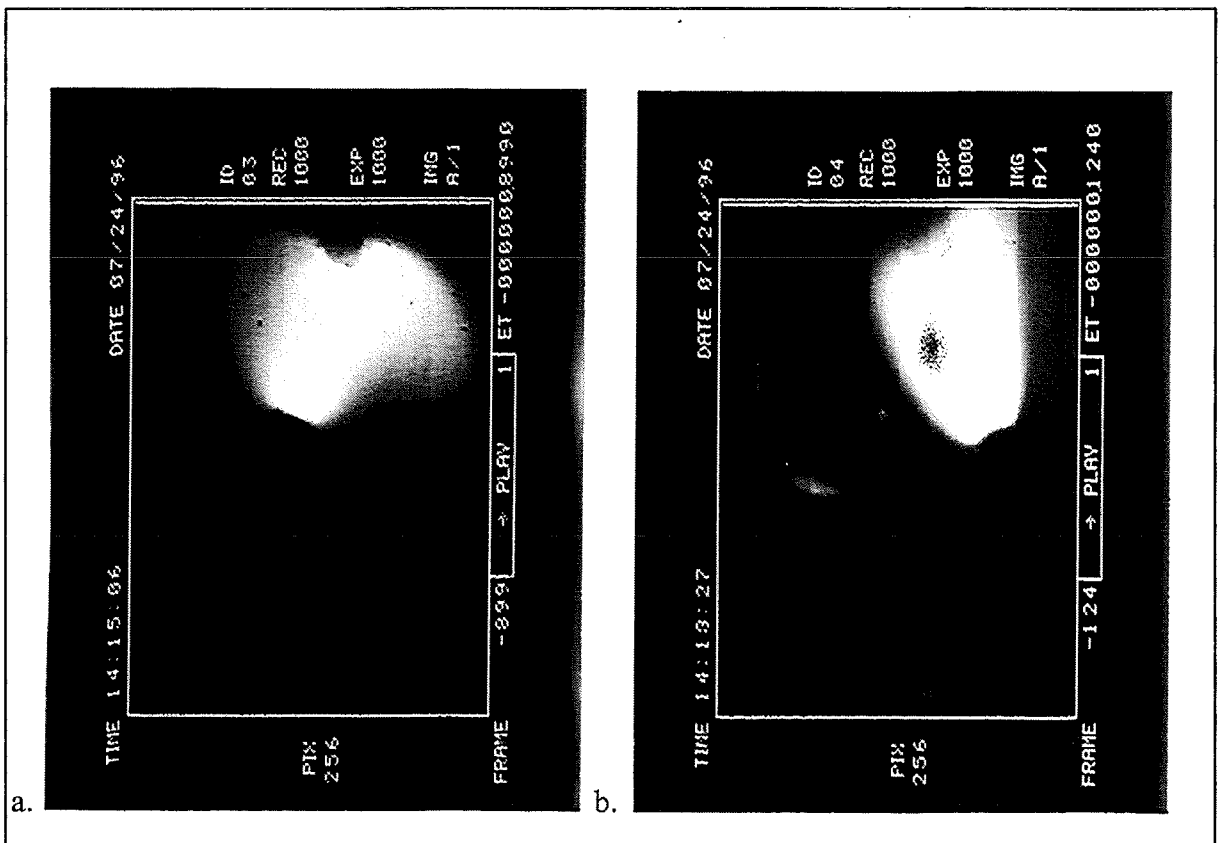


Figure 49: Position of arc during experiments on pins. Conditions: arc: 20 A/4 ms; laser: 0.5 kW/3 ms; delay = 1.0 ms;  $I_a = 2.0$  mm; air;  $I_l = 420$   $\mu$ m.

ding of some phenomena which occur during the attraction of the arc to the laser spot position, the process is recorded with a high speed video camera. Several attraction tests have been recorded. The speed of filming is 1000 images per second.

The image is slightly deformed in the vertical direction on the screen. As the camera was tilted while filming, this distortion in the image is in reality thus in the horizontal direction. From the video tape pictures were made with a video printer. These pictures will be shown here, in order to spread some light upon the attraction process.

First, in figure 45a a picture is shown of successful attraction under standard conditions ( $l = 1.0$  mm). It can clearly be seen that the arc diverges from the straight path towards the workpiece surface. Figure 45b shows the situation if there is no attraction (same conditions,  $l = 2.0$  mm); then the straight line to the surface is being followed.

In figure 46 the creation of the "double spots" is shown (in argon). At the beginning of the TIG pulse (a) the arc goes to a position of the workpiece surface which does not lie exactly straight under the electrode. The laser spot position can also be seen at the right of the arc spot. In the next time step (b) it can be seen that the arc is being split into two parts. One part of the arc is attracted to the laser plume position, the other stays at the arc spot position. In the next two time steps (c and d) it is shown that more of the arc is being drawn to the laser plume and finally, in (e), the arc has entirely moved to the position of the laser plume.

If the laser power is increased to 1.0 kW and the other conditions remain the same as they were in figure 46 then the arc moves immediately to the laser plume position. This is shown in figure 47b+c. In figure 47a only the laser plume is visible. The argon flow blows the plume in a direction away from the electrode, which is totally wrong for the attraction effect. In (b) and (c) the attraction to the laser plume is shown. Here too, the deflection of the arc from the straight line can be seen. In comparison with the situation shown in figure 46 the laser plume now reaches higher which results in an immediate attraction instead of the "double spots" situation.

It was also seen that an arc pulse duration of 9.9 ms (20 A/0.5 kW/3 ms,  $l_c = 1.0$  mm, arc length = 5.0 mm) resulted in "double spots" (or no attraction), whereas, under the same conditions but for a pulse duration of 4 ms, there was successful attraction.

Next, the situation during the experiments on the phosphor bronze pins is recorded. Figure 48 shows the situation before pulsing as was described in § 5.2, figure 42a. When only triggering the TIG, the arc moves only towards pin ① which is shown in figure 49a. If the laser is triggered too (laser is positioned onto pin ②) the arc moves only to pin ②, figure 49b. Once the arc moved to both at the same time (divided into two) which is shown in figure 50. This dividing of the arc occurs every time if the tests are conducted in an argon environment.

#### 5.4 Model

From the previous paragraphs it becomes clear that in micro arc welding the arc can be guided (attracted) by a laser. The main parameters determining the attraction are: arc current, arc length, TIG pulse duration, laser pulse duration, delay time between triggering laser and TIG, workpiece material, laser intensity, welding atmosphere, workpiece geometry and the critical distance.

The delay time and both pulse durations are related which makes their influence somewhat complicated, especially that of the delay time and the TIG pulse duration.

Next, an attempt will be made to explain what happens during the combined spot welding process as a consequence of which a general equation will be derived for the critical distance.

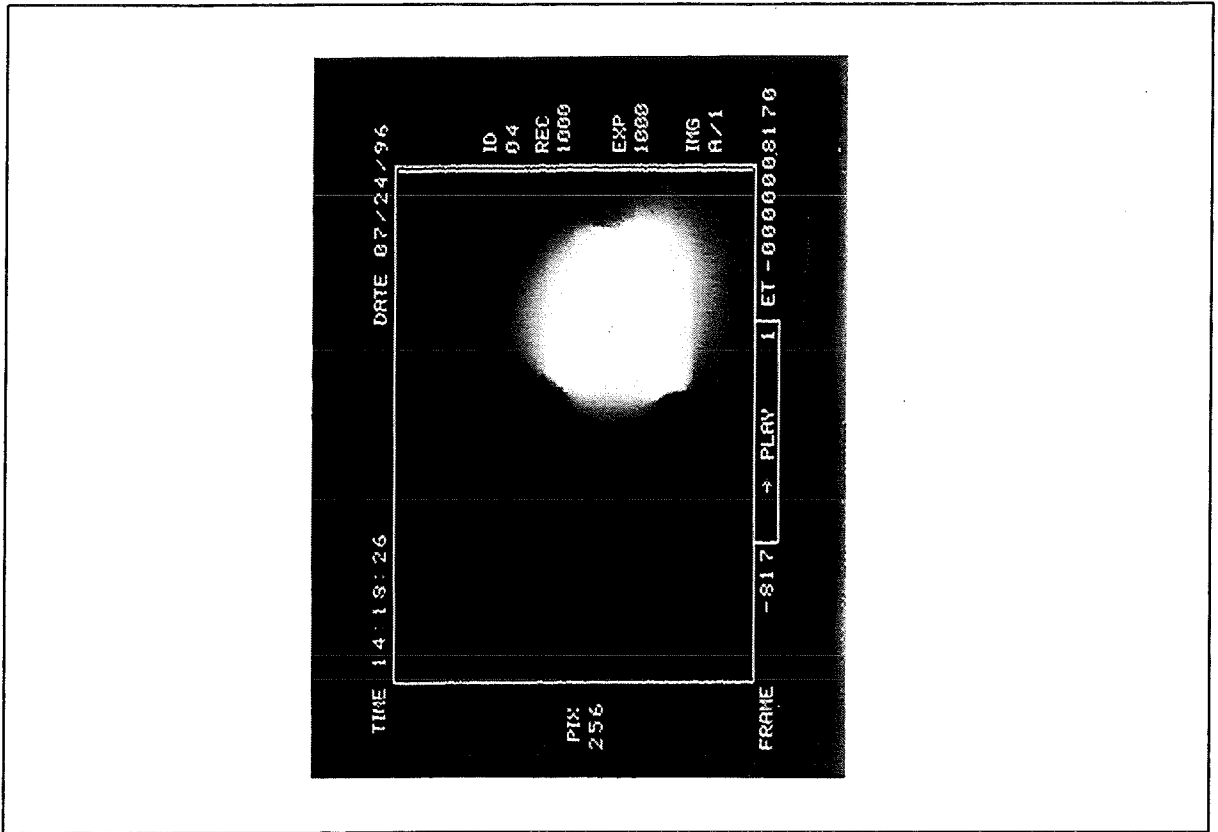


Figure 50: Deviding of arc (every time when argon is used). Conditions: arc: 20 A/4 ms; laser: 0.5 kW/3 ms; delay = 1.0 ms;  $l_a = 2.0$  mm; argon;  $I_L = 420$   $\mu$ m.

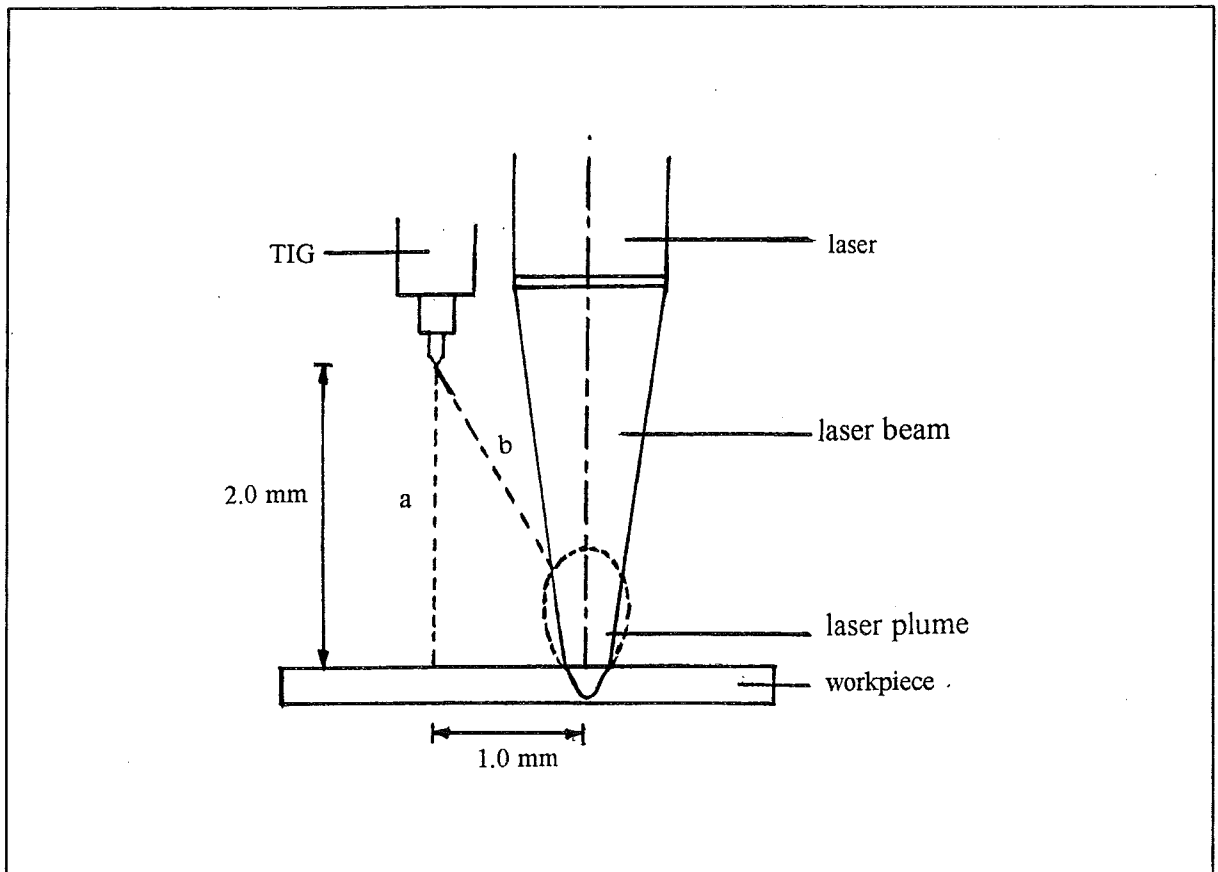


Figure 51: Schematic view of laser plume and arc “attraction” ( $l_a = 2.0$  mm,  $l = 1.0$  mm).

In figure 51 the laser, TIG and workpiece are schematically shown. The figure shows how they are placed with respect to each other and where the arc and the laser plume are. What occurs during the combined pulses is the following. The laser beam is directed to the workpiece and will melt the surface of the workpiece locally if the energy is high enough. Initially, only electrons are released from the workpiece surface, by the transferred heat of the laser beam. But when melting occurs, metal vapour is also formed right above the melt pool (chapter 3).

The electron current density can be calculated with help of Richardsons equation (1) (§ 2.2). With the temperature of the surface increasing above the boiling temperature, metal atoms (vapour) are also released. The electrons and metal vapour form the laser plume which is seen above the weld pool. The metal atoms in the plume can absorb energy from the laser beam and it is possible that a small part of the atoms is ionised, according to Saha's equation (2). Thus, all these elements in the plume (plasma like) make the plume electric conductive. Now, consider the electrode positioned at 1.0 mm in horizontal and 2.0 mm in vertical direction from the laser spot centre, see figure 51. If the laser is triggered at first, a plume will be formed as was mentioned above, assuming that the energy and intensity are high enough. The arc is triggered at a time when the plume is already formed. Then the arc will go to the workpiece surface following the "easy path" created by the laser plume, instead of going to the workpiece following the common route (straight to the surface as shown by the dashed line a in figure 51). The conduction in the plume is higher than that of the metal workpiece, and the distance (line b) between the plume and electrode tip is also shorter than the vertical distance to the workpiece (line a). Thus the laser plume will operate as a conductor or a kind of antenna. In figure 52 a different situation is presented. In comparison with the situation in figure 51 the electrode was moved 1.0 mm to the left. Thus both distances are now 2.0 mm. From the results of the influence of  $l_a$  (table 11) it can be seen that the attraction at these distances is medium. Half of the combined pulses results in a successful attraction. This can be considered as a critical situation. In figure 52 it can be seen that in this situation the distances a and b are almost equal. Thus, when the arc is triggered (after the laser) it will randomly go to the laser plume position or straight to the workpiece. If the horizontal distance (l) increases further, the arc is no longer attracted by the laser plume as the distance b has become larger than distance a. Now, if  $l=2.0$  mm and the arc length  $l_a$  increases from 2.0 mm to 3.5 mm (see figure 52) the situation is no longer critical and the distance to the plume is again shorter as to the surface. Therefore, this will again result in successful attraction.

Returning again to the situation in figure 51. If the arc current is increased, the arc will expand (becomes wider) and is able to reach the plume at a bigger distance.

If the laser power is increased (which is in fact the increase in laser intensity), it results in an expansion of the laser plume (height as well as width). As a consequence, distance b in figure 52 decreases and the arc is attracted to the plume all the time. Thus  $l_c$  increases. The same effect is reached when the laser pulse duration is increased, except on a smaller scale.

Changing the magnification factor (spot size now  $\pm 300 \mu\text{m}$  instead of  $\pm 420 \mu\text{m}$ ) but with the same laser energy results in the energy being transferred into a smaller area (increase in intensity). Therefore more particles are released from the melt pool and thus a lower energy will result in a similar laser plume (similar in height and conductivity) as with a higher laser energy with a higher magnification factor.

In a workpiece with a geometry which allows the heat to flow away in three directions (plate like) the heat will not be build up as high as when the geometry is such that the heat can only flow away in one direction (pin like). Thus, in the latter situation the melting and boiling temperature will be reached earlier and with less energy.

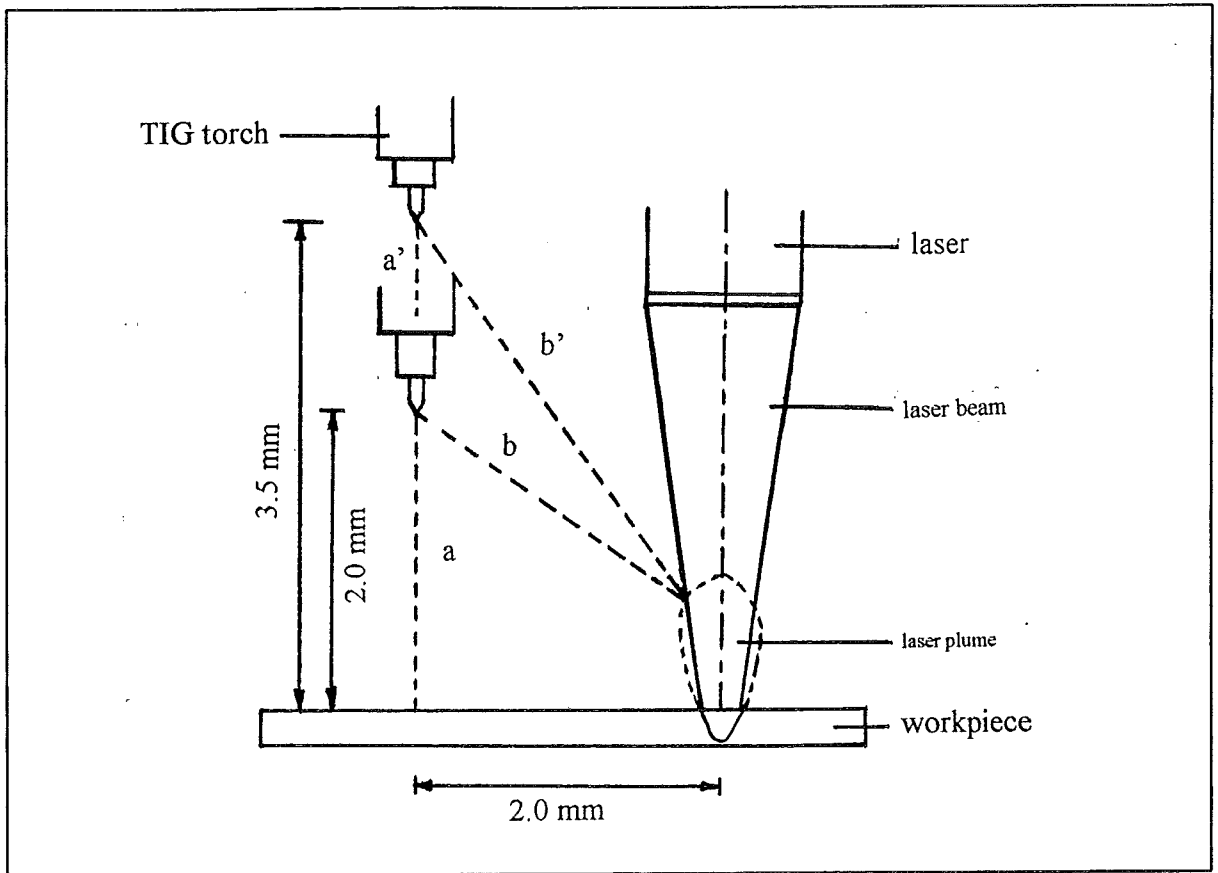


Figure 52: Schematic view of laser plume and arc “attraction” for different situations.

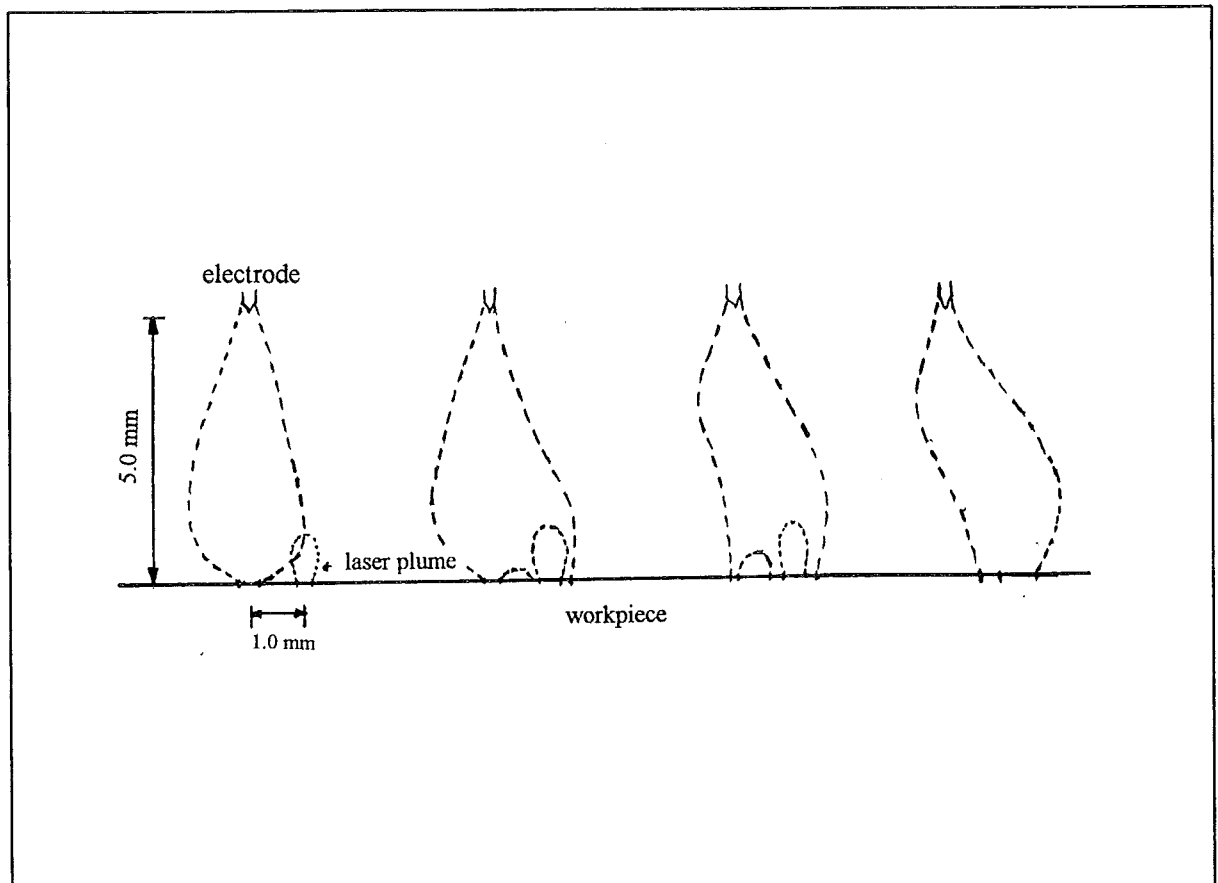


Figure 53: Schematic view of “arc deviding” in argon at higher arc lengths (> 4.0 mm).

The plume needs time to develop. If the arc is triggered too soon, there is no attraction, because the plume is not high or conductive enough. Therefore a delay time is needed between the triggering of the laser pulse and the TIG pulse.

Also the type of material determines the heat conductivity, the electrical conductivity, the boiling and melting temperatures etc. This means that the height and width of the plume and the character of the particles in the plume are dependent on the type of material.

How the TIG pulse duration fits in this model is not yet understood exactly. The width of the arc increases with increasing pulse duration. Anyway, the influence of the TIG pulse duration depends on the delay time and the laser pulse duration.

In argon the critical distance increases at first, because the arc length can be increased (as was explained in figure 52 where the  $l_a$  was increased from 2.0 to 3.5 mm, which resulted in successful attraction). However, above an arc length of 4.0 mm  $l_c$  decreases and the "double spots" are created. As could be seen in the video prints (§ 5.3) the argon flow blows the plume away from the electrode. If the arc length has reached a certain distance (5.0 mm in this case) the distance between the electrode and plume is no longer smaller as the distance to the workpiece and the conductivity is not high enough to attract the arc immediately to the plume. The arc initially goes straight to the workpiece surface, but part of the arc reaches the better conductive plume and therefore is drawn to the plume position (if  $l$  is small enough). This is shown schematically in figure 53. Gradually all energy of the arc is transferred to the plume position and a small arc spot stays behind. Knowing all this, it may be possible to derive a general equation with the influencing parameters in it. However, it is not possible to give an exact equation, as the conducted tests are not sufficient. In order to determine the exact relations, the influences have to be examined more thoroughly. Smaller steps have to be taken and there has to be more knowledge of the laser plume. This is currently not fully understood. First of all, the critical distance can be seen as a function of:

$$l_c = f(I, l_a, I_L, t_l, t_a, \Delta t, \text{geometry (d,h), material, welding atmosphere}),$$

in which:  $I$  = arc current

$l_a$  = arc length

$I_L$  = laser intensity

$t_l$  = laser pulse duration

$t_a$  = TIG pulse duration

$\Delta t$  = delay time

$d$  = laser spot diameter (presented area)

$h$  = visible welding area

From the figures shown in the results and the discussion in the previous sections, the relations should be as follows:

$I$ : from figure 23 it is seen that the relation is not linear. The relation will be stated as  $\sim I^b$ .

$l_a$ : this relation is given in figure 21. A straight line could be drawn through the points, but it is not yet known if that is allowed (too little measuring points). Thus the relation will be expressed as  $\sim l_a^f$ .

$t_a$ : this relation is initially a decreasing  $l_c$  with increasing pulse duration, but after a few milliseconds there is an increase. However the arc pulse duration is also dependent on the laser pulse duration and the delay time. How they are related is not yet understood and therefore this parameter will not be included.

$t_l$ : from section 5.1.7 the relation seems to be  $\sim t_l^g$



$\Delta t$ : an initiation time and an overlap time are needed. This is dependent on the material type and laser values. How to relate this parameter is not yet understood either so it will not be included.

$I_L$ : increasing  $I_c$  with increasing laser intensity. There is a threshold value ( $I_{L0}$ ) to overcome in order to create a plume, which is dependent on the material type. Thus the relation will be  $\sim I_L^k + I_{L0}$ .

geometry: The influence can be expressed as the ratio of the presented area (area of laser spot; proportional to  $d^2$  in which  $d$  is the spot diameter) and the visible area ( $h$ ). Thus the relation will be presented as  $\sim (d^2/h)^m$

material type: this parameter indirectly influences all parameters. The material influence can be taken into the equation as coefficients with which the other parameters have to be multiplied.

welding atmosphere: if a shielding gas is used it will have an influence on the plume creation. This influence manifests itself in i.g. slower/faster plume creation, longer/smaller arc lengths. This parameter will be accounted for in the coefficients with which the other parameters will be multiplied.

Taking all these relations into account, the critical distance, which is a measure of the attraction of the arc by the laser, can be expressed as:

$$I_c = C_0 + \alpha I^b + \beta I_a^f + \varepsilon t_1^g + \eta (I_L^k + I_{L0}) + \lambda (d^2/h)^m \quad (15)$$

in which  $C_0$  is a constant. All coefficients ( $\alpha, \beta, \varepsilon, \eta, \lambda$ ) are dimensional coefficients, whereas the exponents ( $b, f, g, k, m$ ) are non-dimensional.

The values of the coefficients and exponents can be obtained by means of a fitting procedure, using the experimental data as input, when more small (measuring) steps are made.



## 6. CONCLUSIONS & RECOMMENDATIONS

### Conclusions:

From the foregoing chapters the following can be concluded:

- \* It is possible to attract the arc to the laser spot position when pulsed micro welding is concerned. Thus the arc can be manipulated with the laser in order to force the arc to a precisely defined position.
- \* A model for the attraction effect has been derived and this resulted in a general equation for the critical distance, which is the maximum (horizontal) distance over which the arc is still attracted.
- \* The critical distance varies between 0 and 3.0 mm. This is strongly dependent on the conditions. The influencing parameters are: arc current, arc pulse duration, laser power, laser pulse duration, delay time between triggering laser and TIG, laser intensity, material type, workpiece geometry and the welding atmosphere.
- \* Welding in air results in no "double spots", welding in argon does. However, this only occurs at arc lengths higher than 5.0 mm. In argon the spot welds are much cleaner and there is no spatter.
- \* The minimum laser energy at which attraction occurs is 0.45 J (150 W/3 ms with f 50 lens, for the Cr/Ni steel plates (N286)).

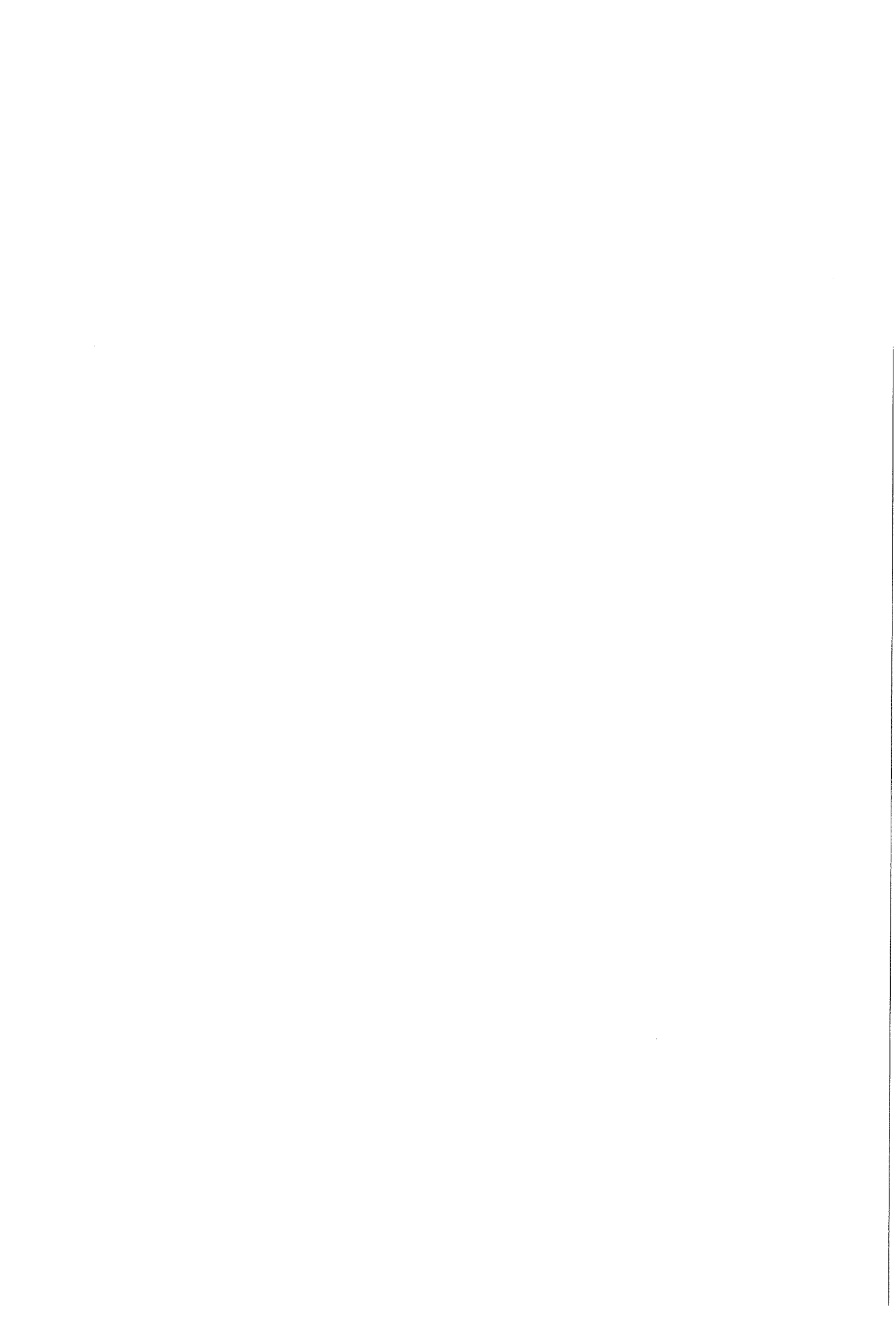
A possible application of the combined welding process is pulsed micro TIG welding of phosphor bronze pins used in various components. The electrode can be placed at a fixed position and through means of positioning the laser on the pins surrounding the electrode, it is possible to weld a group of pins without having to move the electrode. The laser energy has to be as low as possible to make this an attractive (not too expensive) process.

Also this manipulating with the laser can be used for precision micro arc welding processes, because, in case of plates, the position of the arc spot no longer will be random but can be determined precisely.

### Recommendations:

Looking at the model and the derived general equation it becomes clear that the influences are not precisely known. In order to fully understand the attraction process various tests need to be conducted. Therefore some recommendations are:

- \* In order to determine the exact influence of the parameters, more tests have to be conducted with smaller steps.
- \* The influence of the arc pulse duration on the attraction and its relation to the laser pulse duration and delay time needs to be investigated more thoroughly.
- \* Optimising the welding conditions will reduce the required laser energy which is needed in order to have attraction.
- \* The TIG testing device has to be made more reliable. There is too much disturbance in the results which originate from the TIG power source. Also the used gas cup needs to be adapted/redesigned in order to manipulate the argon flow and to exclude the gas cup being electrically charged (which happened a few times during testing).
- \* The resistivity of the arc during the combination process should also be monitored. This could contribute to a better understanding (explanation) of the attraction behaviour.
- \* It is important to know what precisely happens during the laser plume formation; which particles are released, how much particles are released, which height they reach under



certain conditions, if a plasma is formed at these short laser pulse durations etc. Knowing all these facts will make it possible to determine the size of the plume. Then an empirical expression can possibly be determined in which the size of the plume will be given as a function of the already known parameters and in which  $l_c$  is also a parameter; because of the importance of the laser plume in the whole attraction process.

- \* The material influence on the critical distance has not been examined properly. More material types have to be tested in order to determine the influence.
- \* The arc-ignition-by-laser test should be tested with other arc welding power units in order to determine if this is a possibility.



## REFERENCES

- [1] Z.Z. Moeniralam  
Wisselwerking tussen laserlassen en booglassen  
Literatuurscriptie, Delft, 1996
- [2] G. den Ouden  
Lastechnologie  
Delftse Uitgevers Maatschappij b.v., Delft, 1993
- [3] J.W. Hooijmans  
Hydrogen absorption in iron and steel during gas tungsten arc welding  
Thesis, Delft University Press, Delft, 1994
- [4] L.P. Connor (editor)  
Welding Handbook vol. 1 & 2, 8th edition  
American Welding Society, Miami (USA), 1991
- [5] J.P. Zijp  
Heat Transport during Gas Tungsten Arc Welding  
Thesis, Delftse Uitgevers Maatschappij b.v., Delft, 1994
- [6] J.F. Lancaster  
The Physics of Welding, 2nd Edition  
International Institute of Welding
- [7] W.G. Essers (author)  
TIG- en Plasmalassen  
VM-publikatie, voorlichtingsblad NIL-project (Nederlands Instituut voor Lastechniek)
- [8] H. Cui  
Untersuchung der Wechselwirkungen zwischen Schweißlichtbogen und fokussiertem  
Laserstrahl und der Anwendungsmöglichkeiten kombinierter Laser-Lichtbogentechnik  
Dissertation, Braunschweig (Germany), 1991
- [9] C. Dowes  
Laser Welding  
Abington Publishing, Cambridge (England), 1992
- [10] C.J. Nonhof  
Material Processing with Nd-lasers  
Electrochemical Publications Limited, Ayr (Scotland), 1988
- [11] W.M. Steen  
Laser material processing  
Springer-Verlag London Ltd., Germany, 1991
- [12] A.G. Grigoryants  
Basics of laser material processing  
CRC Press, Inc., Florida (USA), 1994
- [13] E. Beyer, U. Dilthey, R. Imhoff, C. Maier, J. Neuenhahn and K. Behler  
New aspects in laser welding with increased efficiency  
From: Proceedings of the laser welding materials processing-ICALEO'94  
Orlando (USA), 17-20 october 1994, 183-192



## APPENDIX A

Table 1: Results arc current influence. Conditions: arc: 4 ms; laser: 0.5 kW/3 ms; air; delay = 1 ms;  $I_L = 420 \mu\text{m}$ .

25 A:

l (mm)	arc length (mm)						
	1.0	1.5	2.0	2.5	3.0	3.5	4.0
0.5	++	++	++	++	++	++	+-
1.0	+-	++	++	++	++	++	--
1.5	--	--	+-	++	++	++	--
2.0	--	--	--	++	++	++	--
2.5	--	--	--	+-	+-	+--	--

30 A:

l (mm)	arc length (mm)						
	1.0	1.5	2.0	2.5	3.0	3.5	4.0
0.5	++	++	++	++	++	++	+-
1.0	+-	++	++	++	++	++	+-
1.5	+-	++	++	++	++	++	+-
2.0	--	--	+-	++	++	++	--
2.5	--	--	--	++	+-	+--	--

40 A

l (mm)	arc length (mm)						
	1.0	1.5	2.0	2.5	3.0	3.5	4.0
0.5	++	++	++	++	++	++	++-
1.0	+-	++	++	++	++	++	+-
1.5	+-	++	++	++	++	++	--
2.0	--	+-	+-	++	++	++	--
2.5	--	--	+--	++	++-	+--	--

50 A:

l (mm)	arc length (mm)						
	1.0	1.5	2.0	2.5	3.0	3.5	4.0
0.5	++	++	++	++	++	++	++
1.0	++-	++	++	++	++	++	+-
1.5	+-	++	++	++	++	++	+--
2.0	--	+-	+-	++	++	++	--
2.5	--	--	+-	++	++	+-	--



Table 2: Results influence laser power experiments

100 W:

l (mm)	arc length (mm)						
	1.0	1.5	2.0	2.5	3.0	3.5	4.0
0.5	--	--	+-	+-	+-	--	--
1.0	--	--	--	--	+-	++	--
1.5	--	--	--	--	+-	+--	--
2.0	--	--	--	--	--	--	--
2.5	--	--	--	--	--	--	--

200 W:

l (mm)	arc length (mm)						
	1.0	1.5	2.0	2.5	3.0	3.5	4.0
0.5	+-	++	++	++	++	++	--
1.0	--	+-	+-	++	++	+-	--
1.5	--	--	--	+-	+-	++	--
2.0	--	--	--	--	--	+-	--
2.5	--	--	--	--	--	--	--

500 W:

l (mm)	arc length (mm)						
	1.0	1.5	2.0	2.5	3.0	3.5	4.0
0.5	++	++	++	++	++	++	--
1.0	+--	+-	++	++	++	++	--
1.5	--	--	+-	+-	++-	++-	--
2.0	--	--	--	--	++	+-	--
2.5	--	--	--	--	--	--	--

750 W:

l (mm)	arc length (mm)							
	1.0	1.5	2.0	2.5	3.0	3.5	4.0	4.5
0.5	++	++	++	++	++	++	++	+-
1.0	+-	++	++	++	++	++	++	+--
1.5	+-	++	++	++	++	++	++-	--
2.0	--	++-	++	++	++	++	+-	--
2.5	--	++-	++	++	++	++	--	--
3.0	--	+-	++-	++	++	+-	--	--
3.5	--	--	--	++	+-	+-	--	--

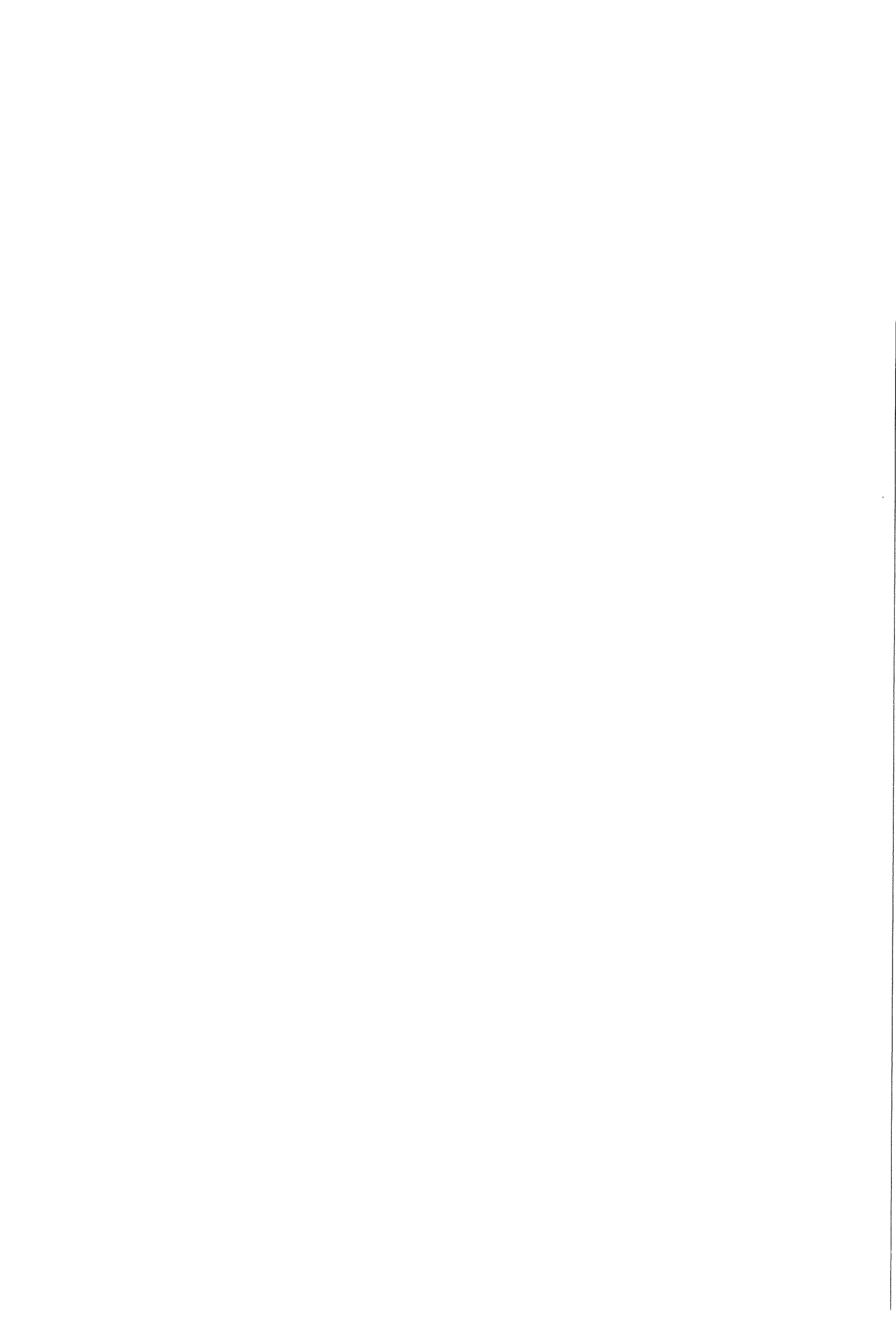


Table 3: Results influence of laser pulse duration experiments

1 ms:

l (mm)	arc length (mm)						
	1.0	1.5	2.0	2.5	3.0	3.5	4.0
0.5	++	++	++	++	++	++	--
1.0	+-	+-	++	++	++	++	--
1.5	--	--	--	+-	+-	+-	--
2.0	--	--	--	--	--	--	--
2.5	--	--	--	--	--	--	--

2 ms:

l (mm)	arc length (mm)						
	1.0	1.5	2.0	2.5	3.0	3.5	4.0
0.5	++	++	++	++	++	++	--
1.0	--	+-	++	++	++	++	--
1.5	--	--	+-	+-	+-	+-	--
2.0	--	--	--	+-	+-	--	--
2.5	--	--	--	--	--	--	--

5 ms:

l (mm)	arc length (mm)						
	1.0	1.5	2.0	2.5	3.0	3.5	4.0
0.5	++	++	++	++	++	++	+-
1.0	--	++	++	++	++	++	--
1.5	+-	+-	++	++	++	++	--
2.0	--	+-	++	++	++	+-	--
2.5	--	--	+-	+-	++	+-	--

Table 4: Results delay time experiments in air

$P_{\text{laser}}$ (kW)	$t_l$ (ms)	$I_{\text{arc}}$ (A)	$t_a$ (ms)	l (mm)	$l_a$ (mm)	delay (ms)	result
0.5	1.0	20	4.0	1.0	2.0	0	+-
0.5	2.0	20	4.0	1.0	2.0	0	+-
0.5	3.0	20	4.0	1.0	2.0	0	+-
0.5	5.0	20	4.0	1.0	2.0	0	+-

comment: The longer the laser pulse duration, the bigger the laser spot and the smaller the arc spot becomes. A bigger part of the arc is drawn towards the laser spot as the laser pulse duration increases (figure 31)



Table 5: Results delay experiment with TIG pulse duration variation. Conditions: arc: 20 A; laser: 0.5 kW/3 ms; delay = 0 ms;  $I_L = 420 \mu\text{m}$ ;  $l = 1.0 \text{ mm}$ ;  $l_a = 2.0 \text{ mm}$ ; air.

$t_a$ (ms)	delay (ms)	result
1.0	0	--
4.0	0	+-
9.9	0	++-
1.0	2.0	++
4.0	2.0	++
9.9	2.0	++

Table 6: Results minimum delay time experiments. Conditions: arc: 20 A/4 ms; laser: 0.5 kW;  $l = 1.0 \text{ mm}$ ;  $l_a = 2.0 \text{ mm}$ ; air

delay (ms)	$t_1$ (ms)	result
0.2	1.0	++-
0.2	2.0	++
0.2	3.0	++-
0.4	1.0	++
0.4	2.0	++
0.4	3.0	++
0.6	1.0	++
0.6	2.0	++
0.6	3.0	++
0.8	1.0	+-
0.8	2.0	+-
0.8	3.0	++
1.0	1.0	++
1.0	2.0	+-
1.0	3.0	++

Table 7: Results reference measurement in argon. Conditions: arc 20 A/4 ms; laser: 0.5 kW/3 ms; delay: 1 ms;  $I_L : 420 \mu\text{m}$ ; argon flow: 1 l/min.

$l$ (mm)	arc length ( $l_a=2.0 \text{ mm}$ )
1.0	++
1.5	++
2.0	+-
2.5	--

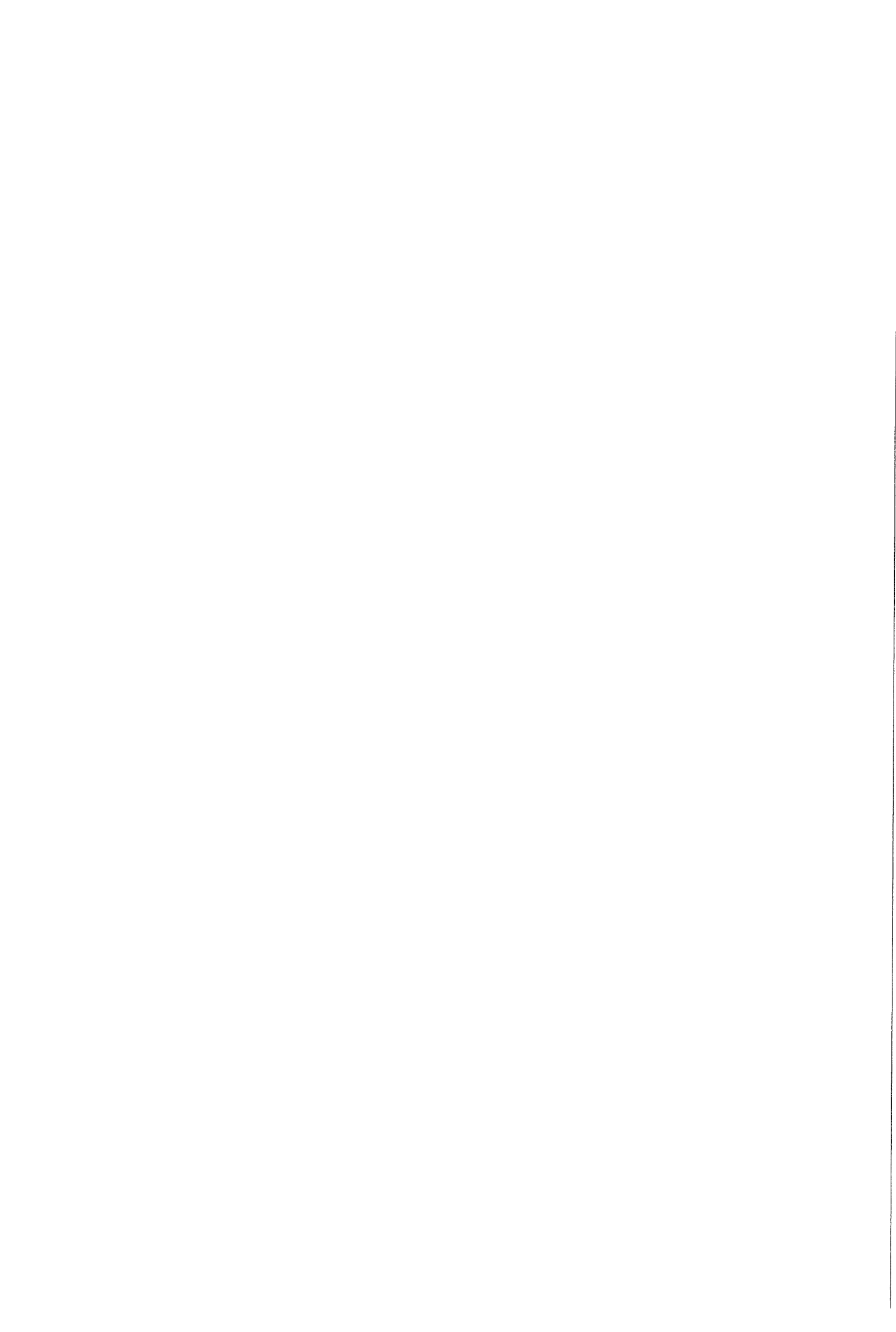


Table 8: Results of influence of arc length on  $l_c$  experiments. Conditions: arc = 20 A/4 ms; laser = 0.5 kW/3 ms; delay = 1 ms;  $I_L = 420 \mu\text{m}$ ; argon flow = 1 l/min.

l (mm)	arc length (mm)									
	1.0	1.5	2.0	3.0	4.0	5.0	6.0	7.0	8.0	9.0
1.0	++	++	++	+-	++	++	++	++	++	+-
1.5	+-	+-	++	++	++	++	++	++-	+-	+-
2.0	--	+-	+-	++	++-	+-	+-	+-	--	--
2.5	--	--	--	+-	+-	--	--	--	--	--

Table 9: Results delay time experiments with variation in TIG pulse duration in argon. Conditions: arc: 20 A; laser: 0.5 kW/3 ms;  $l = 1.0 \text{ mm}$ ;  $l_a = 2.0 \text{ mm}$ ;  $I_L = 420 \mu\text{m}$ ; delay = 0 ms.

delay (ms)	$t_a$ (ms)	result
0	1.0	--
0	4.0	++
0	9.9	++-

Table 10: Results minimum delay time experiments. Conditions: arc: 20 A/4 ms; laser: 0.5 kW;  $l = 1.0 \text{ mm}$ ;  $l_a = 2.0 \text{ mm}$ ; argon

delay (ms)	$t_l$ (ms)	result
0.2	1.0	++
0.2	2.0	++
0.2	3.0	++
0.4	1.0	++
0.4	2.0	++
0.4	3.0	++
0.6	1.0	++
0.6	2.0	++
0.6	3.0	++
0.8	1.0	++
0.8	2.0	++
0.8	3.0	++
1.0	1.0	--
1.0	2.0	++
1.0	3.0	++

comment: at a delay of 0.8 ms the spots are oblong. This oblong form starts already at a delay of 4 ms. Furthermore, there are small "double spots" very faintly visible for all attractions.



## Arc ignition by laser

During the attraction experiments it became clear that the laser beam facilitates the ignition of the TIG arc. For instance, at an arc length of 3.6 mm in air with 20 A current and pulse duration of 4 ms it was not possible to get the arc started, there is only a spark formed.

When the laser is also triggered, thus when the combination spots are made, it was possible to have an arc at higher arc lengths (3.6-4.5 mm). Therefore trying to get the arc started by laser should be investigated.

Hereto the high voltage ignition of 12 kV has to be shut off. The measured open voltage between cathode and anode is 75 V. Several tests were conducted. Varying arc length, critical distance, laser power, pulse durations and delay time. None of them proved to be successful in igniting the arc, not even a spark.

The open voltage is too low, it needs to be at least 150 V, but the electrical components in the TIG power unit are not designed for such high voltages. Thus the ignition test would have to be conducted with other power sources. There must also be looked into the theoretical possibility of igniting the arc with a laser.

